REPORT DOCU

AD-A255 824

Form Approved
OMB No 0704-0188

(2)

Public reporting burden for this collection of information is estimated to average ... hour per response, including the time for reviewing instructions, searching existing data sources, gathering and maintaining the data needed, and completing and reviewing the collection of information. Send comments regarding this burden estimate or any other aspect of this collection of information, including suggestions for reducing this burden, to Washington Headquarters Services, Directorate for Information Operations and Reports, 1215 Jefferson Davis Highway, Suite 1204, Arlington, VA 22202-4302, and to the Office of Management and Budget, Paperwork Reduction Project (0704-0188), Washington, DC 20503.

1. AGENCY USE ONLY (Leave blank)	2. REPORT DATE	3. REPORT TYPE AND DATES COVERED
		Final Report 1 Apr 92/31 Jul 92

4. TITLE AND SUBTITLE
XXth Informal Conference on Photochemistry
April 26 - 1 May 1992

5. FUNDING NUMBERS
61102F 2303/ES

6. AUTHOR(S) Dr Paul H. Wine, Project Director
School of Chemistry, Georgia Institute of Tech
Atlanta, GA 30332

7. PERFORMING ORGANIZATION NAME(S) AND ADDRESS(ES)
Georgia Tech Research Corporation

8. PERFORMING ORGANIZATION REPORT NUMBER
AFOSR-TR- 92 0880

9. SPONSORING/MONITORING AGENCY NAME(S) AND ADDRESS(ES)
AFOSR/NC
Bolling AFB DC 20332-6448

DTIC
OCT 1 1992

10. SPONSORING/MONITORING AGENCY REPORT NUMBER
F49620-92-J-0180

11. SUPPLEMENTARY NOTES

12a. DISTRIBUTION/AVAILABILITY STATEMENT
APPROVED FOR PUBLIC RELEASE:
DISTRIBUTION UNLIMITED

12b. DISTRIBUTION CODE

13. ABSTRACT (Maximum 200 words)

The XXth Informal Conference on Photochemistry was held at the Colony Square Hotel in Atlanta, Georgia during the period April 26 - May 1, 1992. A total of 74 oral papers and 105 poster papers were presented. Most participants agreed that the scientific level of the conference was very high. One of the goals of this conference was to bring together leading researchers in a variety of basic and applied sub-areas of physical photochemistry. In this regard, discussion was stimulated which hopefully will lead to new interdisciplinary research initiatives. The support provided by AFOSR was used to (a) cover the $50 registration fee for students/postdocs who attended the conference and presented papers and (b) cover lodging costs for some of the sam students/postdocs.

92 9 30 052

92-26248

236pp

14. SUBJECT TERMS

15. NUMBER OF PAGES

16. PRICE CODE

17. SECURITY CLASSIFICATION OF REPORT	18. SECURITY CLASSIFICATION OF THIS PAGE	19. SECURITY CLASSIFICATION OF ABSTRACT	20. LIMITATION OF ABSTRACT
UNCLASSIFIED	UNCLASSIFIED	UNCLASSIFIED	

NSN 7540-01-280-5500

Standard Form 298 (Rev. 2-89)
Prescribed by ANSI Std. 239-18
298-102

XXth INFORMAL CONFERENCE ON PHOTOCHEMISTRY

AFOSR Grant No. F49629-92-J-0180
Georgia Tech Project No. A-9171

Final Report

A-1

Submitted to:

Air Force Office of Scientific Research
Directorate of Chemistry and Materials Science
Bolling Air Force Base
Washington, DC 20332-6448
Attn: Dr. Michael Berman

Submitted by:

Dr. Paul H. Wine, Project Director
School of Chemistry and Biochemistry, School of Earth and
Atmospheric Sciences, and Electro-Optics and Physical Sciences Laboratory-GTRI
Georgia Institute of Technology
Atlanta, GA 30332

XXTH INFORMAL CONFERENCE ON PHOTOCHEMISTRY

The XXth Informal Conference on Photochemistry was held at the Colony Square Hotel in Atlanta, Georgia during the period April 26 - May 1, 1992. A total of 74 oral papers and 105 poster papers were presented. Most participants agreed that the scientific level of the conference was very high. One of the goals of this conference was to bring together leading researchers in a variety of basic and applied sub-areas of physical photochemistry. In this regard, discussion was stimulated which hopefully will lead to new interdisciplinary research initiatives.

The support provided by AFOSR was used to (a) cover the $50 registration fee for students/postdocs who attended the conference and presented papers and (b) cover lodging costs for some of the same students/postdocs. A list of students/postdocs whose registration fees were covered is attached.

The main body of this report is the book of abstracts.

STUDENTS AND POSTDOCS WHOSE REGISTRATION FEES WERE COVERED USING AFOSR FUNDS

Student/Postdoc	Affiliation
Allen, John M.	Duke University
Anastasio, Cort	Duke University
Bevilacqua, Thomas J.	NOAA Aeronomy Laboratory
Bishenden, Elizabeth	University of Toronto, Canada
Bohac, E. J.	University of North Carolina
Bu, Y.	Emory University
Chen, Junyi	York University, Canada
Chin, Mian	Harvard University
Cronkhite, Jeffrey M.	Georgia Institute of Technology
Daniels, Michael	Cornell University
Davis, H. Floyd	University of California-Berkeley
Easter, David C.	Naval Research Laboratory
Erickson, Matthew	Emory University
Fei, Suli	Emory University
Glenewinkel-Meyer, Thomas	University of Wisconsin
Grantier, David R.	Georgia Institute of Technology
Harvey, Lilia	Georgia Institute of Technology
Hippler, Michael	Heriot-Watt University, U.K.
Horwitz, Ron	University of Cincinnati
Hunter, Martin	University of Southern California
Irikura, Karl K.	National Institute of Standards and Technology
Jefferson, Anne	University of Colorado
Joslin, Evelyn	Imperial College, U.K.
Kaledin, Leonid	Emory University
Kash, Phillip W.	University of Chicago
Lee, Seong-Poong	Emory University
Lee, Yin-Yu	National Tsing Hua University, Taiwan
Lovejoy, Christopher M.	University of Colorado

Morris, Vernon R.	University of California-Davis
Navratil, Amy J.	University of Denver
Nickolaisen, Scott L.	Jet Propulsion Laboratory
Nien, Chia-Fu	University of Miami
Nur, Abdullahi	Howard University
Padmaja, S.	National Institute of Standards and Technology
Pounds, Andrew J.	Georgia Institute of Technology
Robbins, David L.	University of Georgia
Sapers, Steven P.	Battelle Pacific Northwest Laboratory
Schafer, Pamela	Emory University
Schnupf, Udo	Emory University
Seakins, Paul W.	University of Colorado
Shackelford, Christie J.	Georgia Institute of Technology
Shi, Jichun	Ford Motor Company
Singleton, Steven	University of Denver
Stevens, Philip S.	Pennsylvania State University
Su, Yali	University of Notre Dame
Tarr, J. A.	Emory University
Thompson, John E.	NOAA Aeronomy Laboratory
Thorn, R. Peyton	Georgia Institute of Technology
Waldeck, Janet	Weizmann Institute, Israel
Wang, Desheng	Emory University
Washewsky, Gabriella	University of Chicago
Weston, Gareth	Oxford University, U.K.
Willey, Kenneth	University of Georgia
Winstead, Chris	Georgia Institute of Technology
Yang, D. L.	Emory University
Yen, Chen-Sheng	University of Georgia
Yu, Tao	Emory University
Zhen, Gao	Georgia Institute of Technology
Zheng, Xiaonen	Emory University

XXth Informal Conference on PHOTOCHEMISTRY

April 26 - May 1, 1992
Atlanta, Georgia

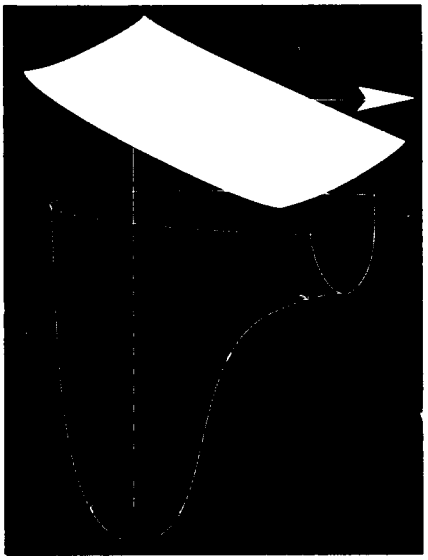

Georgia Institute of Technology
A Unit of the University System of Georgia

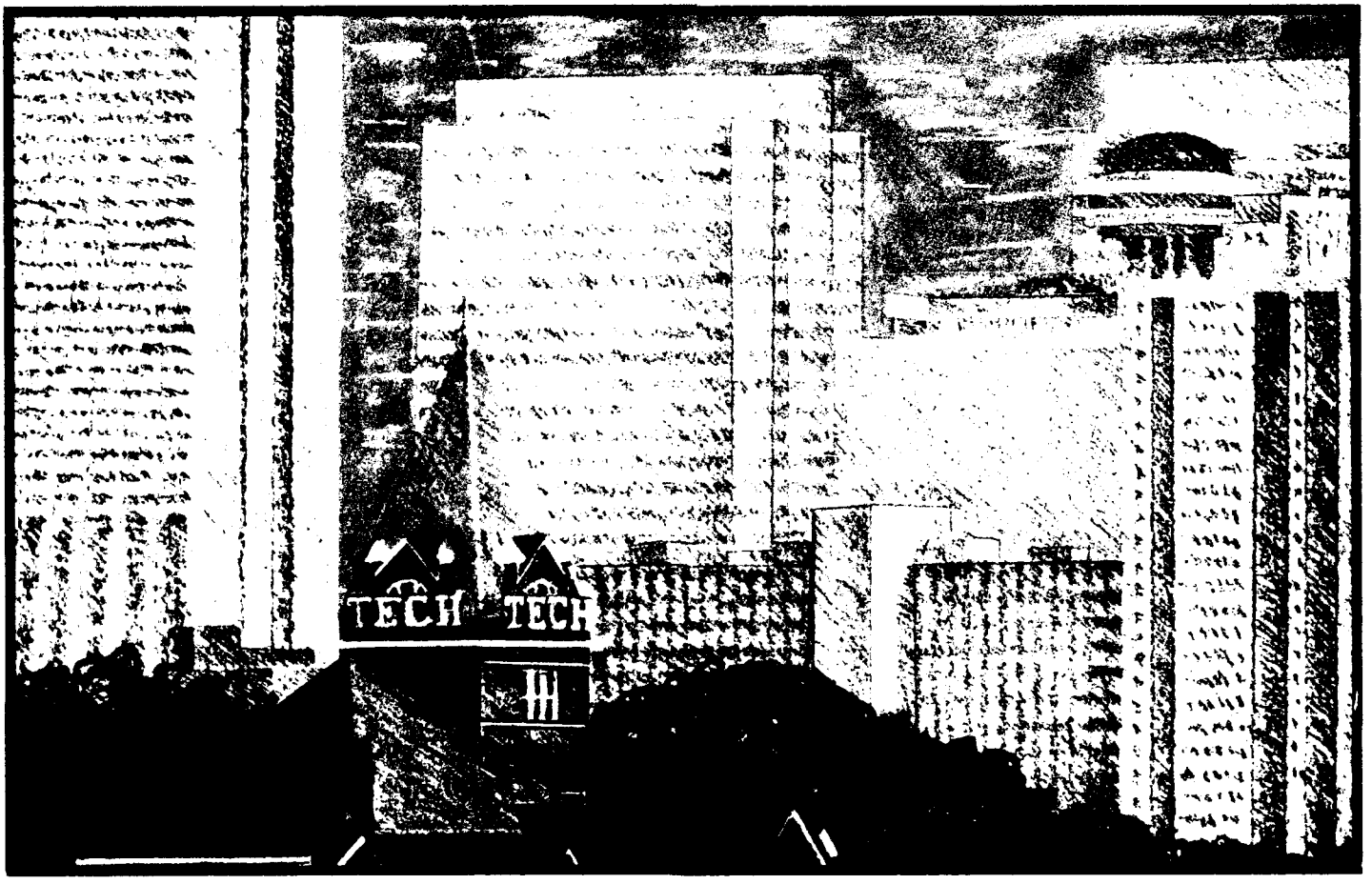

XXth INFORMAL CONFERENCE ON PHOTOCHEMISTRY

Sponsors

National Science Foundation, Atmospheric Chemistry Program

National Aeronautics and Space Administration, Upper Atmosphere Research Program

U.S. Environmental Protection Agency, Exploratory Research Program

Air Force Office of Scientific Research, Directorate of Chemistry and Materials Science

School of Chemistry and Biochemistry, Georgia Tech

School of Earth and Atmospheric Sciences, Georgia Tech

School of Physics, Georgia Tech

Physical Sciences Laboratory, Georgia Tech Research Institute

Department of Chemistry, Emory University

Organizing Committee

P. H. Wine, Chairman

J. M. Bowman

D. D. Davis

J. L. Gole

M. C. Heaven

M. C. Lin

INFORMAL CONFERENCE ON PHOTOCHEMISTRY

I.	University of California, Los Angeles (Blacet)	1952
II.	University of Rochester (Noyes)	1954
III.	National Research Council, Ottawa (Steacie)	1958
IV.	National Bureau of Standards (Ausloos & McNesby)	1959
V.	University of Alberta (Gunning)	1961
VI.	University of California, Davis (Brinton & Volman)	1964
VII.	Rensselaer Polytechnic Institute (Harteck & Strong)	1966
VIII.	National Research Council, Ottawa (Kutschke)	1968
IX.	Ohio State University (Calvert)	1970
X.	Oklahoma State University (Mains)	1972
XI.	Vanderbilt University (Martin)	1974
XII.	National Bureau of Standards (Braun & Kurylo)	1976
XIII.	University of South Florida (Stevens)	1978
XIV.	University of California, Irvine, (Lee, Molina & Rowland)	1980
XV.	Stanford Research Institute (Slanger & Golden)	1982
XVI.	Harvard University (Anderson)	1984
XVII.	University of Colorado (Ravishankara)	1986
XVIII.	University of Southern California (Reisler & Wittig)	1989
XIX.	University of Michigan (Barker)	1990
XX.	Georgia Institute of Technology (Wine)	1992

PROGRAM

April 26

5:00 - 9:00 Registration

7:00 - 9:00 Reception

April 27

8:10 - 8:15 Opening Remarks

Photodissociation Dynamics I (Session Chairman: P.H. Wine)

8:15 - 8:45 A1 A. Zewail, "Recent Developments in Femtochemistry"

8:45 - 9:05 A2 L.D. Ziegler, "Frequency and Time Domain Studies of Ultrafast Molecular Photodissociation"

9:05 - 9:25 A3 Y.B. Fan and D.J. Donaldson, "Cluster Induced Photochemistry of CH_3I at 248 nm"

9:25 - 9:45 A4 B.K. Andrews, K.A. Burton, and R.B. Weisman, "Dynamics of Azomethane's Two-Step Photodissociation"

BREAK

Photodissociation Dynamics II (Session Chairman: R.E. Weston)

10:15 - 10:45 B1 M. Shapiro, "Theory of Transient Effects in Photodissociation and Continuum Raman Spectroscopy with Pulses"

10:45 - 11:05 B2 K. Obi, "Hydrogen Abstraction in Molecular Cluster of Benzophenone with Hydrogen Donors"

11:05 - 11:25 B3 Y. Matsumi, K. Tonokura, and M. Kawasaki, "Fine-Structure Branching Ratios and Doppler Profiles of $Cl(^2P_j)$ Photofragments from Photodissociation of Chlorine Molecule Near and in the Ultraviolet Region"

11:25 - 11:45	B4	S. Rosenwaks, T. Arusi-Parpar, Y. Cohen, D. David, A. Strugano, I. Bar, and J.J. Valentini, "State-to-State Photodissociation of H_2O and HOD in the First Absorption Band"

LUNCH

Photodissociation Dynamics III (Session Chairman: Y.T. Lee)

1:30 - 2:00	C1	H.F. Davis, B. Kim, H.S. Johnston, and Y.T. Lee, "Photodissociation Dynamics of NO_3 and ClO_2"
2:00 - 2:20	C2	D.R. Peterman, R.G. Daniel, and J.A. Guest, "Characterization of Acetic Acid Photochemical Dynamics: Isotopic Substitution Effects"
2:20 - 2:40	C3	J.L. Brum, S. Deshmukh, and B. Koplitz, "Site-Specific Photochemistry"
2:40 - 3:00	C4	S.P. Sapers and W.P. Hess, "Photodissociation of $BrCH_2CH_2OH$ and ICH_2CH_2OH: Formation and Characterization of OH ($X^2\pi$)"

BREAK

Photodissociation Dynamics IV (Session Chairman: S. Rosenwaks)

3:30 - 3:50	D1	E.J. Bohac and R.E. Miller, "State-to-State Vibrational Predissociation of H_2-HF and D_2-HF: A Direct Comparison Between Theory and Experiment"
3:50 - 4:10	D2	Y. Rudich and R. Naaman, "State-to-State Vibrational Photodissociation of Van der Waals Molecules"
4:10 - 4:30	D3	J. Manz, "Model Studies on Laser Control of Bond Fissions and Isomerizations for Organic and Organometallic Molecules"
4:30 - 4:50	D4	M.A. Duncan, "Photochemistry and Spectroscopy of Metal Ion-Molecule Complexes"

DINNER

8:00 - 10:00 POSTER SESSION I

April 28

Free Radical Spectroscopy I (Session Chairman: J. Tellinghuisen)

8:15 - 8:45 E1 E. Hirota, "High-Resolution Spectroscopy of Free Radicals and its Applications to Photochemical Reactions"

8:45 - 9:05 E2 B. Gazdy and J.M. Bowman, "Ab initio Spectroscopy of HCO(X,J=1 → J=0) and HCN (X,J=0)

9:05 - 9:25 E3 G.N.R. Tripathi, "Time-Resolved Raman Spectra and Reaction Dynamics of Solvated Radicals"

9:25 - 9:45 E4 G.W. Faris, M.J. Dyer, P.C. Cosby, D.L. Huestis, and T.G. Slanger, "Experiments on the Quartet States of Nitric Oxide"

BREAK

Free Radical Spectroscopy II (Session Chairman: R. McDiarmid)

10:15 - 10:45 F1 T.A. Miller, "Spectroscopy of Radicals and Their Complexes"

10:45 - 11:05 F2 M.C. Heaven, S. Fei, X. Zheng, and U. Schnupf, "Electronic Spectroscopy and Predissociation Dynamics of OH/D-Kr"

11:05 - 11:25 F3 K.K. Irikura, R.D. Johnson III, and J.W. Hudgens, "The 2 + 1 REMPI Spectrum of $SiCl_2$"

11:25 - 11:45 F4 K.D. Setzer, O. Shestakov, and E.H. Fink, "Spectroscopic and Kinetic Studies of the Upper Spin-Orbit Components of Widely Split $^2\Sigma^-$ and $^2\pi$ Ground States of Diatomic Radicals"

LUNCH

Photochemistry on Surfaces I (Session Chairman: J.M. White)

1:30 - 2:00	G1	J.C. Polanyi, "The Dynamics of Photodissociation and Photoreaction in the Adsorbed State"
2:00 - 2:20	G2	R.V. Weaver, Y. Zeiri, and T. Uzer, "Competition Between Adsorbate Dissociation and Desorption on Laser-Heated Surfaces: A Stochastic Trajectory Study"
2:20 - 2:40	G3	V. Barclay, D. Jack, J.C. Polanyi, and Y. Zeiri, "Surface Aligned Photochemistry: A Theoretical Study of the HX/LiF(100) System (X=Cl, Br, and I)"
2:40 - 3:00	G4	P.L. Houston, M. Asscher, F.M. Zimmenrmann, L.L. Springsteen, and W. Ho, "Translational and Internal Energy Distributions of CO Photochemically Desorbed from Oxidized Ni(111)"

BREAK

Photochemistry on Surfaces II (Session Chairman: P.L. Houston)

3:30 - 4:00	H1	T.J. Chuang, "Laser-Stimulated Gas-Surface Photochemistry: Basics and Applications"
4:00 - 4:20	H2	A. Hoffman, B. Carraway, and M.R. Hoffmann, "Photocatalysis on Q-Sized Semiconductor Particles"
4:20 - 4:40	H3	S.-P. Lee, J. Tarr, and M.C. Lin, "Photochemistry of Organometallics on Insulators"
4:40 - 5:00	H4	J.M. White, "Molecular Photochemistry on Surfaces"

DINNER

8:00 - 10:00 POSTER SESSION II

April 29

Atmospheric Photochemistry I (Session Chairman: A.R. Ravishankara)

8:15 - 8:45	I1	S.P. Sander, "Atmospheric Reactions of Chlorine Oxide Reservoirs"
8:45 - 9:05	I2	F. Maguin, G. Laverdet, G. LeBras, and G. Poulet, "The Reactions IO + HO_2 and BrO + HO_2: Kinetic Results and Atmospheric Impact"
9:05 - 9:25	I3	T.K. Minton, C.M. Nelson, T.A. Moore, and M. Okumura, "Direct Observation of ClO from Chlorine Nitrate Photolysis"
9:25 - 9:45	I4	D.R. Worsnop, G.N. Robinson, M.S. Zahniser, C.E. Kolb, X. Shi, and D.R. Herschbach, "Chemical Kinetics and Dynamics of the Sodium Nightglow"

BREAK

Optical Diagnostic Techniques (Session Chairman: A.J. Hynes)

10:15 - 10:45	J1	J. Wolfrum, "Laser Diagnostics in Photochemistry: Elementary and Industrial Processes"
10:45 - 11:05	J2	K.L. McNesby and R.A. Fifer, "Tomographic Analysis of Line of Sight Infrared Spectra of Flames"
11:05 - 11:25	J3	D.B. Oh and J.A. Silver, "Visible Diode Laser Detection of HCO"
11:25 - 11:45	J4	J.D. Bradshaw and S.T. Sandholm, "Application of Photofragmentation Laser Induced Fluorescence to the Measurement of Important Atmospheric Gases"

LUNCH

Free Radical Kinetics (Session Chairman: M.R. Berman)

1:30 - 2:00	K1	M.J. Pilling, "Kinetics of Free Radical Reactions of Importance in Combustion"

2:00 - 2:20	K2	L.J. Medhurst, N.L. Garland, and H.H. Nelson, "Temperature Dependence of the Kinetics of the Reaction: CH + N_2"
2:20 - 2:40	K3	J.M. Nicovich, K.D. Kreutter, C.A. van Dijk, and P.H. Wine, "Temperature-Dependent Kinetics Studies of the Reactions $Br(^2P_{3/2})$ + H_2S ⇔ SH + HBr and $Br(^2P_{3/2})$ + CH_3SH ⇔ CH_3S + HBr. Heats of Formation of SH and CH_3S Radicals"
2:40 - 3:00	K4	H. Hippler, R. Forster, M. Frost, A. Schlepegrell, and J. Troe, "High Pressure Limiting Rate Constants for Reactions of OH-Radicals with NO, NO_2, CO, and OH from Saturated Laser Induced Fluorescence Studies"

BREAK

Condensed Phase Environmental Photochemistry
(Session Chairman: M.R. Hoffmann)

3:30 - 3:50	L1	R.G. Zepp and W.L. Miller, "Production of Atmospheric Trace Carbon Gases from Photodegradation of Humic Substances"
3:50 - 4:10	L2	B.C. Faust, C. Anastasio, and J.M. Allen, "Aqueous-Phase Photochemical Formation of Oxidants in Authentic Cloud Waters"
4:10 - 4:30	L3	G.N. Robinson, D.R. Worsnop, M.S. Zahniser, C.E. Kolb, W.DeBruyn, S. Duan, and P. Davidovits, "Heterogeneous Chemistry of Trace Gases on Aqueous and Sulfuric Acid Liquid Droplets"
4:30 - 4:50	L4	S. Padmaja, P. Neta, and R.E. Huie, "Laser-Flash Photolysis of H_2S Solutions"

DINNER

8:00 - 10:00 POSTER SESSION III

April 30

Reaction Dynamics I (Session Chairman: I.W.M. Smith)

8:15 - 8:45	M1	F.F. Crim, "Bond- and State-Selected Photodissociation and Bimolecular Reaction"
8:45 - 9:05	M2	D. Wang and J.M. Bowman, "Quantum Calculations of Mode Specificity in $H + H_2O \leftrightarrow OH + H_2$ and $H + HOD \rightarrow H_2 + OD$, $HD + OH$"
9:05 - 9:35	M3	G.C. Schatz, "Theoretical Studies of Vibrational and Electronic State Specificity in Chemical Reactions: $H + H_2O \rightarrow OH + H_2$ and $Cl + HCl \rightarrow ClH + Cl$"
9:35 - 9:55	M4	A.P. Baronavski and S. McCauley, "Ultrafast Studies of Electron Photodetachment and Solvation in Aqueous Iodide Anion Solutions"

BREAK

Reaction Dynamics II (Session Chairman: R.D. Coombe)

10:15 - 10:45	N1	P.J. Dagdigian, "The Dynamics of the Electronic Quenching and Chemical Reactions of the Imidogen Radical"
10:45 - 11:05	N2	N. Balucani, P. Casavecchia, and G. G. Volpi, "Reaction Dynamics of Radical Species from Crossed Beam Studies"
11:05 - 11:25	N3	K.H. Gericke and K. Mikulecky, "Influence of Vibrational and Translational Motion on the Reaction Dynamics of $O(^1D) + H_2(v) \rightarrow OH(v,J) + H$"
11:25 - 11:45	N4	J. Shao, L. Yuan, H. Yang, Y. Gu, K. Li, K. Wang, and Y. Tao, "Preliminary Investigation of the $O(^1D) + H_2$, D_2, HD Reactions: Chemical Laser Determination of Nascent Product Vibrational Distributions and the $O(^1D)$ + HD Macroscopic Branching Ratio"

LUNCH

Photophysics and Energy Transfer I (Session Chairman: R.W. Carr)

1:30 - 2:00	O1	J.R. Barker, "Mechanisms for the Vibrational Deactivation of Large Molecules"
2:00 - 2:20	O2	U. Hold, T. Lenzer, K. Luther, and A. Symonds, "Collisional Deactivation of Highly Excited Azulene: Transition Probabilities of Energy Transfer Determined by Kinetically Controlled Selective Ionization Measurements"
2:20 - 2:40	O3	A.J. Sedlacek, G.E. Hall, R.E. Weston, Jr., and G.W. Flynn, "Diode Laser Studies of Energy Transfer from Highly Vibrationally Excited Aromatic Molecules"
2:40 - 3:00	O4	J. Troe, "Supercollision Effects on Thermal Unimolecular Reactions"

BREAK

Photophysics and Energy Transfer II (Session Chairman: J. Troe)

3:30 - 3:50	P1	M.J. Frost, M. Islam, I.W.M. Smith, and J.F. Warr, "Infrared-Ultraviolet Double Resonance Experiments on Collisional Energy Transfer in NO, HCN, and C_2H_2"
3:50 - 4:10	P2	A. Kaes and F. Stuhl, "Collisions of NH($A^3\pi$,J,N,e/f,v=0) with NH_3, Ar, He"
4:10 - 4:30	P3	J.L. Gole, K.K. Shen,, C.B. Winstead, and D. Grantier, "Chemically Driven Pulsed and Continuous Visible Chemical Laser Amplifiers and Oscillators"
4:30 - 4:50	P4	C.M. Lovejoy and S.R. Leone, "Translation-to-Vibration Excitation of H_2O(001) by 2.2 eV H Atoms: Rotational Alignment of an Asymmetric Top"
4:50 - 5:10	P5	L.R. Williams and D.R. Crosley, "Collisional Vibrational Energy Transfer of OH($A^2\Sigma^+$, v'=1)"

Evening BANQUET (Guest Speaker: Y.T. Lee)

May 1

Atmospheric Photochemistry II (Session Chairman: H. Niki)

8:15 - 8:45	Q1	P.D. Goldan, S.A. Montzka, W.C. Kuster, M. Trainer, and F.C. Fehsenfeld, "The Influence of Volatile Organic Compounds of Natural Origin on the Photochemical Production of Ozone"
8:45 - 9:05	Q2	M. O. Rodgers and W. L. Chameides, "The Role of Hydrocarbons in the Production of Ozone Episodes in the Southern United States"
9:05 - 9:25	Q3	R. Koch, M. Elend, J. Nowack, M. Siese, and C. Zetzsch, "The Secondary Reactions in the Tropospheric Degradation of Aromatics: Rate Constants for O_2 + Benzene-OH, Toluene-OH, p-Xylene-OH and Phenol-OH"
9:25 - 9:45	Q4	D. Boglu, R. Meller, and G.K. Moortgat, "Photooxidation Studies by FTIR Spectroscopy of CF_3COCl and CF_3CFH_2 (HCFC-134a)"

Atmospheric Photochemistry III (Session Chairman: D.D. Davis)

10:15 - 10:45	R1	S.C. Wofsy, "The Influence of the Biosphere on Important Atmospheric Gases"
10:45 - 11:05	R2	P.S. Stevens, J.H. Mather, and W. H. Brune, "In-Situ Measurements of Tropospheric OH and HO_2 by Laser Induced Fluorescence at Low Pressures"
11:05 - 11:25	R3	F.L. Eisele and D.J. Tanner, "Ion-Assisted Tropospheric OH Measurements"
11:25 - 11:45	R4	F. Wu and R.W. Carr, "The Photodissociation of Carbonyl Halides"
11:45 - 12:05	R5	R.R. Friedl, S.P. Sander, and Y.L. Yung, "Chloryl Nitrate: A Novel Product of the OClO + NO_3 + M Recombination"

LUNCH

1:30 - 5:30 Laboratory Tours at Georgia Tech and Emory

POSTER SESSION I

I-1 M. Daniels, "Production of Vibrationally Excited Oxygen from the 248 nm Photodissociation of Ozone"

I-2 D. C. Robie, M. Hunter, J. L. Bates, and H. Reisler, "Product State Distributions in the Photodissociation of Expansion - Cooled NO_2 Near the $NO(X^2\pi)$ v = 1 Threshold"

I-3 Th. Glenewinkel-Meyer, J. A. Bartz, and F. F. Crim, "Photodissociation of Silane in a Supersonic Expansion"

I-4 J. S. Keller, E. Jensen, P. W. Kash, and L. J. Butler, "Photodissociation Dynamics of Methanethiol Excited in the First Absorption Band"

I-5 P. W. Kash, M. D. Person, G. C. G. Waschewsky, and L. J. Butler, "Nonadiabaticity and the Competition Between Alpha, Beta, and Gamma Bond Fission Upon $^1(n,\pi^*(C=O))$ Excitation in Acetyl, Bromoacetyl, and Bromopropionyl Chloride"

I-6 A. Jefferson, E. C. Richard, and V. Vaida, "Gas and Condensed Phase Photochemistry of OClO"

I-7 E. Bishenden and D. J. Donaldson, "Cl Atom Production from Near UV Photolysis of OClO"

I-8 S. Baumgärtel, K.-H. Gericke, T. Haas, M. Lock, and C. Maul, "Photodissociation Dynamics of $RN_3 + h\nu \rightarrow R + N_3$, R = H,D,CN"

I-9 M. Hippler and J. Pfab, "Photodissociation of Jet-Cooled Nitrosyl Chloride Near 380 nm"

I-10 D. V. Kupriyanov and O. S. Vasyutinskii, "Absorption Spectroscopy of Polarized Tl Photofragments"

I-11 J. R. Waldeck and M. Shapiro, "Time-Evolution of the Photofragment Angular Distribution: $\beta(t)$"

I-12 G. Hancock and D. G. Weston, "Time Resolved FTIR Studies of the Photolysis of CH_2CFCl"

I-13 G. E. Hall, J. T. Muckerman, J. M. Preses, R. E. Weston, Jr., and G. W. Flynn, "A Time-Resolved FTIR Study of the Photodissociation of Pyruvic Acid"

I-14 K. Seki and H. Okabe, "Photodissociation of Methylacetylene and Acetylene at 193 nm"

I-15 D. B. Exton and J. V. Gilbert, "Photolysis of $NFCl_2$"

I-16 L. D. Waits, R. J. Horwitz, R. G. Daniel, and J. A. Guest, "Photofragmentation of CF_3I^+ Produced by Resonant Multiphoton Ionization"

I-17 C. S. Yeh, K. F. Willey, D. L. Robbins, J. E. Salcido, and M. A. Duncan, "Photoinitiated Reactions in Mass-Selected Magnesium Ion-Molecule Complexes"

I-18 D. L. Robbins, K. F. Willey, C. S. Yeh, J. S. Pilgrim, B. J. Salcido, and M. A. Duncan, "Spectroscopy and Photochemistry of Metal Dimer Rare Gas Complexes"

I-19 K. F. Willey, C. S. Yeh, D. L. Robbins, J. S. Pilgrim, and M. A. Duncan, "Photochemistry and Charge-Transfer in Mass-Selected Organometallic Clusters"

I-20 M. J. McQuaid and R. C. Sausa, "The ArNO Van der Waals' Complex: Observation and Analysis of the A-X Electronic Transition"

I-21 S. Fei and M. C. Heaven, "Electronic Spectroscopy and Predissociation of Ne-CN"

I-22 U. Schnupf, J. M. Bowman, and M. C. Heaven, "Development of a Three-Dimensional Potential Energy Surface for the A State of OH/D-Ar"

I-23 B. Gazdy and J. M. Bowman, "Resonances and Predissociation Dynamics of Ar-OH* (v=0,1)"

I-24 D. Chapman, J. Bentley, B. Gazdy, and J. M. Bowman, "Wavepacket Relaxation and Complete Absorption Spectrum of HO_2"

I-25 Y.-Y. Lee, Y.-P. Lee, and I.-C. Chen, "Laser-Induced Fluorescence of Jet-Cooled CH_3O: Vibronic Analysis of the $\tilde{X}$ State"

I-26 A. H. Nur, X. Zhu, and P. Misra, "Laser Excitation Spectroscopy of Jet-Cooled Hydroxyl and Methoxy Radicals in the Overlapping 308-317 nm Spectral Region"

I-27 K. K. Irikura and J. W. Hudgens, "Detection of $CH_2(\tilde{X}^3B_1)$ Radicals by 3 + 1 REMPI"

I-28 T. F. Hanisco, C. Yan, and A. C. Kummel, "The Effect of Molecular Orientation in CO/Ag(111) Scattering Probed by REMPI"

I-29 S.-P. Lee and M. C. Lin, "KrF Laser-Induced Photochemistry of Nitrosobenzene Adsorbed on a Cold $Al_2O_3(11\bar{2}0)$ Surface: Desorption Dynamics of the NO Photofragment"

I-30 Y. Bu, S.-P. Lee, and M. C. Lin, "Photodesorption of Benzene Adsorbed on Single Crystals of SiO_2 and LIF at 308, 248, and 193 nm"

I-31 K.-D. Shiang and J. M. Bowman, "Vibrational Overtone-Induced Desorption of HF from LiF(001)"

I-32 X.-Y. Zhu and J. M. White, "Photochemistry of Group V Hydrides on GaAs: Dynamics and Mechanism"

I-33 H. P. Gillis, J. L. Clemons, and J. P. Chamberlain, "Low Energy Electron Enhanced Etching of Semiconductor Surfaces"

I-34 H. A. Bender, W. T. Silfvast, and K. M. Beck, "Investigation of Distortion and Damage of Mo-Si Multilayer Reflective Coatings with High Intensity UV Radiation"

I-35 B. Marciniak and G. L. Hug, "Energy and Electron Transfer Processes in the Quenching of Triplet States of Organic Compounds by 1,3 Diketonate Metal Chelates. Laser Flash Photolysis Studies"

POSTER SESSION II

II-1 D. Grosjean, E. L. Williams II, and J. H. Seinfeld, "Atmospheric Oxidation of Selected Terpenes and Related Carbonyls: Gas Phase Carbonyl Products"

II-2 D. Grosjean, "Peroxyacyl Nitrates: Atmospheric Formation and Removal Processes"

II-3 M. M. Maricq, "Time Resolved UV Spectroscopy of CF_3CFHO_2"

II-4 T. G. Slanger, "The Action Spectrum of the O_2 10-0 Schumann-Runge Band in the Atmosphere"

II-5 J. J. Orlando, G. S. Tyndall, G. K. Moortgat, and J. G. Calvert, "Quantum Yields for Oxygen Atoms from the Photolysis of NO_3"

II-6 N. S. Wang, J. M. Jen, and Y.-P. Lee, "Kinetic Study of the Reaction of CH_3S with NO_2"

II-7 D. D. Nelson, Jr., M. S. Zahniser, and C. E. Kolb, "Chemical Kinetics of the Reactions of the OH Radical with Several Hydrochlorofluoropropanes"

II-8 T. E. Kleindienst, D. F. Smith, E. E. Hudgens, and C. D. McIver, "Kinetics and Mechanism for the Reaction of OH with Ethyl t-Butyl Ether in the Presence of NO_x"

II-9 J. M. Nicovich, S. Wang, and P. H. Wine, "Kinetics and Thermochemistry of C_2Cl_5 Formation from the $Cl(^2P_J)$ + C_2Cl_4 Association Reaction"

II-10 R. P. Thorn, J. M. Cronkhite, J. M. Nicovich, and P. H. Wine, "Laser Flash Photolysis Studies of Radical-Radical Reaction Kinetics: The $O(^3P)$ + BrO Reaction"

II-11 S. L. Nickolaisen, R. R. Friedl, and S. P. Sander, "Determination of Rates Constant for the ClO Self Reaction"

II-12 J. E. Thompson and A. R. Ravishankara, "A Study of the Reactions of $O(^1D)$ with Bromocarbons"

II-13 J. B. Burkholder, R. L. Mauldin III, R. Yokelson, and A. R. Ravishankara, "Cl_2O_3: A Kinetic and Spectroscopic Study"

II-14 T. J. Bevilacqua, D. R. Hanson, and C. J. Howard, "Gas Phase Reaction Kinetics of CF_3O_2 and CF_3O"

II-15 J. Chen, T. Zhu, and H. Niki, "Long Path FTIR Study of Atmospheric Reactions Involving CF_3OO and CF_3O Radicals"

II-16 A. J. Pounds, A. J. Hynes, T. McKay, J. D. Bradshaw, and P. H. Wine, "Detailed Mechanistic Studies of the OH-Initiated Oxidation of Dimethylsulfide Under Atmospheric Conditions"

II-17 M. Chin and D. D. Davis, "Stratospheric Photochemistry of OCS and its Possible Contribution to the Stratospheric Background Aerosol"

II-18 G. Chen, G. Sachse, J. Collins, J. Bradshaw, S. Sandholm, G. Gregory, B. Anderson, J. Barrick, and D. D. Davis, "An Examination of the NO_x Photostationary State Based on NASA GTE CITE-3 Data From the Tropical Atlantic"

II-19 R. E. Stickel, M. Chin, C. A. van Dijk, Z. Zhao, and P. H. Wine, "Tunable Diode Laser Studies of Atmospheric Reaction Mechanisms"

II-20 L. Herbert, K. Li, P. Sharkey, I.W.M. Smith, A. Defrance, J. L. Queffelec, C. Rebrion, B. R. Rowe, and I. R. Sims, "Kinetics of Elementary Reactions at Low Temperatures"

II-21 J. Shi, E. W. Kaiser, and L. Rimai, "Time-Resolved Infrared Spectral Photography: Applications in Atmospheric Chemistry"

II-22 H. Berresheim and F. L. Eisele, "Real-Time Detection of Atmospheric DMS, DMSO, and SO_2 Using Selected Ion Chemical Ionization Mass Spectrometry"

II-23 J. J. Schwab and M. Hankin, "The Measurement of H_2O_2 and CH_4 in the Atmosphere Using Fixed-Frequency Infrared Gas Lasers and FM Detection Techniques"

II-24 J. M. Allen and B. C. Faust, "Characterization of the Aqueous-Phase Photochemical Formation of Peroxyl Radicals and Singlet Molecular Oxygen in Cloud Water Samples from Across the United States"

II-25 C. Anastasio, J. M. Allen, and B. C. Faust, "Aqueous-Phase Photochemical Formation of Peroxides in Authentic Cloud Waters"

II-26 S. Padmaja, P. Neta, and R. E. Huie, "One-Electron Oxidation of Inorganic Anions by Inorganic Radicals. Temperature Dependence in Aqueous Acetonitrile Solutions"

II-27 C. J. Shackelford, J. M. Nicovich, K. D. Kreutter, E. P. Daykin, S. Wang, and P. H. Wine, "Chemical Kinetic, Thermochemical, and Spectroscopic Characterization of the $(CH_3)_2S$-Br Adduct"

II-28 J. M. Cronkhite, S. Wang, R. P. Thorn, J. M. Nicovich, and P. H. Wine, "Kinetics of the Reactions of $O(^3P)$ with CF_3NO and $(CF_3NO)_2$"

II-29 A. A. Viggiano, R. A. Morris, J. S. Paschkewitz, and J. F. Paulson, "Kinetics of the Gas Phase Reactions of Cl^- with CH_3Br and CD_3Br: Strong Evidence for Nonstatistical Behavior"

II-30 D. L. Yang, T. Yu, and M. C. Lin, "Kinetics of CN Radical Reactions with Selected Cycloalkanes: CN Reactivity Towards Secondary C-H Bonds"

II-31 M. T. Butterfield, T. Yu, and M. C. Lin, "Kinetics of CN Reactions with C_3H_6, $C_3H_3D_3$, C_3D_6, and C_2H_3CN"

II-32 S.-P. Lee, J. A. Tarr, and M. C. Lin, "REMPI/MS Kinetic Spectrometer: A Test with CH_3 Radical Reactions"

II-33 V. I. Lang and A. T. Pritt, Jr., "Vacuum UV Absorption Spectra of Hydrazine Fuels"

II-34 G. L. Vaghjiani, "Photochemistry of Hydrazine: UV Absorption Cross Sections and Photoproduct Yields Between 200 and 285 nm"

II-35 C. E. Brown, M. A. Blitz, S. A. Decker, and S. A. Mitchell, "Multiphoton Dissociation of Nickelocene for Gas-Phase Kinetic Studies of Nickel Atom Association Reactions"

POSTER SESSION III

III-1 P. W. Seakins and S. R. Leone, "FTIR Studies of Mechanisms of HF Production from H Atom/Radical Reactions"

III-2 I.W.M. Smith, R. P. Tuckett and C. J. Whitham, "Product State Distribution from the Reaction: N + OH → NO + H, and the Influence of Reagent Vibrational Excitation on the Reaction: N + NO(v) → N_2 + O"

III-3 S. Singleton and R. D. Coombe, "Dynamics of the O(^{1}D) + ClNCO Reaction"

III-4 A. J. Navratil and R. D. Coombe, "Radiative and Collisional Relaxation of NCl($a^1\Delta$)"

III-5 R. McDiarmid, "On the Vibrational Substructure of the 195 nm Transition of Acetone"

III-6 R. Gopal, K. N. Uttam, and M. M. Joshi, "Thermal Emission Spectrum of YbCl Molecule"

III-7 X. Zheng and M. C. Heaven, "Ion-Pair to Valence Transitions of Jet-Cooled IBr"

III-8 L. A. Kaledin and M. C. Heaven, "The Low-Lying Electronic States of Uranium Monoxide"

III-9 P. Schafer and J. M. Bowman, "Numerical Truncation/Recoupling Calculations of the High Energy Vibrational Spectrum of Hydrogen Peroxide"

III-10 C. W. Larson, M. E. Fajardo, J. D. Mills, P. W. Langhoff, P. S. Erdman, and W. C. Stwalley, "Visible Absorption Spectroscopy of Dense, High Temperature Lithium Vapor"

III-11 Y. Su, G. N. R. Tripathi, and R. H. Schuler, "Time-Resolved Resonance Raman Study of Isonicotinamide Radicals"

III-12 B. H. Weiller, "Time-Resolved IR Spectroscopy of Transient Organometallics in Liquid Rare Gas Solvents"

III-13 K. I. Barnhard, M. He, and B. R. Weiner, "Fluorescence Lifetimes of the Vinoxy Radical: Evidence for Predissociation"

III-14 M. Erickson, M. Macler, H.-S. Lin, and M. C. Heaven, "Spectroscopy and Fluorescence Decay Dynamics of Matrix Isolated Iodine Monobromide"

III-15 F. Castaño, M. N. Sanchez Rayo, F. Beitia, and D. Husain, "Time-Dependent Study of the Dynamics of the Collision-Induced Intramultiplet Mixing of Ca(4s4p(^3P_J)) by Helium at 750K"

III-16 C.-F. Nien and J. M. C. Plane, "A Comparison Between Oxidation Reactions of the Alkali and Alkaline Earth Atoms"

III-17 R. E. McClean, H. H. Nelson, N. L. Garland, and M. Campbell, "Collisional Quenching of AlO($B^2\Sigma^+$)"

III-18 R. A. Caporusso and M. Cacciatore, "Semiclassical Calculations of V-V and V-T/R Rate Constants in N_2 - N_2"

III-19 J. M. Thomas, G. Stark, and D. H. Katayama, "The Preferential Excitation of the CO($a^3\pi$, v') Product Observed in the N_2 ($A\ ^3\Sigma_u^+$, v') + CO ($X\ ^1\Sigma^+$, v" = 0) Energy Transfer Reaction"

III-20 B. M. Toselli and J. R. Barker, "Isotope Effects in the Vibrational Deactivation of Large Molecules"

III-21 J. Shi and J. R. Barker, "The Kinetics of Ozone Recombination at High O_2 Pressures: The Effects of a Metastable Electronic State"

III-22 E. M. Joslin, H. Yu, and D. Phillips, "Laser Induced Fluorescence of Jet-Cooled 4-Aminobenzonitrile - The Onset of Intramolecular Vibrational Redistribution"

III-23 D. C. Easter and A. P. Baronavski, "Ultrafast Vibrational Relaxation in the Fluorescent State of 4-(Dicyanomethylene)-2-methyl-6(p-dimethylaminostyryl)-4H-pyran"

III-24 R. W. Schwenz, J. V. Gilbert, and R. D. Coombe, "Halogen Amine Chemistry and the Excitation of Iodine Atoms"

III-25 J. B. Koffend, B. H. Weiller, and R. F. Heidner III, "Kinetics of Chemically Pumped NF($b^1\Sigma^+$): Study of the NF($a^1\Delta$) + $I^*(^2P_{1/2})$ ⇔ NF($b^1\Sigma^+$) + $I(^2P_{3/2})$ Equilibrium"

III-26 D. Grantier, K. K. Shen, C. B. Winstead, S. H. Cobb, and J. L. Gole, "Chemically Driven Continous Visible Chemical Laser Amplifiers"

III-27 C. B. Winstead, K. X. He, T. Hammond, D. Grantier, and J. L. Gole, "Laser Induced Plasma Spectroscopy of Silicon and Germanium Based Molecules and Jet Cooled Metal Based Ion-Molecule Complexes"

III-28 H. T. Liou, H. Yang, and P. Dan, "Laser Induced Lasing in the CS_2 Vapor"

III-29 L. M. Tolbert and L. C. Harvey, "Ortho-Allyl Phenols: The Case Against Excited State Proton Transfer"

III-30 H. Suzuki, T. Abe, and N. Koto, "Cyclobutanetetracarboxylic Dianhydride (CBDA) Synthesis by Photodimerization of Maleric Anhydride (MA) and the Practical Usage"

III-31 N. Berenguer, F. Borondo, J. M. Gomez-Llorente, and R. M. Benito, "Simulation of Stimulated Emission Pumping Spectra in LiCN"

III-32 J. Tellinghuisen, C. W. Wilkerson, Jr., and R. A. Keller, "A Study of Bias and Precision in the Estimation of First-Order Decay Rates from Sparse Data"

III-33 Z. Gao, N. Zhang, and F. Kong, "Cluster Ion Formation by Laser Ablation and Photofragmentation"

III-34 X. B. Xie, H. P. Yang, T. J. Cui, Q. Zhuang, and C. H. Zhang, "Nature of the New Emission Resulting from $O_2(a^1\Delta_g)$, Cl_2, and Heated Metal (Cu)"

III-35 V. R. Morris, F. Mohammed, and W. M. Jackson, "Chemical Dynamics Studies Using Time Resolved Infrared Emission Spectroscopy"

Abstract

Recent Developments in Femtochemistry

Ahmed Zewail

Arthur Amos Noyes Laboratory of Chemical Physics

California Institute of Technology

In this talk, we will present some recent developments in the study of elementary chemical reactions on the femtosecond time scale. The focus is on the dynamics of the transition state in reactions involving atom-molecule collisions (A + BC) and photon-molecule half-collisions ($h\upsilon$ + AB). Studies, in real-time, of the nature of bonding in the transition state and the dynamics on the reactive potential will be presented in an effort to compare the status of theory versus experiments.

FREQUENCY AND TIME DOMAIN STUDIES OF ULTRAFAST MOLECULAR PHOTODISSOCIATION

L. D. Ziegler, Department of Chemistry, Boston University

Analysis of the spontaneous resonance Raman emission of molecules in the gas phase is a sensitive probe of subpicosecond photodissociation dynamics with *rovibronic* specificity. A Kramers-Heisenberg based formulism has been developed to extract photodissociation rates corresponding to excited state lifetimes in the regime between a vibrational and a rotational period. This information is determined by excitation profile and polarization analysis of resonance Raman features.

The photodissociation of NH_3 (ND_3) and CH_3 (CD_3) on their lowest lying excited electronic surfaces will be contrasted. Lifetimes in the range from 40 fs to ~1 ps are determined by our approach as a function of vibrational and rotational specificity on these excited state surfaces. The emission of CH_3I due to resonance with the photodissociative A and B states will be compared. Dramatic mode-specific photodissociation rate effects are found for the CH_3I B-state. The resonance scattering of methyl iodide in a supersonic jet has been observed. The jet resonance emission provides evidence for strong orientational effects and new photochemistry pathways in methyl iodide clusters.

A direct time domain approach will be contrasted with frequency domain based techniques. The transient resonant birefringent and dichroism excited and probed with 30 fs pulses will be discussed for I_2 in solution. A B-state predissociation lifetime of 200 fs has been determined by this technique.

Cluster-Induced Photochemistry of CH_3I at 248 nm

Y.B. Fan and D.J. Donaldson

Department of Chemistry and Scarborouph Collage
University of Toronto
80 St. George Street, Toronto, Ontario, Canada M5S 1A1

ABSTRACT

We have carried out a systematic study of the 248 nm excimer-laser photodissociation of small methyl iodide clusters in a free jet expansion. Ground electronic state I_2 is formed from the photolysis of methyl iodide dimers and detected *via* the laser induced fluorescence (LIF) excitation spectrum of its (B-X) transition. The internal energy of the I_2 is approximately 1.7 kJ/mol and is the same for CH_3I seeded in CO_2, Ar, Xe, O_2 and He, as well as for the neat expansion and deuterated sample. A room temperature flow cell experiment shows that the reaction channel $I^* + CH_3I \longrightarrow I_2 + CH_3I$ does not contribute to the measured I_2 signal. The results strongly imply that a cluster-induced *cooperative effect* is responsible for the I_2 - producing chemistry.

Dynamics of Azomethane's Two-Step Photodissociation

B. Kim Andrews, Katherine A. Burton, and R. Bruce Weisman

Department of Chemistry and Rice Quantum Institute
Rice University
Houston, Texas 77251

The photodissociation of gas phase azomethane into methyl radicals and molecular nitrogen (CH_3-N=N-CH_3 $\rightarrow$ CH_3 + N_2 + CH_3) has been explored using a combination of experimental and computational methods. Nanosecond time-resolved CARS spectroscopy permits the detection of both the nitrogen and the methyl radical products. The measured appearance kinetics of these species shows that dissociation occurs through two distinct steps of bond-breaking in which the methyldiazenyl radical (CH_3NN) exists as an intermediate. Under thermalized conditions, the methyldiazenyl radical lives for 5 ns before dissociating into nitrogen and the second methyl radical.

CARS spectra of the photoproducts provide information about their nascent internal energy contents and distributions. Methyl radicals are observed with 0 to 4 quanta of vibrational excitation in the ν_2 out-of-plane deformation mode, and kinetic analysis shows that the first-step methyls carry far more ν_2 energy than the second-step methyls. A rotational temperature is estimated for the vibrationally unexcited second-step methyl radicals. In addition, the nitrogen's nascent vibrational and rotational distributions are deduced. Impulsive and statistical models of energy partitioning are applied to help interpret these data on product energies, and although much information remains unmeasured, it seems that the first step may have substantial impulsive character, whereas the second step may show specific exit channel interactions superimposed on statistical energy partitioning. *Ab initio* CASSCF quantum calculations of the second-step potential surface have also been performed and the results used to help understand the dissociation dynamics.

THEORY OF TRANSIENT EFFECTS IN PHOTODISSOCIATION AND CONTINUUM RAMAN SPECTROSCOPY WITH PULSES

MOSHE SHAPIRO

DEPARTMENT OF CHEMICAL PHYSICS,
THE WEIZMANN INSTITUTE OF SCIENCE,
REHOVOT, 76100 ISRAEL

ABSTRACT

THEORY OF PHOTODISSOCIATION AND RAMAN SCATTERING VIA AN INTERMEDIATE DISSOCIATIVE MANIFOLD UNDER CONDITIONS OF SHORT-PULSE EXCITATION ITdDISCU**q"! I
)qhONTEXT OF RAMAN SCATTERING, WE
SHOW THAT TRANSIENT EFFECTS LEAD TO THE APPEARANCE OF ADDITIONAL TERMS, NOT INCLUDED IN THE KRAMERS-HEISENBERG FORMULA. THE ROLE OF TRUE RAMAN SCATTERING VS. RESONANCE FLUORESCENCE IN CONTRIBUTING TO THE OBSERVED SIGNAL IS ELUCIDATED. A SIMPLE NEW INTERPRETATION OF VIRTUAL STATES WHICH COMES AS A NATURAL CONSEQUENCE OF OUR THEORY WILL BE DESCRIBED.

APPLICATION OF THIS FORMULATION TO THE CALCULATION OF FEMTOSECOND TRANSITION STATE SPECTRUM IN NAI AND RAMAN LINE-INTENSITIES OF DISSOCIATING IBR AND CH3I IS PRESENTED. THE COMPUTATIONS REVEAL THE DEPENDENCE OF THE OBSERVED QUANTITIES ON THE LASER PARAMETERS. THE INTERPLAY BETWEEN RESONANCE FLUORESCENCE AND RAMAN SCATTERING RESULTS IN A COMPLEX DEPENDENCE OF THE RAMAN LINE INTENSITIES ON THE EXCITATION WAVELENGTH. THIS DEPENDENCE IS LARGELY AFFECTED BY THE TOPOLOGICAL IMPRINTS OF THE INITIAL AND FINAL VIBRATIONAL STATES.

THE PRESENT THEORY IS VERIFIED BY OUR RECENT EXPERIMENTS ON IBR IN WHICH THE TOPOLOGY OF HIGH LYING VIBRATIONAL STATES IS CLEARLY IN EVIDENCE. EXCELLENT QUANTITATIVE AGREEMENT BETWEEN OUR PARAMETER-FREE THEORY AND THE EXPERIMENTS IS OBTAINED.

THE CONNECTION BETWEEN THE CONTINUUM RAMAN EXPERIMENTS AND IDEAL ULTRA-SHORT PULSE WAVEPACKET PROPAGATION IS THEN MADE. IT WILL BE ARGUED THAT WAVEPACKET PROPAGATION, FOLLOWING ULTRA-SHORT PULSE EXCITATION, CAN IN PRINCIPLE BE EXTRACTED FROM CW CONTINUUM RAMAN SCATTERING.

Hydrogen Abstraction in Molecular Cluster of Benzophenone with Hydrogen Donors

Kinichi Obi

Department of Chemistry, Tokyo Institute of Technology, Ohokayama, Meguroku, Tokyo 152, Japan

Photochemical reactions in neutral molecular clusters of benzophenone with hydrogen donors formed in the supersonic free jet have been investigated. The hydrogen donors studied were ethanol, 2–propanol, 1,4–cyclohexadiene and triethylamine. One–color three–photon ionization spectra of benzophenone clusters are broad and diffuse, though bare benzophenone shows sharp band structures of the totally symmetric torsional mode. The broadening of the spectra in benzophenone–hydrogen donor mixed expansion indicates the generation of molecular clusters; a broad spectral feature would result from the spectral congestion due to low–frequency intermolecular modes of the van der Walls vibration. Phosphorescence of the benzophenone clusters were measured by the excitation in the 0–0 band region. 1,4–Cyclohexadiene and triethylamine quench the phosphorescence, but ethanol and 2–propanol do not alter the phosphorescence intensity.

The emission of produced benzophenone ketyl radical (BPK) was measured. The clusters were excited with pulses from a XeCl or dye laser, and BPK generated was subsequently excited with visible light from a dye laser. The formation of BPK was observed only in the benzophenone–1,4–cyclohexadiene clusters. BPK was also formed with one–color irradiation at 308 nm, which showed a square laser power dependency. This suggests that BPK formed with the first photon absorbs the second photon within the same laser pulse. The fluorescence and its excitation spectra of BPK in the jet are very similar to those in the condensed phase. The action spectrum for BPK formation was almost the same with MPI spectrum. The fast formation time of BPK and good agreement between the action and MPI spectra indicate that BPK is formed by the intracluster reaction after photoexcitation of benzophenone. The reactivity of hydrogen donors will be discussed.

Fine-structure branching ratios and Doppler profiles of $Cl(^2P_j)$ photofragments from photodissociation of chlorine molecule near and in the ultraviolet region

Yutaka Matsumi, Kenichi Tonokura, and Masahiro Kawasaki
Research Institute of Applied Electricity,
Hokkaido University, N12W6, Sapporo 060, Japan

Abstract

Photofragment chlorine atoms in the ^2P_j states from Cl_2 at 266 - 500 nm are measured by a resonant-enhanced multiphoton ionization technique. The branching ratios of $[Cl^*(^2P_{1/2})]/[Cl(^2P_{3/2})]$ increase monotonically with dissociation wavelengths from $(3.8 \pm 0.7) \times 10^{-3}$ at 308 nm to $(1.87 \pm 0.19) \times 10^{-1}$ at 475 nm. At 375 nm $\leq \lambda \leq$ 475 nm, the Doppler profiles of chlorine atoms indicate adiabatic formation of two $Cl(^2P_{3/2})$ from the $^1\Pi(1_u)$ state and $Cl(^2P_{3/2}) + Cl^*(^2P_{1/2})$ from the $B^3\Pi(0_u^+)$. On the other hand, at short wavelength (308 nm), $Cl^*(^2P_{1/2})$ is generated from the $^1\Pi(1_u)$ state through nonadiabatic transitions during the dissociation. The relative contribution of the $^1\Pi(1_u) \leftarrow X^1\Sigma_g^+)$ and $B^3\Pi(0_u^+) \leftarrow X^1\Sigma(0_g^+)$ transitions in the photoabsorption is estimated from the obtained branching ratios at 375 nm $\leq \lambda \leq$ 475 nm.

State-to-state photodissociation of H_2O and HOD in the first absorption band

S. Rosenwaks, T. Arusi-Parpar, Y. Cohen, D. David, A. Strugano and I. Bar

Department of Physics, Ben-Gurion University of the Negev, Beer-Sheva 84105, Israel

James J. Valentini

Department of Chemistry, Columbia University, New York, NY 10027

The photodissociation of H_2O and HOD at the leading edge of the first absorption band is studied from particular rotational states of vibrationally excited H_2O and HOD. Stimulated Raman excitation and coherent anti-Stokes Raman scattering prepare and detect, respectively, H_2O molecules excited with *one* quantum of vibration in the symmetric stretch mode, H_2O (1,0,0), and HOD molecules with one quantum of vibrational excitation in the O-H, HOD (0,0,1), or O-D, HOD (1,0,0), stretch vibration. This selective vibrational excitation prepares densities of the excited molecules in particular rotational levels that are sufficient for state-to-state molecular dynamics studies. The subsequent photodissociation at 193 nm favors product formation from these particular vibrational states for H_2O (1,0,0) and HOD (0,0,1), but not from HOD (1,0,0). The H_2O and HOD molecules dissociate to produce OH + H and OH + D or OD + H fragments, respectively. The OH and OD photoproducts are detected state specifically via laser induced fluorescence. The photodissociation of HOD (0,0,1) selectively leads to OD + H yield of 2.5 ± 0.5 times greater than that of OH + D, while the photodissociation of HOD (1,0,0) does not enhance the yield of any of the fragments. The analysis of the OH product in different rotational, Λ-doublet and spin states formed as a result of the photodissociation of H_2O (1,0,0) for several initial rotational states is currently in progress. Our results show that even this low level of excitation can effect mode specific bond fission. Also, these results agree with theoretical calculations indicating that the yield of the fragments depend on the Franck-Condon overlap of the ground state vibrational wavefunction with the continuum wave function on the repulsive surface of the upper state.

Photodissociation Dynamics of NO_3 and ClO_2

H. Floyd Davis, Bongsoo Kim[1], Harold S. Johnston[1], and Yuan T. Lee
Materials and Chemical Sciences Division,
Lawrence Berkeley Laboratory and Department of Chemistry,
University of California, Berkeley CA 94720

The photochemical decomposition of NO_3 and ClO_2 in the atmosphere is of potential importance in the balance of global ozone. Despite this, there has been considerable uncertainty regarding the excited state dynamics of these molecules. For each radical, two chemically distinct photodissociation pathways are possible:

$$NO_3 \rightarrow NO_2(X^2A_1) + O(^3P) \quad (1)$$

$$\rightarrow NO(^2\Pi) + O_2(^3\Sigma^-_g, ^1\Delta_g) \quad (2)$$

$$OClO \rightarrow ClO(^2\Pi) + O(^3P) \quad (3)$$

$$\rightarrow Cl(^2P) + O_2(^3\Sigma^-_g, ^1\Delta_g) \quad (4)$$

We have studied the dynamics of these processes using photofragment translational energy spectroscopy with a tunable excitation laser. We have clearly observed both fragment partners in each of processes (1)-(4) above.

In the case of NO_3, the translational energy distributions and wavelength dependence for channel (1) leads us to a revised O-NO_2 bond energy and $\Delta H_f°(NO_3)$. Whereas the NO_3 visible absorption spectrum is broad and poorly understood, the ClO_2 ($A^2A_2 \leftarrow X^2B_1$) absorption spectrum possesses a well defined progression primarily resulting from excitation to the (ν_1,0,0),(ν_1,1,0),(ν_1,0,2), and (ν_1,1,2) levels of the excited electronic state. We have measured the ClO fragment vibrational state populations from dissociation of ClO_2 prepared in a range of these well defined levels. We find that the ClO vibratitonal state distributions are strongly dependent on the initial vibrational state of the parent molecule.

Channels (2) and (4) lead to a net loss of atmospheric ozone and are particularly interesting since they result from concerted unimolecular decomposition with a large release of product translational energy. For both molecules, the quantum yields for O_2 production were found to be strongly wavelength dependent. The structure in the product time-of-flight spectra not only provides information about the electronic states of the O_2 molecule, but in several favorable cases, information on its vibrational states as well.

Our results on NO_3 solve most unanswered questions arising from the earlier work of Magnotta and Johnston. We believe that the present work on ClO_2 photodissociation resolves some of the recent controversy regarding its primary photochemistry and will hopefully stimulate further theoretical work on its excited state potential energy surfaces.

[1] Collaborators on NO_3 Project

Characterization of Acetic Acid Photochemical Dynamics: Isotopic Substitution Effects

Dean R. Peterman, Robert G. Daniel, and Joyce A. Guest
Department of Chemistry
University of Cincinnati
Cincinnati, OH 45221-0172

We are continuing our studies of the photochemical α-cleavage pathways and dynamics of carbonyl compounds. The photolysis of deuterated acetic acid has been examined to elucidate details of the dissociation dynamics by comparison to previous studies of non-deuterated acetic acid [1]. Nascent OD photofragment distributions have been measured. The change in the center-of-mass of OD compared to OH allows us to evaluate whether fragment rotation originates from an impulse along the C-O bond axis or from in-plane and out-of-plane bending vibrations in the parent.

Results for the OD photofragment from 218-nm dissociation of CH_3COOD show that the mean rotational energy increases by less than 15% compared to OH from CH_3COOH. An impulsive dissociation model for acetic acid predicts that the OD fragment rotational energy content should be twice that of OH.

OD photofragment translational energy distributions provide intruiging information related to the parent dissociation dynamics. Specifically, the breadth of the OD distributions varies significantly with N". These observations can be explained by proposing that the lowest N" fragments acquire their rotational angular momentum from parent bending vibrations, while the higher N" fragments acquire much of their rotational angular momentum from the impulse imparted to the OD upon bond fission. Further interpretation of these observations will be presented.

---

1. S. S. Hunnicutt, L. D. Waits, and J. A. Guest, *J. Phys. Chem.*, 95, 562 (1991); 93, 5188 (1989).

Site-Specific Photochemistry

Jeffrey L. Brum, Subhash Deshmukh, and Brent Koplitz
Department of Chemistry
Tulane University
New Orleans, Louisiana 70118

ABSTRACT

We present results on "site-specific" H-atom production in photolysis experiments conducted under collisionless conditions. H and D atoms are used as labels to investigate the site(s) at which C-H (or C-D) bond cleavage occurs in a variety of haloalkane systems. The site(s) (e.g. α, β, or γ) where C-H (or C-D) bond cleavage occurs is dependent not only the nature of the molecule, but also on the photolysis wavelength. H and D atoms are useful as labels to investigate photolysis involving competition between chemically distinct reactive sites. For example, results on selectively deuterated *n*-iodopropanes: $ICD_2CH_2CH_3$, $ICH_2CD_2CH_3$, and $ICH_2CH_2CD_3$ demonstrate a clear preference for C-H (or C-D) bond cleavage at the β position when using 248 nm radiation. In contrast, experiments involving 2-iodopropane show enhancement of C-H bond cleavage at the α, not the β site, when compared with data obtained using 193 nm radiation. Power dependence studies and experiments using two photolysis lasers clearly indicate that photon absorption by an intermediate, presumably an alkyl radical, is important in many of the systems studied. As a diagnostic tool, H- and D-atom Doppler spectroscopy allows us to gain insight into the energetics associated with the various dissociation processes. Our overall aim is to gain a further understanding of the photolysis properties of a variety of molecules and their associated radicals.

Photodissociation of $BrCH_2CH_2OH$ and ICH_2CH_2OH: Formation and Characterization of OH ($X\ ^2\Pi$).

Steven P. Sapers[a] and Wayne P. Hess
Pacific Northwest Laboratory[b]
P.O. Box 999
Richland, WA 99352

ABSTRACT

This work studies the dissociation of $BrCH_2CH_2OH$ and ICH_2CH_2OH following laser excitation to the electronic $\tilde{A}$ state. The direct subpicosecond dissociation cleaves the C—X bond to produce CH_2CH_2OH and the halogen atom in either the ground ($^2P_{3/2}$) or excited ($^2P_{1/2}$) state. The initial dissociation produces excited CH_2CH_2OH in a distribution of internal states, some of which have sufficient energy to undergo secondary, *non-photoinduced* dissociation to form OH and C_2H_4. We probe the OH translational and rotational product states following this secondary dissociation using laser-induced-fluorescence in both flow cell and pulsed jet apparatus. 202 nm excitation of $BrCH_2CH_2OH$ produces OH with no vibrational excitation and a non-Boltzmann rotational distribution with an average rotational energy of 8 kJ/mole. Doppler analysis of the rotational lineshape shows that on average 39% of the energy available for the secondary dissociation is partitioned into relative translation of OH and C_2H_4. 266 nm excitation of ICH_2CH_2OH also produces OH but at much lower quantum yields due to energetic constraints. We find that the CH_2CH_2OH radical also absorbs at 266 nm to produce OH. The rotational and translational energy distribution of OH from secondary dissociation of CH_2CH_2OH radical is qualitatively described by a simple rotational model.

a) NORCUS Postdoctoral Research Associate.
b) Pacific Northwest Laboratory is operated for the U.S. Department of energy by Battelle Memorial Institute under contract DE-AC06-76RLO 1830.

STATE-TO-STATE VIBRATIONAL PREDISSOCIATION OF H_2-HF AND D_2-HF: A DIRECT COMPARISON BETWEEN THEORY AND EXPERIMENT

E.J. Bohac and R.E. Miller
Department of Chemistry
University of North Carolina
Chapel Hill, N.C. 27599.

The vibrational predissociation of weakly bound complexes is of fundamental importance in photochemistry since it promises us the opportunity of making quantitative comparisons between experiment and theory. For atom-diatom systems there has already been considerable progress in this direction [1,2]. Unfortunately, there is a wide range of dynamical processes which cannot be studied in these simple systems, for example, the transfer of vibrational energy from one molecule in the complex to another. The study of this intermolecular V-V process clearly requires at least the complexity of a diatom-diatom system. From both the theoretical and experimental points of view, systems with large rotational constants are desirable in order to minimize the number of open channels. The H_2-HF and D_2-HF systems are excellent choices from this point of view. They have been studied using high resolution infrared spectroscopy [3-5] and ab initio methods [6], so that reasonably good intermolecular potentials are thought to exist for these systems. Very recently Clary [7] has reported close-coupling calculations of the final state distributions of D_2-HF, based upon an ab-initio potential surface. The stage has therefore been set for making direct comparisons between this fully ab-initio calculation and state-to-state experiments.

We will report on recent experiments, based upon the use of the opto-thermal detection method, designed to measure these state-to-state probabilities for both H_2-HF and D_2-HF. The method involves measurement of the photofragment angular distributions resulting from vibrational predissociation of these complexes. The low density of fragment rotational channels allows us to resolve structure in the angular distribution which can be related to the final rotational state distribution, including the scalar intermolecular rotational correlations. The dependence of these angular distributions upon the laser polarization direction is also used to determine the μ-v vector correlation. The results of these experiments are compared directly with the theoretical calculations of Clary [7].

REFERENCES:

1. J.I. Cline, N. Sivakumar, D. Evard, C.R. Bieler, B.P. Reid, N. Halberstadt, S.R. Hair and K.C. Janda, J.Chem.Phys., 90, 2605, (1989).
2. J.I. Cline, B.P. Reid, D.D. Evard, N. Sivakumar, N. Halberstadt and K.C. Janda, J.Chem.Phys., 89, 3535, (1988).
3. C.M. Lovejoy, D.D. Nelson,Jr. and D.J. Nesbitt, J.Chem.Phys., 89, 7180, (1988).
4. C.M. Lovejoy, D.D. Nelson,Jr. and D.J. Nesbitt, J.Chem.Phys., 87, 5621, (1987).
5. K.W. Jucks and R.E. Miller, J.Chem.Phys., 87, 5629, (1987).
6. D.C. Clary and P.J. Knowles, J.Chem.Phys., 93, 6334, (1990).
7. D.C. Clary, J. Chem. Phys., in press.

State to State Vibrational Photodissociation of van der Waals Molecules

Y. Rudich and R. Naaman
Department of Chemical Physics
Weizmann Institute, Rehovot, Israel

High resolution infrared spectroscopy of van der Waals (vdW) molecules is an important tool in understanding their structure and the interaction potential energy surfaces (PES) near the equilibrium configuration. To gain comprehensive knowledge about vdW molecules, dynamical properties such as predissociation lifetimes and state distributions after dissociation are required. However, rotational energy distribution following IR vibrational excitation, has been studied for only a few systems.

An IR pump-resonance enhanced multiphoton ionization probe experiments allow the investigation of the energy distribution in molecules following vibrational predissociation of van der Waals complexes in their electronic ground state.

In our setup, the infrared photons are generated by frequency substraction of 1.06 μm from the output of a Nd:Yag pumped dye laser in a $LiNbO_3$ crystal. The probe laser is another Nd:Yag pumped dye laser. By continuously varying the delay between the pump and probe lasers, the lifetime of the vibrationally excited complex can be probed.

Among and the systems investigated was the C_2H_2-HCl complex. The symmetric CH stretch of acetylene is excited to v=1 by IR absorption at ~3270 cm^{-1}. The signal of the emerging HCl(v=1,J) was monitored as function of the delay between the pump and probe lasers. The intensity of the signal showed no variation for delays at the range of 10-100ns. This indicates that the lifetime of the vibrationally excited complex is shorter than the experimental resolution of 10 ns. The rotational energy distribution in HCl(v=1) was probed at a delay of 20 ns and averaged over 500 laser shots for each rotational level. Only rotational states between J=0 to J=3 were populated and no signal could be detected at J=4. The distribution was fitted to a Boltzman distribution with a temperature of 53±5 K. This is indicative of the slow dissociation process. From this rotational distribution the calculated new upper limit for the dissociation energy of the complex is $\leq$260 cm^{-1}. Since J=3 is populated, but no population is observed at J=4, the dissociation energy must be between $260>D_0>170$ cm^{-1}. This is lower than the 350cm^{-1} which has been calculated using atomic charges.

By monitoring a single J state in the product as function of the infrared laser wavelength, the absorption spectrum of the complex can be obtained over a very broad wavelength region.

MODEL STUDIES ON LASER CONTROL OF BOND FISSIONS AND ISOMERIZATIONS FOR ORGANIC AND ORGANOMETALLIC MOLECULES

J. Manz

Institute fur Physikalische Chemie
Universität Würzburg
8700 Würzburg, Marcusstrasse 9/11, Germany

Selective fissions of metal-ligand bonds may be achieved by cw IR + UV photodissociation. Selective isomerizations may be induced by series of ps IR laser pulses. The photodissociation and reaction dynamics are simulated by time dependent wavepackets representing model compounds such as Ni-C_2H_4, $HCo(CO)_4$, $(C_6H_6)Cr(C_6D_6)$, $(C_6H_6)RuCOH_2$, and semibullvalenes. Detailed analyses yield various dynamical effects e.g. asynchronous breaking of competing bonds, and laser driven photochromy.

The results have been obtained by international cooperation including Ch. Daniel (Strasbourg), G. K. Paramonov (Minsk) as well as J. E. Combariza, S. Görtler, B. Just., E. Kolba, F. Seyl, B. Warmuth (Würzburg).

PHOTOCHEMISTRY AND SPECTROSCOPY OF METAL ION-MOLECULE COMPLEXES

Michael A. Duncan

Department of Chemistry
University of Georgia
Athens, Georgia 30602

Metal ion complexes with small molecules (Mg^+-CO_2, Ag^+-benzene, etc.) are produced in a pulsed nozzle laser vaporization cluster source. These cluster complexes are studied with photodissociation spectroscopy in a specially designed reflectron time-of-flight mass spectrometer system. Mass-selected complexes are excited electronically to study decomposition dynamics and their energy dependence.

In metal-benzene ions, the primary process observed is dissociative charge transfer, e.g.,

$$Ag^+\text{-benzene} + h\nu \rightarrow Ag + \text{benzene}^+$$

The energy dependence of this fragmentation channel can be used to determine an upper limit on the metal ion-benzene binding energy. Threshold spectra have been obtained for benzene complexes with silver, iron and magnesium ions.

Magnesium complexes with a variety of small molecules are probed through excitation near the $^2S \rightarrow {}^2P$ atomic transition (280 nm in the isolated ion). Photoinduced excited state reactions are observed for Mg^+-$(CO_2)_X$, Mg^+-$(H_2O)_X$, and Mg^+-$(CH_3OH)_X$ complexes. For example,

$$Mg^+\text{-}CO_2 + h\nu \rightarrow MgO^+ + CO$$

Vibrationally resolved excitation spectra probe the structure of these ions, and studies of increasingly larger complexes investigate the role of solvation on the photochemistry.

High-Resolution Spectroscopy of Free Radicals and its Applications to Photochemical Reactions

Eizi Hirota

The Graduate University for Advanced Studies
4259 Nagatsuta, Midori, Yokohama 227, Japan
and
The Institute for Molecular Science
Okazaki 444, Japan

Recent high-resolution infrared spectroscopic studies on transient molecules will be reviewed, paying special attention to their applications to photochemistry. The following molecules will be discussed in some detail.

(1) XY_3 type molecules

One of the most fundamental examples belonging to this class is the methyl radical. Two of the three infrared-active fundamental bands have been recorded and are readily used to monitor this important species in photochemical reaction systems. One recent example of the applications, $CH_4 + O(^1D) \rightarrow CH_3 + OH$, will be presented. The second species, the silyl radical SiH_3, is of considerable importance in practical applications, namely it has been shown that this species plays the most important role in silane discharge plasma employed to fabricate amorphous silicon. Recent developments will be given. The third example of transient species is BH_3, for which the first high-resolution spectroscopic study was reported in 1987. Kawaguchi has recently made an additional, substantial contribution to the spectroscopic study of this species, *i.e.* he succeeded in observing and analyzing its ν_3 band by using a Fourier transform spectrometer. The last example NO_3 will be discussed together with a linear free radical CCH, separately.

(2) Vibronic interaction in NO_3 and CCH

The NO_3 molecule in the ground vibronic state $\tilde{X}^2A_2'$ has been established to be completely planar. However, a number of anomalies were noticed in the excited state of a degenerate vibrational mode of e' symmetry. An explanation based upon a vibronic interaction with excited electronic states of E' symmetry has been proposed to explain these anomalies. A similar approach is applied to the CCH radical to account for a "negative" anharmonicity of the bending mode in the ground electronic state.

(3) Hydrocarbon radicals C_nH_2 with n = 2, 3, and 5

Thaddeus' group has recently published an epoch-making result; they succeeded in detecting a new carbene H_2CCC (n = 2) together with H_2CCCC by microwave spectroscopy. The former is an isomer of cyclopropenylidene and the latter of diacetylene; they are 0.63 and 1.9 eV, respectively, higher in energy than their parents. Both of them have been detected in interstellar media, and there would be no doubt about that they play some important roles also in the field of photochemistry. Curl and his coworkers have recently succeeded in detecting another interesting radical, the propargyl radical H_2CCCH (n = 3), by means of infrared diode laser kinetic spectroscopy, namely they generated this species by the photolysis of propargyl halides. We have recently identified another transient radical of n = 5, namely the allyl radical H_2CCHCH_2. We generated it mainly by the photolysis of 1,5-hexadiene. The details will be presented at the meeting.

XXth Informal Photochemistry Meeting
April 26- May 1, 1992
Atlanta, GA

ABSTRACT

Ab initio **spectroscopy of HCO(X,J=1 → J=0) and HCN(X,J=0),** Bela Gazdy and Joel M. Bowman, Department of Chemistry, Emory University, Atlanta, GA 30322.

We report "exact" energies and wavefunctions of all bound and numerous quasibound states of HCO in the ground and first excited rotational states. The potential used is the Bowman-Bittman-Harding surface, with small adjustments to improve agreement with available experimental results. Multichannel "golden-rule" calculations of the partial widths of quasibound states are also reported and compared to exact scattering calculations of Cho and Wagner for J=0.

The energies and wavefunctions of many highly excited vibrational states of non-rotating HCN are calculated "exactly" and compared with experiment. Several potential surfaces are considered in these comparisons.

Supported in part by the National Science Foundation.

TIME-RESOLVED RAMAN SPECTRA AND REACTION DYNAMICS OF SOLVATED RADICALS

G.N.R. Tripathi
Radiation Laboratory
University of Notre Dame
Notre Dame, IN 46556

The state-of-the-art Raman methodology, as applied to examine the structure and reactions of short-lived radical intermediates in solution, will be discussed by reference to some selected studies of recent completion. It has been possible to obtain, by this method, structural information on a number of radicals in solution which, for various reasons, do not exhibit well resolved vibronic features in their electronic spectra in the gas phase or in low temperature matrices. A typical example is the O_3^- radical in which the broad absorption in the 430 nm region corresponds to a dissociative excited state. Pronounced effects of hydration have been observed in the Raman spectra of aqueous O_3^-. The harmonic frequency (ω_e) of the O_3^- symmetric stretch in aqueous solution is 30-40 cm^{-1} higher and the anharmonicity constant ($\omega_e x_e$) is almost twice as large as compared to the O_3^- in crystalline matrices. The intensity patterns in the Raman spectra excited in resonance with different electronic transitions of the radicals provide an understanding of the nature of the excited states. In this context, a Raman study of the p-benzosemiquinone radical anion will be briefly discussed. The relationship between the radical structure and chemical properties, such as redox potential, electron transfer and bimolecular reaction rates and reaction sites will be illustrated by the example of oxygen and sulfur containing aromatic radicals. We have observed an electron transfer component in the hydroxyl radical reactions with aromatic molecules which gives a new insight into the reaction mechanism of this radical.

EXPERIMENTS ON THE QUARTET STATES OF NITRIC OXIDE

G. W. Faris, M. J. Dyer, P. C. Cosby, D. L. Huestis, and T. G. Slanger
Molecular Physics Laboratory
SRI International
Menlo Park, CA 94025

ABSTRACT

We report the first demonstration of photoexcitation of the NO($b^4\Sigma^-$) state directly from the ground state. Tuneable Raman-shifted laser radiation at 192-207 nm was used to excite the v = 2-5 levels of the NO(b) state, with emission being monitored on the $b^4\Sigma^-$-$a^4\Pi$ Ogawa bands at 780-960 nm. The oscillator strength for the NO(b-X) transition is about 10^{-3} that of the allowed NO B-X transition, and laser intensities of 10-30 μJ are adequate for NO(b) excitation. The b-X system is spectrally quite complex, and we find that in order to accurately simulate the spectrum, careful account must be taken of the various spin-orbit interactions between the b and X states and other doublet and quartet manifolds. The relative positioning of the NO doublet and quartet states can now be specified to ±0.1 cm^{-1}, an improvement of more than an order of magnitude. The radiative lifetime of the excited levels lies in the 5-7 μs range, somewhat shorter than predicted by theory, and self-quenching by reaction or state-change occurs at every gas kinetic collision. Energy transfer between NO states is rapid, and we find that it is simple to observe NO(b-a) quartet emission after initially exciting the NO doublet states - $A^2\Sigma^+$, $B^2\Pi$, $C^2\Pi$. Since virtually all NO(b) radiatively cascades to the $a^4\Pi$ state, the present technique is a means of directly populating the lower quartet, principally in levels v = 1,2.

Spectroscopy of Radicals and Their Complexes

Terry A. Miller
Ohio Eminent Scholar
Professor of Chemistry
The Ohio State University

Complexes involving closed-shell species have been well studied in recent years and can generally be described as being held together by weak van der Waals interactions. By contrast, the pairing of two open-shell radical species is the classical recipe for the formation of a strong chemical bond. It is clearly of interest to probe the interactions in closed shell radical (both charged and uncharged) complexes. Such complexes are clearly important in the reactions of open shell radical species. We have used high resolution laser induced fluorescence to probe such complexes in a free jet environment. Complexes observed have included both small and large as well as metallic radicals. Similarly, considerable variation in the closed shell partners from inert gases to metals have been investigated. Selected examples of such systems will be discussed.

Electronic Spectroscopy and Predissociation Dynamics of OH/D-Kr.

Michael C. Heaven, Suli Fei, Xiaonan Zheng, and Udo Schnupf.
Department of Chemistry, Emory University, Atlanta, GA 30322.

OH/D-Kr complexes were generated in expansions driven by Ne/Kr mixtures. Bands belonging to the complexes were seen in the vicinity of the OH/D *A-X* 0-0 and 1-0 transitions. Despite the congestion caused by presence of several Kr isotopes, sixteen bands were rotationally resolved and analyzed. For the ground state, the zero-point rotational constant defined a Kr to OH center of mass distance of 3.8 Å. The relatively small effect of H/D isotopic substitution on the ground state rotational constant was consistent with a linear hydrogen-bonded equilibrium geometry. Attempts to obtain a potential energy surface for the OH/D-Kr *A* state are in progress. Preliminary fits indicate a surface much like that obtained for OH-Ar, with a well-depth of approximately 2000 cm^{-1}.

Vibrational predissociation of OH/D(v=1)-Kr causes measurable line broadening in several bands. We are in the process of determining the linewidths, in order to quantify the predissociation rates. However, it is already evident that the linewidths do not show a simple dependence on internal energy, indicating the presence of novel dynamical effects. The results for OH/D-Kr will be compared and contrasted with those for OH/D-Ne and OH/D-Ar.

The 2+1 REMPI Spectrum of $SiCl_3$

Karl K. Irikura, Russell D. Johnson III, and Jeffrey W. Hudgens

Chemical Kinetics and Thermodynamics Division,

National Institute of Standards and Technology, Gaithersburg, Maryland 20899

Abstract. Between 330 and 400 nm the 2+1 REMPI spectrum of $SiCl_3$ exhibits two overlapping vibrational progressions composed of >30 members and one vibrational progression composed of 5 members. These band systems, labeled $\tilde{F}$, $\tilde{G}$, and $\tilde{H}$, are tentatively assigned to three distinct Rydberg states that reside between 50100 and 59600 cm^{-1}. The vibrational progressions have an average spacing of ω_2 = 262 cm^{-1} and are assigned to the ν_2 umbrella modes of the Rydberg states. Electronic origins are not observed. *Ab initio* calculations on $SiCl_3$ and $SiCl_3^+$ yield geometries and harmonic vibrational frequencies consistent with the spectroscopic assignments and provide the adiabatic ionization potential, IP_a = 7.93 ± 0.05 eV. In combination with a recent experimental value for $\Delta H_f(SiCl_3^+)$, this leads to $\Delta H_f(SiCl_3)$ = -353 ± 12 kJ/mol.

Spectroscopic and kinetic studies of the upper spin-orbit components of widely split $^3\Sigma^-$ and $^2\Pi$ ground states of diatomic radicals

K. D. Setzer, O. Shestakov and E. H. Fink
Fachbereich 9 - Physikalische Chemie, Universität Wuppertal
D-5600 Wuppertal, F.R.G.

Emission spectra of transitions between the upper and lower fine structure components of widely split $^3\Sigma^-$ or $^2\Pi$ ground states have been observed in the near-infrared region for 17 diatomic radicals (TeX, BiX, BiY, PbX; X=H(D),F,Cl,Br,I; Y=O,S,Se). The $X_2 1^{\pm}$ or $X_2 {}^2\Pi_{3/2}$ states are excited by chemical reactions or selective E->E or V->E energy transfer processes from metastable $O_2(a^1\Delta_g)$, $NF(a^1\Delta)$ or $H_2(v=1)$ molecules in fast-flow systems. Analysis of high-resolution Fourier-transform spectra of some of the transitions has yielded accurate molecular constants for the ground states including some hyperfine coupling constants.
Time resolved emission of the X_2 -> X_1 transitions is studied following excitation of the X_2 states by excimer laser photolysis of suitable parent compounds or by pulsed dye laser excitation via the X_1 -> A transitions in the visible region. The radiative and collisional processes connecting the $A^2\Sigma^+$, $X_2 {}^2\Pi_{3/2}$ and $X_1 {}^2\Pi_{1/2}$ states of PbF have been studied in detail. Following dye laser excitation of the A,v'=0,1 states, time and wavelength resolved emission of the A -> X_1, A -> X_2 and X_2 -> X_1 transitions has been measured. The radiative lifetime of the A,v=0 state is found to be 5.0±0.2 μs, and the ratio of the transition probabilities A_{u1} for the A -> X_2 and A -> X_1 transitions is 0.08±0.01. Quenching of the A state is found to proceed to the X_2 state for most collision partners, with rate constants ranging from $\leq 10^{-14}$ to $\geq 10^{-10}$ cm^3s^{-1}. The radiative lifetime of the X_2 state is 300±30 μs, and the state is fairly stable towards collisional quenching ($k_q \leq 10^{-14}$ cm^3s^{-1}). Efficient near-resonant E->E and E->V energy transfer is observed in collisions of $PbF(X_2)$ with O_2 and H_2.

20th Informal Conference on Photochemistry
Atlanta, Georgia, April 26-May 1, 1992

THE DYNAMICS OF PHOTODISSOCIATION AND PHOTOREACTION IN THE ADSORBED STATE

John C. Polanyi
University of Toronto, Toronto, Canada

The new field of photochemistry in the adsorbed state has the attraction (a) that one can catalyse photodissociation (particularly through charge-transfer from the substrate), altering its probability, wavelength and molecular dynamics, and (b) that one can catalyse photoreaction by the (in theory) simple expedient of aiming adsorbed reagents at one another. The field of 'surface aligned photoreaction' is the youngest of all the endeavours in this broad area. This talk will review the evidence for photoinduced reaction between co-adsorbed species and for alignment in the adsorbate, and will argue that the infant field shows promise for the future.

COMPETITION BETWEEN ADSORBATE DISSOCIATION AND DESORPTION ON LASER-HEATED SURFACES: A STOCHASTIC TRAJECTORY STUDY+

R. V. Weaver, Y. Zeiri**, and T. Uzer**

+ Supported by the National Science Foundation

* School of Physics, Georgia Institute of Technology, Atlanta, Georgia 30332-0430, USA

** Department of Chemistry, University of Toronto, Toronto, Ontario M5S 1A7, Canada. Permanent Address: Department of Physics, Nuclear Research Center-Negev, P.O. Box 9001, Beersheva, Israel

There is increasing theoretical and experimental interest in energy flow pathways in the adsorbate/substrate system. A number of recent experiments imply that different modes of such systems relax differently, and that depending on the complexity of the adsorbate, intramolecular decay processes can compete effectively with energy flow to the substrate's vibrational and electronic degrees of freedom[1].

As part of our research into pathways and time scales of energy flow processes on surfaces, we present a theoretical study of the consequences of rapid laser heating on an adsorbate containing weak and strong bonds. Our theoretical model is in the spirit of the desorption/dissociation experiments on peptides adsorbed on glass surfaces[2]. Among the numerous interesting results of these experiments are nonstatistical processes where depending on the heating rate the stronger bonds in the adsorbate break before the weaker ones. We model these processes by means of a Stochastic Trajectory approach which folds the vibrations of the surface into a one-dimensional chain using the Generalized Langevin Equation[3]. Results will be shown for model polyatomics of different lengths and configurations as well as different heating rates. We vary the positions of the weak bonds inside the molecule, and investigate the consequences of parallel versus perpendicular adsorption geometry. The branching ratio between desorption and dissociation is found to depend sensitively on a number of these variables.

1. E. g., A. L. Harris and N. J. Levinos, J. Chem. Phys. 90, 3878 (1990).

2. J. H. Hahn, R. Zenobi, and R. N. Zare, J. Phys. Chem. 189, 2842 (1987); F. Engelke, J. H. Hahn, W. Henke, and R. N. Zare, Anal. Chem. 59, 909 (1987).

3. M. Shugard, J. C. Tully, and A. Nitzan, J. Chem. Phys. 66, 2534 (1977); J. C. Tully, Acc. Chem. Res. 14, 188 (1981).

SURFACE ALIGNED PHOTOCHEMISTRY: A THEORETICAL STUDY OF THE HX/LiF(100) SYSTEM (X=Cl, Br and I)

V. Barclay, D. Jack, J. C. Polanyi and Y. Zeiri
Department of Chemistry, University of Toronto, 80 St. George St., Toronto, Ontario M5S 1A1

There is currently considerable experimental and theoretical interest in the photochemistry of actinic molecules adsorbed on solid surfaces. Of particular interest is the photodissociation (PDIS) and subsequent photo-reaction (PRXN) of co-adsorbed species. We report here the results of an investigation of these topics for the HX/LiF(001) system. Molecular dynamics as well as quantum wavepacket techniques have been used to examine the influence of adsorbate structure, coverage, and chemical nature on the angular and energy distributions of the PDIS and PRXN products. For PRXN emphasis is placed on the branching ratios of the various reaction pathways, *i.e.* the relative cross section of abstraction, exchange, and inelastic scattering events. These results are then compared with the experimental values.

Translational and Internal Energy Distributions of CO Photochemically Desorbed from Oxidized Ni(111)

P. L. Houston, M. Asscher, F. M. Zimmenrmann,
L. L. Springsteen, and W. Ho

Department of Chemistry
and
Materials Science Center
Cornell University
Ithaca, NY 14853-1301

Our recent experiments on the photodesorption of CO from oxidized Ni(111) suggest that this process is due to the hot carrier mechanism. We have measured for the first time the translational, rotational, and vibrational energy distributions for CO desorbed from a solid surface. CO was photochemically desorbed from epitaxially grown NiO(111) at 70 K with an excimer pump laser, and the desorbed molecules were monitored using laser-induced fluorescence (LIF) excited by a vacuum ultraviolet probe laser.

The results can be summarized briefly as follows. 1) Photodesorption cross sections for desorption using 4.0 eV photons were measured by monitoring the decrease in LIF signal from a particular rovibrational line as a function of the number of pulses impinging on the initially CO saturated surface. The resulting decay curve was fit by the sum of two exponentials, corresponding to cross sections of 3.3×10^{-18} and 4.5×10^{-19} cm^2, in reasonable agreement with the results of previous studies using an Hg arc lamp. 2) The velocity distribution of the desorbed products was measured by varying the time delay between the pump and probe lasers. Arrival time distributions were characteristic of Boltzmann velocity distributions with translational temperatures of T_{tr} = 1150 ± 150 K, nearly independent of rotational level probed. 3) The rotational and vibrational distributions of the desorbed CO molecules were measured by scanning the probe laser over various bands of the CO $A^1\Pi(v',J') \leftarrow X^1\Sigma(v'',J'')$ transition. The rotational distribution was characterized by a rotational temperature of T_r=196 K for J values less than 11 and by a temperature of T_r=670 K for higher J values. Figure 1 shows a "Boltzmann plot" of the rotational distribution. 4) The vibrational distribution, based on the measured v=1/v=0 ratio was found to be characterized by T_v=1400 K.

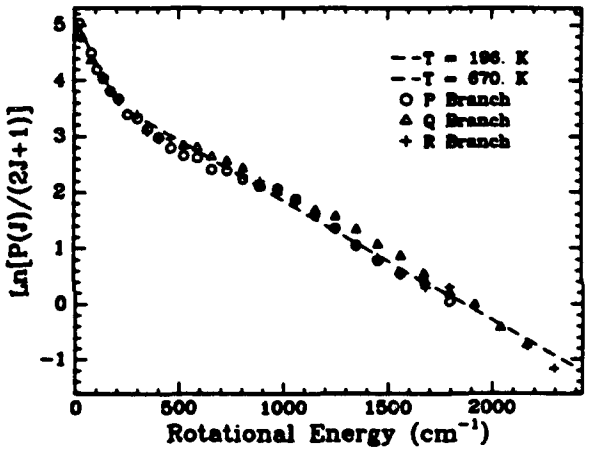

Figure 1 Rotational state populations plotted logarithmically against rotational energy.

The translational, vibrational and rotational distributions are very hot compared to the maximum temperature (82 K) to which the surface could have been heated by the laser, so the desorption is clearly a non-thermal process. It also seems unlikely that the 4.0 eV photon would directly excite electrons involved in the surface-CO bond, since the bond is extremely weak. Charge transfer excitation between the surface and the adsorbate, or hot substrate electron excitation of the adsorbate are the most likely mechanisms to explain the data. The excited vibrational distribution, in particular, is consistent with the formation of a temporary negative ion, CO^-, since the bond for this ion is considerably longer than that in the neutral CO. As the CO^- starts to leave the surface, the electron would jump back to the surface, leaving the CO bond extended and leading to vibrational excitation.

Laser Stimulated Gas-Surface Photochemistry: Basics And Applications

T. J. Chuang
IBM Almaden Research Center
650 Harry Road
San Jose, CA 95120-6099

Abstract: UV lasers have been extensively used in recent years to induce gas-solid interactions and to probe surface molecular dynamics. In this talk, a brief review of recent advances in the field will be given. Some model systems are used to illustrate the many facets of photoexcitation effects. These include photon-enhanced chemisorption, adsorbate-adsorbate and adsorbate-substrate reactions, production formation and desorption of surface species. The dynamics processes associated with vibrational and electronic activation and subsequent energy transfer and relaxation are investigated. The development in the two-dimensional imaging of photofragments for translational and internal energy distributions as well as angle resolved studies will be presented. Applications of photochemical techniques to material processing such as etching and deposition relevant to microelectronics fabrication will also be discussed.

Photocatalysis on Q–Sized Semiconductor Particles

A. Hoffman, B. Carraway and M. R. Hoffmann

California Institute of Technology

Pasadena, California 91125

Semiconductors such as TiO_2, ZnO, Fe_2O_3, CdS and ZnS are known to be photochemical catalysts for a wide variety of reactions in aqueous solution. When a photon with an energy of $h\nu$ matches or exceeds the bandgap–energy, E_g, of the semiconductor, an electron is promoted from the valence band, VB, into the conduction band, CB, leaving a hole behind. Electrons and holes either recombine and dissipate the input energy as heat, get trapped in metastable surface states, or react with electron donors and acceptors adsorbed on the surface or bound within the electrical double layer. Q–sized semiconductors are ultrasmall particles with diameters ranging from 1 to 10 nm which fall in the transition between the molecular level (i.e., clusters) and the bulk phase (i.e., crystals). The most notable property of these particles is a shift in the band gap energy toward higher energies as the diameter of the particle decreases (e.g., a particle–in–the–box effect).

In the case of the photocatalytic destruction of pentachlorophenol in the presence of particulate TiO_2, we have proposed a mechanism for the TiO_2 photoassisted degradation of PCP in which ·OH generated at the semiconductor surface appears to be the active photooxidant. Complete degradation is achieved in less the one hour of irradiation over the wavelength range of 330 to 370 nm and light intensities of 50 μM photons min^{-1} with quantum yields approaching 20%.

In a similar fashion, the photodegradation of chloroform over a broad range of pH, appears to proceed via the following mechanism:

$$h^+_{vb} + OH^-_{surf} \longrightarrow {}^{\cdot}OH_{surf}$$

$$e^-_{cb} + O_{2surf} \longrightarrow O^{\cdot-}_{2surf}$$

$$O^{\cdot-}_{2surf} + H^+ \rightleftharpoons HO^{\cdot}_2$$

$${}^{\cdot}OH_{surf} + CHCl_{3surf} \longrightarrow CCl^{\cdot}_{3surf} + H_2O_{surf}$$

$$CCl^{\cdot}_{3surf} \rightleftharpoons CCl^{\cdot}_3$$

$$CCl^{\cdot}_3 + O_2 \longrightarrow CCl_3O^{\cdot}_2$$

$$2\,CCl_3O^{\cdot}_2 \longrightarrow 2\,CCl_3O^{\cdot} + O_2$$

$$CCl_3O^{\cdot} + HO^{\cdot}_2 \longrightarrow CCl_3OH + O_2$$

$$CCl_3OH \longrightarrow Cl_2C{=}O + H^+ + Cl^-$$

$$Cl_2C{=}O + H_2O \longrightarrow CO_2 + 2\,H^+ + 2\,Cl^-$$

The Q–sized particles have been found to have larger overall quantum yields than their bulk phase counterparts. We have also found the Q–sized particles (e.g., ZnO, TiO_2 and CdS) to be effective photoinitiators for the formation of polymers from vinylic monomers in non–aqueous solvents. In these reactions, quantum yields for the Q–sized particles range from 2 to 20, while their bulk–phase counterparts show little photoactivity.

Photochemistry of Organometallics on Insulators*

S.-P. Lee, J. A. Tarr and M. C. Lin

Department of Chemistry

Emory University

Atlanta, GA 30322

Abstract

The photochemistry of organometallics related to groups III/V and II/VI semiconductor LCVD (laser chemical vapor deposition) processes has been investigated at 248 and 193 nm by time-of-flight / REMPI (or EI)-mass spectrometry.

Recent results obtained from our studies of dimethyl cadmium and trivinyl antimony on quartz surfaces will be presented.

---

* work supported by ONR (contract No. N00014-89-J-1235).

Molecular Photochemistry on Surfaces

J. M. White
Department of Chemistry
Center for Materials Chemistry and
NSF Science and Technology Center
University of Texas
Austin, TX 78712

This report will describe our recent surface photochemistry experiments. We briefly describe recent work, including dynamics, on alkyl halides on Pt(111) and Ag(111) and SO_2 on Ag(111), and, briefly, AsH_3 on GaAs. We will also discuss a novel thin film experiment designed to distinguish direct adsorbate excitation (photon absorption) from indirect substrate-mediated excitation. The alkyl work involves fluorinated C_1 adsorbates and we give special attention to the issue of C-F bond cleavage in mixed Cl- and F-containing molecules. For SO_2 we find interesting wavelength and coverage dependences in both dynamical properties (time-of-flight) and yields (post-irradiation TPD) over the range 6.4 to 3.5 eV. For example, dissociative processes which are readily observed in multilayers, are strongly quenched in monolayer and submonolayers. On the other hand, molecular desorption is strong throughout the full coverage regime. For AsH_3 on Ga-rich GaAs(100), we find evidence for the substrate-mediated formation of As-H and AsH_2 when adsorbed AsH_3 is irradiated with 6.4 eV photons. AsH_2 is photolyzed to As-H and Ga-H. There are strong D-for-H isotope effects and we ascribe these to mass-dependent substrate-mediated quenching of excited states of the adsorbate.

Atmospheric Reactions of Chlorine Oxide Reservoirs

Stanley P. Sander

Chemical Kinetics and Photochemistry Group, Jet Propulsion Laboratory
California Institute of Technology, Pasadena, California 91109

One consequence of the occurrence of reactions on cloud particles in the polar stratosphere is the repartitioning of chlorine-containing species from "reservoir" forms (e.g. $ClONO_2$ and HCl) into "active" forms such as ClO radicals. Enhancements of a factor of 100 or more in the ClO concentration over conditions present in lower latitudes are typical, and are currently the best indicators of perturbations caused by heterogeneous chemistry. The conditions peculiar to the springtime polar lower stratosphere (high ClO, very low temperature, high pressure and intermittent darkness) favor the formation of new species that may act as temporary chlorine reservoirs. These include the higher chlorine oxides (Cl_2O_2, Cl_2O_3, ...), and complexes involving ClO_x and NO_x/HO_x. I will present some recent results from this laboratory on the kinetics and spectroscopy of possible chlorine reservoirs and assess the atmospheric implications of these findings.

THE REACTIONS IO + HO_2 AND BrO + HO_2 : KINETIC RESULTS AND ATMOSPHERIC IMPACT.

F. MAGUIN, G. LAVERDET, G LE BRAS and G. POULET
Laboratoire de Combustion et Systèmes Réactifs
CNRS - 45061 ORLEANS cedex 2 - FRANCE.

Absolute kinetic investigations of the title reactions have been performed using the discharge-flow mass spectrometry method. For the IO + HO_2 reaction, the rate constant obtained at 298 K is : (1.03 ± 0.13) x 10^{-10} cm^3 $molecule^{-1}s^{-1}$. HOI, detected as the reaction product, could be a major reservoir for iodine species in the remote marine boundary layer (where low NOx levels are present). For the BrO + HO_2 reaction the rate constant obtained at 298 K, (3.3 ± 0.5) x 10^{-11} cm^3 $molecule^{-1}s^{-1}$, is six times higher than the value considered in the previous modelling of stratospheric ozone depletion due to bromine compounds. A new modelling has shown that this global ozone depletion, as well as the bromine partitioning, are significantly affected by the present laboratory data. These effects are shown to be very sensitive to the branching ratio of the BrO + HO_2 reaction if two channels forming HOBr and HBr, respectively, are considered. Experiments are in progress to measure the rate constant and product distribution of the BrO + HO_2 reaction at the lower temperatures of the stratosphere. The kinetic and mechanistic data for the XO + HO_2 reactions (X = Cl, Br, I) will be also discussed.

Direct Observation of ClO from Chlorine Nitrate Photolysis

Timothy K. Minton
Jet Propulsion Laboratory, M.S. 67-201
California Institute of Technology
4800 Oak Grove Drive
Pasadena, CA 91109

Christine M. Nelson, Teresa A. Moore, and Mitchio Okumura
Department of Chemistry, M.S. 127-72
California Institute of Technology
Pasadena, CA 91125

Although the mechanisms for polar ozone depletion are believed to be well understood, our recent investigation of the photodissociation of chlorine nitrate ($ClONO_2$) in a molecular beam indirectly raises questions about the presumably dominant ozone destruction cycle involving ClO:

$$\begin{array}{rcl} ClO + ClO + M & \longrightarrow & ClOOCl + M \\ ClOOCl + h\nu & \longrightarrow & ClOO + Cl \\ ClOO + M & \longrightarrow & Cl + O_2 + M \\ 2(Cl + O_3 & \longrightarrow & ClO + O_2) \\ \hline \text{Net:} \quad 2O_3 & \longrightarrow & 3O_2 \end{array}$$

A crucial assumption made in the second step of this cycle is that ClOOCl photodissociation leads to atomic chlorine. This assumption requires the Cl-O bond (21 kcal/mol) to break preferentially over the weaker O-O bond (18 kcal/mol), and it is based on the argument that excitation of an $n \rightarrow \sigma^*$ transition localized on the chlorine yields selective dissociation of the Cl-O bond. This idea arose from previous photolysis experiments on $ClONO_2$ in a flow cell. The concensus from these experiments is that the quantum yield for Cl atoms is ~ 0.9.[a] Recently, a very similar study on ClOOCl reported a quantum yield of 1.0 for Cl atoms produced from the primary photochemical reaction (step 2).[b]

However, our results show conclusively that in the photodissociation of $ClONO_2$ at 193 and 248 nm the $ClO + NO_2$ channel is significant, accounting for about 35 percent of the dissociation events. The only other channel observed was $Cl + NO_3$. Our experiments were carried out on a crossed molecular beams apparatus and employed the technique of photofragment translational spectroscopy. All primary photoproducts were observed directly, and their velocity and angular distributions have been measured. A photodissociation experiment was also performed on Cl_2O, which fragments to Cl + ClO and thus provides a means to calibrate the mass spectrometer detector so that the branching ratio between the two dissociation pathways in $ClONO_2$ can be accurately determined.

Even though the weaker O-N bond (26 kcal/mol) does break 35 percent of the time, the dominant channel is still Cl-O bond fission, which requires 40 kcal/mol. This result is consistent with the picture of a transition localized on the Cl-O moiety. Nevertheless, the large fraction of ClO product was not seen in the previous photolysis studies. Therefore, the report of only Cl atoms from ClOOCl photolysis becomes questionable. If ClO is in fact an important product of ClOOCl photodissociation, then the catalytic cycle above may not account for as much ozone destruction as currently believed.

---

[a] *Chemical Kinetics and Photochemical Data for Use in Stratospheric Modeling*, JPL Publication 90-1, edited by W.B. DeMore, et al. (Jan. 1, 1990).

[b] M.J. Molina, A.J. Colussi, L.T. Molina, R.N. Schindler, and T.-L. Tso, Chem. Phys. Lett. 173, 310 (1990).

CHEMICAL KINETICS AND DYNAMICS OF THE SODIUM NIGHTGLOW

D.R.Worsnop, G.N.Robinson, M.S.Zahniser and C.E.Kolb
Aerodyne Research, Inc., Billerica, MA 01821

X.Shi and D.R.Herschbach
Harvard University, Cambridge, MA 02138

The mesospheric sodium nightglow is believed to be produced by the chemiluminescent reaction of sodium monoxide with atomic oxygen. Sodium monoxide is formed by the reaction of atomic sodium with ozone. We have investigated the kinetics and dynamics of the $Na + O_3$ reaction using both fast flow reactor and molecular beam techniques. In particular, we have used magnetic deflection analysis in a crossed beam experiment to examine product electronic states from reaction of atomic Na, K and Rb with ozone. Those experiments show that these ozone reactions form the alkali monoxide in the $^2\Sigma^+$ state, which, in the case of NaO, lies 0.25 eV above the $^2\Pi$ ground state. Under mesospheric conditions the lifetime of this excited $^2\Sigma^+$ state of NaO should be long relative its rate of chemical reaction with O atoms. Molecular correlation analysis of the NaO + O reaction indicates that the electronic state of the NaO reactant may control the electronic branching ratio for excited $Na^*(^2P)$ formation. The implications of these results for the sodium nightglow will be discussed.

"Laser Diagnostics in Photochemistry: Elementary and Industrial Processes"

Jürgen Wolfrum

Physikalisch-Chemisches Institut der Universität Heidelberg

Germany

Results of experiments on the microscopic dynamic of the reactions of hydrogen atoms with O_2, CO_2, H_2O and the determination of absolute cross sections using tunable UV-laser systems for excitation and detection are compared with theoretical predictions.

Excimer laser photolysis of metalorganic complexes of platinum and palladium has been used to generate mono- and bimetallic noble metall clusters over a wide range of compositions. The temperature in the reaction volume could be determined by LIF-spectroscopy of electronic states of Pt atoms. Results on the structure and catalytic activities of mono- (Pt, Pd) and bimetallic (Pt-Pd) clusters will be described.

The ignition of O_3/O_2 and CH_3OH/O_2 mixtures by irradiation with a CO_2-laser along the axis of a cylindrical vessel is described as a model system for the unsteady interaction of elementary chemical reactions with transport processes in the gas phase. Experimental data on temperature and flame propagation using IR-absorption and 2D-LIF for time- and spatially resolved flame detection are compared with model calculations.

The last part describes experimental results on 2D-imaging of laminar and turbulent flame fronts, flame quenching processes, concentration and temperature fields using tunable UV-laser systems in industrial scale flames, Otto- and Diesel-engines.

Tomographic Analysis of Line of Sight Infrared Spectra of Flames

Kevin L. McNesby and Robert A. Fifer
U.S. Army Ballistic Research Laboratory
Attn: SLCBR-IB-I
Aberdeen Proving Ground, MD 21005-5066

Line of sight absorption spectra of combusting systems are often difficult to interpret. One of the main reasons for this is that the probe beam usually must pass through several regions of varying species concentration, temperature and density. The absorbance reported through, for instance, a flame is really the absorbance integrated over the entire beam path. Frequently, species outside the region of interest (e.g., exhaust gases) mask or obliterate small absorbances due to species within the region of interest (e.g., the preheat zone of a low pressure flame).

We are using a radiological imaging technique, computed tomography, to obtain species profiles within a flame as a function of height above the burner surface and lateral position at that height. This information is extracted from parallel line of sight absorbance data using a technique known as Abel inversion. This process yields two dimensional "slices" of the flame. At any point within each slice the infrared spectrum of the species present may be obtained. Abel inversion is a special application of computerized tomography which may be applied only to systems possessing axial symmetry.

We have used this technique to evaluate a low pressure premixed methane / nitrous oxide burner flame. The flame is supported on a water cooled stainless steel cylindrical frit which sits inside a low pressure chamber. Data are collected using crossed beams from a Fourier transform infrared spectrometer and from an infrared diode laser. Species and temperature profiles for inverted and "normal" line of sight absorbance spectra are compared and contrasted with data taken on similar systems by different methods.

Visible Diode Laser Detection of HCO

Daniel B. Oh and Joel A. Silver
Southwest Sciences, Inc
1570 Pacheco St., Suite E-11
Santa Fe, New Mexico 87501

ABSTRACT

There are a wide variety of laser-based spectroscopic techniques that enable detection of reaction intermediates and facilitate a better understanding of chemical reactions. These methods (LIF, Stimulated Raman scattering, REMPI, CARS and 2-D fluorescence imaging, etc.) provide highly selective, time-resolved and non-intrusive detection of species of interest. They provide, however, only a relative measure of number densities. Even fluorescence measurements of a diatomic radical such as OH, for which reliable calibrations are theoretically possible, suffer from uncertainties in quenching cross sections due to changing concentrations of collision partners. This limits the quantitative aspect of LIF measurements.[1]

We have been developing a new laser-based detection method that combines two recent technological advances-the use of visible and near-IR wavelength diode lasers and high frequency wavelength modulation spectroscopy-to achieve quantitative, highly selective and rapid time response detection of reaction intermediates. We access the visible and near-IR absorption bands present in many open shell reaction intermediates.[2] We chose to study the formyl radical (HCO) because of its importance in oxidation of alkyl radicals that lead to the formation of CO and CO_2. Using InGaAlP laser diodes (~680 nm, ~0.003 cm^{-1} linewidth, 4-20 mW), we access the rotational absorption features in the (0,7,0) $A^2A'' \leftarrow$ (0,0,0) X^2A' transition of HCO.[3] Fluorine atoms from microwave discharge of F_2 react with excess H_2CO in a low pressure discharge flow reactor. A multi-pass optical arrangement (Herriott type) perpendicular to the flow allows absorption detection by high frequency wavelength modulation. Quantitative chemical titration of F atoms provides the HCO concentration and thus the line strengths. We will report on our progress in detecting HCO and measuring HCO line strengths.

REFERENCES

(1) N. L. Garland and D. R. Crosley, "On the Collisional Quenching of Electronically Excited OH, NH and CH in Flames," Twenty-first Int'l Symp. on Combustion, 1986, pp.1693-1702.

(2) M.E. Jacox, "Electronic Energy Levels of Small Polyatomic Molecules," J. Phys. and Chem. Ref. Data, 17(2), 269-512 (1988) and references therein.

(3) G. Hertzberg and D.A. Ramsey, "The 750 to 450nm Absorption System of the Free HCO Radical," Proc. Roy. Soc. (London), A233, 34-54 (1955).

Application of Photofragmentation Laser Induced Fluorescence to the Measurement of Important Atmospheric Gases.

J.D. Bradshaw and S.T. Sandholm
School of Earth and Atmospheric Sciences
Georgia Institute of Technology
Atlanta, Georgia 30332

The applicability of photofragmentation coupled with laser induced fluorescence (PF-LIF) as a technique for quantitatively measuring important atmospheric compounds has now been established at the few parts-per-trillion (ppt) level. In this report we give results of a PF-LIF ammonia sensor's performance as evaluated in laboratory, field, and intercomparison studies. In this approach, the two-photon- photofragmentation of NH_3 at 193 nm produces a significant yield of NH fragments in the metastable $b^1\Sigma^+$ state. This state is then probed via laser excitation of the $NH(b^1\Sigma^+) \rightarrow NH(c^1\Pi)$ transition near 452 nm. The resulting fluorescence from the $NH(c^1\Pi) \rightarrow NH(a^1\Delta)$ transition is monitored at a wavelength near 325 nm. In this scheme, the background noise generated from the 193 nm photolysis laser is allowed to decay to nearly insignificant levels prior to probing the long-lived $NHb^1\Sigma^+$ metastable state population. The monitoring of the $NH(c^1\Pi) \rightarrow NH(a^1\Delta)$ transition occurs at a wavelength shorter than the LIF probe wavelength, thus allowing complete segregation of probe laser generated background fluorescence and scatter. The limit-of-detection for the instrument presented here is < 4 pptv (1×10^8 molecule/cm^3) for a one minute sigmal integration period, under ambient sampling conditions. The technique is free from interferences and system performance does not significantly degrade under adverse sampling conditions (i.e. rain, fog, haze. clouds, etc.). Spectroscopic selectivity in laser excitation of the $NH(b^1\Sigma^+) \rightarrow NH(c^1\Pi)$ transition is sufficient to resolve $^{15}NH_3$ and $^{14}NH_3$ contributions for use in atmospheric tracer studies of $^{15}NH_3/^{14}NH_3$ ratios. The design of a sensitive PF-LIF NH_3 sensor that is capable of making high temporal resolution (10 sec) gradient flux measurements of $^{14}NH_3$ and $^{15}NH_3$ will also be discussed along with the future application of the PF-LIF technique to other important atmospheric compounds.

Kinetics of free radical reactions of importance in combustion

M J Pilling
School of Chemistry, University of Leeds, Leeds LS2 9JT, U.K.

Two reaction systems will be discussed:

1. The isomerisation of an alkyl peroxy radical to form a hydroperoxy radical is a key rate determining step in the oxidation of alkanes at moderate temperatures and is of significance in the chemistry of autoignition (knock) in petrol engines. No direct studies have been made of the kinetics of such reactions.

   We have measured rate constants for the neopentyl peroxy radical, generating the alkyl radical by laser flash photolysis of the iodide and detecting OH, generated by fragmentation of the hydroperoxy radical, by LIF. At high $[O_2]$, the isomerisation is the rate determining step in the formation of OH. As $[O_2]$ is reduced the rate constant for formation of OH increases, enabling the rate constant for the peroxy radical decomposition to be determined.

2. Rate constants for CH_3 + OH and for $^1CH_2$ + H_2O have recently been determined by Oser *et al*[1] and by Hack *et al*[2] respectively. The pressure dependence of the former, when combined with k($^1CH_2$ + H_2O), is incompatible with the thermochemistry of the reactions.

$$CH_3 + OH \longrightarrow {}^1CH_2 + H_2O$$

$$\xrightarrow{M} CH_3OH$$

Master equation calculations have been carried out to examine this inconsistency.

1. H. Oser, N.D. Stothard, R. Humfer and H.H. Grotheer, J. Phys. Chem., in press

2. W. Hack, H.Gg. Wagner, and A. Wilms, Ber. Bunsenges. Phys. Chem., 1988, **92**, 620.

TEMPERATURE DEPENDENCE OF THE KINETICS OF THE REACTION: CH + N_2

Laura Jane Medhurst, Nancy L. Garland and H.H. Nelson
Chemistry Division, Code 6111
Naval Research Laboratory
Washington, D.C. 20375-5000

The chemical reaction of CH + N_2 has been proposed as the initial step in the formation of "prompt" NO in hydrocarbon combustion, especially under fuel-rich conditions.[1] We measured the rate constant of this reaction at a total pressure of 100 Torr between 600 and 1200 K, the temperature regime where there is a change in the chemical mechanism. Formation of a CHN_2 complex dominates near room temperature while H-atom abstraction to form HCN + N dominates at temperatures above 2000 K.

CH radicals are generated by 248-nm photolysis of $CHBr_2Cl$ and probed by laser-induced fluorescence via the $B^2\Sigma^+ - X^2\Pi_r$ (0,0) band near 387 nm. Temperatures were determined from rotational scans of the B-X (0,0) band of CH. Results from these experiments will be discussed and compared to the results of other kinetic studies.

1. Fenimore, C.P., Thirteenth Symposium (International) on Combustion, p.373 The Combustion Institute, 1971).

TEMPERATURE-DEPENDENT KINETICS STUDIES OF THE REACTIONS $Br(^2P_{3/2}) + H_2S \leftrightarrow SH + HBr$ and $Br(^2P_{3/2}) + CH_3SH \leftrightarrow CH_3S + HBr$. HEATS OF FORMATION OF SH AND CH_3S RADICALS

J. M. Nicovich, K. D. Kreutter[a], C. A. van Dijk, and P. H. Wine

Physical Sciences Laboratory, Georgia Tech Research Institute,
Georgia Institute of Technology, Atlanta, GA 30332

Time-resolved resonance fluorescence detection of $Br(^2P_{3/2})$ atom disappearance or appearance following 266 nm laser flash photolysis of $CF_2Br_2/H_2S/H_2/N_2$, $CF_2Br_2/CH_3SH/H_2/N_2$, $Cl_2CO/H_2S/HBr/N_2$, and $CH_3SSCH_3/HBr/H_2/N_2$ mixtures has been employed to study the kinetics of the reactions $Br(^2P_{3/2}) + H_2S \rightleftarrows SH + HBr$ (1, -1) and $Br(^2P_{3/2}) + CH_3SH \rightleftarrows CH_3S + HBr$ (2, -2) as a function of temperature over the range 273 - 431K. Arrhenius expressions in units of 10^{-12} $cm^3molecule^{-1}s^{-1}$ which describe the results are $k_1 = (14.2 \pm 3.4) \exp[(-2752 \pm 90)/T]$, $k_{-1} = (4.40 \pm 0.92) \exp[(-971 \pm 73)/T]$, $k_2 = (9.24 \pm 1.15) \exp[(-386 \pm 41)/T]$, and $k_{-2} = (1.46 \pm 0.21) \exp[(-399 \pm 41)/T]$; errors are 2σ and represent precision only. By examining $Br(^2P_{3/2})$ equilibration kinetics following 355 nm laser flash photolysis of $Br_2/CH_3SH/H_2/N_2$ mixtures, a 298K rate coefficient of $(1.7 \pm 0.5) \times 10^{-10}$ $cm^3molecule^{-1}s^{-1}$ has been obtained for the reaction $CH_3S + Br_2 \rightarrow CH_3SBr + Br$. To our knowledge, these are the first kinetic data reported for each of the reactions studied. Measured rate coefficients, along with known rate coefficients for similar radical + H_2S, CH_3SH, HBr, Br_2 reactions are considered in terms of possible correlations of reactivity with reaction thermochemistry and with IP - EA, the difference between the ionization potential of the electron donor and the electron affinity of the electron acceptor. Both thermochemical and charge-transfer effects appear to be important in controlling observed reactivities.

Second and third law analyses of the equilibrium data for reactions 1 and 2 have been employed to obtain the following enthalpies of reaction in units of kcal mol^{-1}: for reaction 1, $\Delta H_{298} = 3.64 \pm 0.43$ and $\Delta H_0 = 3.26 \pm 0.45$; for reaction 2, $\Delta H_{298} = -0.14 \pm 0.28$ and $\Delta H_0 = -0.65 \pm 0.36$. Combining the above enthapies of reaction with the well-known heats of formation of Br, HBr, H_2S, and CH_3SH gives the following heats of formation for the RS radicals in units of kcal mol^{-1}: $\Delta H_f^\circ_0(SH) = 34.07 \pm 0.72$, $\Delta H_f^\circ_{298}(SH) = 34.18 \pm 0.68$, $\Delta H_f^\circ_0(CH_3S) = 31.44 \pm 0.54$, $\Delta H_f^\circ_{298}(CH_3S) = 29.78 \pm 0.44$; errors are 2σ and represent estimates of absolute accuracy. The SH heat of formation determined from our data agrees well with literature values but has reduced error limits compared to other available values. The CH_3S heat of formation determined from our data is near the low end of the range of previous estimates and is 3-4 kcal mol^{-1} lower than values derived from recent molecular beam photofragmentation studies. The heats of formation determined in this study represent the most uncertain parameter required to evaluate a number of S-H, S-C, and S-S bond dissociation energies.

This work was supported by the National Science Foundation and the National Aeronautics and Space Administration.

(a) Present address: Dept. of Biochemistry, Duke Univ., Durham, NC 27706.

High Pressure Limiting Rate Constants for Reactions of OH-Radicals with NO, NO_2, CO, and OH from Saturated Laser Induced Fluorescence Studies.

H.Hippler, R.Forster, M.Frost, A.Schlepegrell, and J.Troe
Institut für Physikalische Chemie der Universität Göttingen,
Tammannstraße 6, W-3400 Göttingen, Germany

Reactions of OH-radicals often dominate oxidation processes in many complex chemical systems like combustion or atmospheric chemistry. The recombinations of OH with NO, NO_2, CO, and OH play a particular important role as a sink of OH-radicals. Only a detailed knowledge of the falloff behaviour of the rate constants of these reactions can lead to a complete understanding of complex oxidative systems. A prediction of these rate constants under given experimental conditions can be made with the help of unimolecular rate theory and an analysis of complete falloff curves which are obtained from experiments. Total pressures of several 100 bar are needed in order to achieve direct access to the high pressure limiting rate constants of recombination reactions for such small molecules. The problem of a sensitive time-resolved detection method for these reactions under high pressure conditions has been solved by using "saturated" LIF of OH-radicals.

OH-radicals were produced by laser photolysis of HNO_3 (248 nm) or of N_2O (193 nm) in the presence of water. After a time-delay a second laser excited the $Q_1(2)$ line of the 0-0 band of the X-A transition of OH for fluorescence detection. Complete falloff curves including new high pressure limiting rate constants for the reactions above will be presented together with an interpretation in terms of a statistical unimolecular rate theory.

PRODUCTION OF ATMOSPHERIC TRACE CARBON GASES FROM PHOTODEGRADATION OF HUMIC SUBSTANCES

Richard G. Zepp and William L. Miller*

Environmental Research Laboratory
U.S. Environmental Protection Agency
Athens, Georgia 30613
*(ASci Corp., Athens, GA)

Humic substances are hydrophobic, biologically-refractory components of the organic matter in wetlands, rivers, lakes and the sea. Field studies by others have indicated that photoreactions of humic substances are a significant source of atmospheric carbon monoxide and carbonyl sulfide. Because the reactions enhance the oxidation of humic substances to carbon dioxide and biologically-labile organic compounds, they may play an important role in the carbon cycle. In this study we present kinetic data from laboratory studies of the photoreactions of humic substances exposed to solar and monochromatic radiation under varying reaction conditions.

Laboratory studies of the direct photoreactions of humic substances were conducted with water samples and aqueous solutions of well-characterized humic substances isolated from wetlands, rivers and near coastal ecosystems in North America. Exposure of the humic substances to both sunlight and simulated solar irradiation resulted in the loss of absorbance at near ultraviolet and visible wavelengths (i.e. photobleaching) with a simultaneous, rapid formation of carbon monoxide and carbon dioxide. Using fading at 350 nm to quantify photochemical conversion of humic substances from various sources, we determined that chemical yields of CO_2 are in the 20 to 50 percent range, CO yields are 1 to 2 percent, and other identifiable low-molecular-weight products are 1 percent or less. Quantum yield studies indicated that ultraviolet and blue radiation produce carbon monoxide most efficiently.

Other studies showed that the photoproduction of carbonyl sulfide in coastal sea water samples and synthetic seawater involves the humus-sensitized photooxidation of organosulfur compounds in the water. Kinetic studies of the photooxidation of various organosulfur compounds in solutions of humic substances in artificial sea water demonstrated that compounds with non-bonded electrons on the sulfur atom are most efficiently oxidized to carbonyl sulfide. Quantum yield studies indicated that radiation in the UV-B region (280-320 nm) was most efficient at inducing the photooxidations.

These reactions involve the intermediacy of short-lived, chemically reactive transients that include triplet states, singlet molecular oxygen, oxygen-centered free radicals, and radical cations that directly result from primary photochemical processes of the humic substances. Moreover, hydrogen peroxide formed by the photoreduction of dioxygen by humic substances reacts efficiently with reduced transition metals (e.g, iron, copper) to produce hydroxyl radicals that may be involved in these reactions. Laser flash photolytic and steady-state kinetic methods that are being used to study the role of these transients in producing atmospheric gases will be discussed.

AQUEOUS-PHASE PHOTOCHEMICAL FORMATION OF OXIDANTS IN AUTHENTIC CLOUD WATERS

Bruce C. Faust, Cort Anastasio, and John M. Allen
School of the Environment, Environmental Chemistry Laboratory,
Duke University, Durham, North Carolina 27706 USA

Aqueous-phase redox reactions in tropospheric cloud drops significantly affect the: i) oxidation of SO_2 to H_2SO_4 by peroxides and other oxidants (1), ii) destruction of O_3 by $^{\bullet}O_2^-$ (2), and iii) oxidation of organic matter by free radicals (3). Very few studies have focused on aqueous-phase photochemistry as a source of oxidants in atmospheric water drops, and none of these investigations have studied authentic atmospheric waters.

A study was therefore initiated (4-6): i) to identify photo-oxidants formed from aqueous-phase photochemical reactions in authentic cloud and fog waters, ii) to quantify their aqueous-phase photo-stationary state concentrations and formation rates, iii) to elucidate possible mechanisms of formation of the photo-oxidants, and iv) to assess the impact of this source of oxidants to tropospheric chemistry.

From 1988-1991, authentic cloud water samples were obtained, through researchers, from: i) mountain top sites in North Carolina, Virginia, New York, Washington, and Oregon, and ii) aircraft above Ontario. Filtered (0.5 μm Teflon) authentic cloud waters exhibit a characteristic UV-visible absorption that overlaps the spectral irradiance of sunlight (Figure 1). Similar absorption spectra were observed for all cloud and fog waters.

Chromophores present in atmospheric water absorb solar UV light, which initiates the aqueous-phase photochemical formation of peroxides (Figure 2; ref. 6). The initial rate of peroxide photo-formation is linearly dependent on actinic flux (Figure 3). Aqueous-phase photochemical formation rates of peroxides were typically 1-2 μM/hour in the cloud waters studied (midday, equinox sunlight; ref. 6). The photochemical formation of peroxides also provides evidence for the formation of peroxyl radicals (HOO$\bullet$ and ROO$\bullet$), since peroxyl radicals are thought to be the dominant precursors of peroxides in clouds.

Additional evidence for the aqueous-phase photochemical formation of peroxyl radicals is provided by the photo-oxidation of 2,4,6-trimethylphenol, a classic chemical probe for peroxyl radicals (7). Typical aqueous-phase photo-stationary state concentrations of peroxyl radicals range from 1-40 nM in numerous authentic cloud waters (4,5).

Singlet molecular oxygen is also formed from aqueous-phase photochemical reactions in atmospheric waters. Typical photo-stationary state concentrations and formation rates of $O_2(^1\Delta_g)$ ranged from 30-1500 fM and 7-340 nM/sec, respectively (4,5).

From this work we conclude that aqueous-phase photochemical reactions are a significant, and in some cases dominant, source of these oxidants to tropospheric cloud drops.

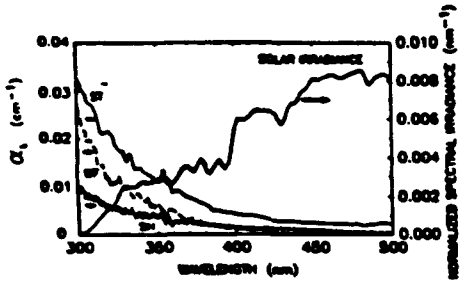

Fig. 1. Left: Absorbance per cm. of filtered authentic cloud water, α_λ. ST Stampede Pass, WA; WF Whiteface Mtn., NY; SH Shenandoah Pk., VA. Distilled water reference. Right: Sunlight spectrum.

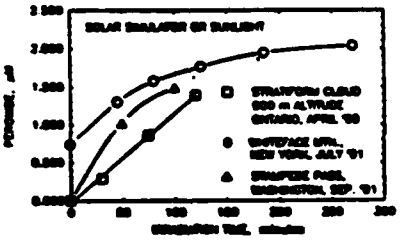

Fig. 2. Photochemical formation of peroxides in authentic cloud waters. KB aircraft sample 900 m over Ontario; WF Whiteface Mtn., NY; ST Stampede Pass, WA.

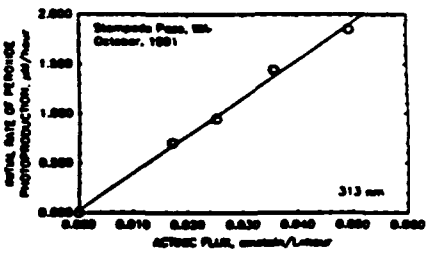

Fig. 3. Inital rate of peroxide photoformation versus actinic flux.

References

1. Gunz, D.W.; Hoffmann, M.R. *Atmos. Environ.* 1990, *24A*, 1601.
2. Lelieveld, J.; Crutzen, P.J. *Nature* 1990, *343*, 227.
3. Graedel, T.E.; Mandich, M.L.; Weschler, C.J. *J. Geophys. Res.* 1986, *91*, 5205.
4. Faust, B.C.; Allen, J.M. in *Effects of Solar Ultraviolet Radiation on Biogeochemical Dynamics in Aquatic Environments*, Woods Hole Oceanographic Institution Technical Report 90-09 (eds. N.V. Blough and R.G. Zepp) 1990.
5. Faust, B.C.; Allen, J.M. submitted to *J. Geophys. Res.* 1991.
6. Faust, B.C.; Anastasio C.; Allen, J.M. in preparation.
7. Faust, B.C.; Hoigné, J. *Environ. Sci. Tech.* 1987, *21*, 957-964.

HETEROGENEOUS CHEMISTRY OF TRACE GASES ON AQUEOUS AND SULFURIC ACID LIQUID DROPLETS

G.N. Robinson, D.R. Worsnop, M.S. Zahniser, C.E. Kolb
Aerodyne Research, Inc., Billerica MA 01821

W. DeBruyn, S. Duan, and Paul Davidovits,
Boston College, Chestnut Hill, MA 02167

Heterogeneous gas/liquid processes play an important role in atmospheric chemical transformations, ranging from acid rain formation in tropospheric clouds to ozone depletion in the stratosphere. Using an experimental technique that passes a train of fast moving liquid droplets through a low pressure flow tube, we have measured the gaseous uptake rates of trace gases into aqueous and sulfuric acid solutions. By measuring gas uptake as a function of millisecondgas/liquid interaction times, we can resolve rates of mass accommodation from surface saturation due to liquid solubility constraints. Based on measurements of mass accommodation coefficients for a range of molecules including organic and halogenated alcohols and organic/inorganic acids, we have developed a model of mass accommodation on liquid water using critical cluster size homogeneous nucleation theory. For SO_2 and CH_3CHO, we see evidence for chemisorption of gas molecules on the liquid surface. Other recent results have placed limits on the solubility and hydrolysis rates of halogenated carbonyls that are expected to be produced by tropospheric degradation of proposed fluorocarbon substitutes. Current experiments are measuring the uptake of HCl, HNO_3, and N_2O_5 on cold sulfuric acid droplets that are representative of background aerosols in the stratosphere.

LASER-FLASH PHOTOLYSIS OF H_2S SOLUTIONS

S. Padmaja, P. Neta, and R. E. Huie
Chemical Kinetics and Thermodynamics Division
National Institute of Standards and Technology
Gaithersburg. MD 20899

The photochemistry of H_2S has been investigated in aqueous solutions by excimer laser flash photolysis at 248 nm (KrF) and 193 nm (ArF). At neutral pH and above, and with 248 nm photolysis, an optical absorption at 380 nm, ascribed to the radical dimer $H_2S_2\cdot^-$, formed with a rate constant of 2×10^9 $M^{-1}s^{-1}$. At 193 nm, the formation of the radical dimer was coincident with the pulse, suggesting the photolysis of a dimeric precursor. The yield in this case was at a maximum near the pK_a of H_2S, 6.97, and decreased at higher and lower pH. At very low pH, H_2S photolysis by 193 nm radiation was observed to lead to the HS· radical, absorbing at 240 nm. This radical was found to react with O_2, forming the intermediate product $\cdot SO_2^-$, which has an absorption maximum at 260 nm, and ultimately leading to $HO_2\cdot$, which absorbs at 225 nm.

Several reactions associated with aqueous H_2S and its radical products also have been investigated, both by flash photolysis and pulse radiolysis. These include the oxidation of HS^- by a number of oxidizing radicals, such as $\cdot SO_4^-$, $\cdot(SCN)_2^-$, and $\cdot I_2^-$; the reaction of e_{aq}^- with H_2S; the reaction of H· with H_2S; and several reactions of the $\cdot H_2S_2^-$ and HS· radicals. The HS· radical is found to react with unsaturated alcohols, aldehydes and nitriles through addition to the double bond. The rate constants for these reactions range from 1×10^8 - 1×10^9 $M^{-1}s^{-1}$. The dimer radical reacts with unsaturated compounds with rate constants of the order of 1×10^7 $M^{-1}s^{-1}$.

Bond- and State-Selected Photodissociation and Bimolecular Reaction

F. Fleming Crim
Department of Chemistry
University of Wisconsin-Madison
Madison, Wisconsin

Controlling the course of chemical reactions by exciting particular vibrations of the reactants is an intriguing prospect with fundamental and, potentially, practical consequences. We have exploited the isolation of the O-H stretching vibration in H_2O and HOD to demonstrate such control in the photodissociation and reaction of water. We prepare single eigenstates by vibrational overtone excitation and subsequently photodissociate or react them. In vibrationally mediated photodissociation of H_2O, the selection of different initial stretching states having roughly the same energy leads to drastically different populations of the vibrational states of the OH photolysis product. By exciting the O-H stretching overtone in HOD, we can selectively photolyze that bond. In bimolecular reaction experiments, we react vibrationally excited water molecules with H atoms to produce H_2 and OH or with translationally energetic Cl atoms to produce HCl and OH. The reactions, which are endothermic, proceed at an undetectable rate in our room temperature measurements. Vibrationally excited water, however, reacts at roughly the gas kinetic collision rate. Different initially excited vibrational states have very different reaction rates and dynamics, depending on the distribution of the excitation among the vibrations. Applying this technique to HOD($4\nu_{OH}$) allows us to demonstrate bond selected bimolecular chemistry, in which the reaction produces only OD. This observation suggests a general approach to assessing and performing bond controlled chemistry in a variety of molecules.

XXth Informal Photochemistry Meeting
April 26- May 1, 1992
Atlanta, GA

ABSTRACT

Quantum calculations of mode specificity in $H+H_2O \rightarrow OH + H_2$ and $H + HOD \rightarrow H_2 + OD$, $HD + OH$, Deshang Wang and Joel M. Bowman, Department of Chemistry, Emory University, Atlanta, GA 30322

We report reduced dimensionality quantum calculations of mode specificity in the above reactions using the semi-empirical potential of Schatz and Elgersma. The three stretching degrees of freedom are fully coupled by effective potentials given by the full six degree-of-freedom potential minimized with respect to the three angular degrees of freedom plus the local bending energy. We consider energies sufficient to excite the third overtone states of H_2O and the fourth overtone states of HOD. Comparisons are made with recent experiments of Crim and co-workers, with recent reduced dimensionality calculations of Clary, and previous trajectory calculations of Schatz and co-workers.

Supported in part by the Department of Energy

Theoretical Studies of Vibrational and Electron State Specificity in Chemical Reactions: $H + H_2O \rightarrow OH + H_2$ and $Cl + HCl \rightarrow ClH + Cl$

George C. Schatz

Department of Chemistry
Northwestern University
Evanston, IL 60208-3113

This talk will be divided between two projects which are currently being actively pursued in my group. The first is concerned with vibrational state and bond specific reaction dynamics in the reactions $H + H_2O$ and H + HOD. This work is aimed at interpreting the very exciting experiments recently reported by the Crim and Zare groups, and it follows up earlier theoretical work done at Northwestern. Our new calculations have used the fourier transform method for defining semiclassical vibrational eigenstates in H_2O and HOD, followed by trajectories to determine reactive cross sections and product state distributions. Comparison with experiment is generally good, but there are some areas of disagreement that could tell a lot about the ability of classical mechanics to describe coupled vibrational modes during reaction.

The second part of the talk is concerned with electronic state specificity in chemical reactions, particularly with the effects of spin orbit excitation and orbital alignment. Here we have developed an accurate quantum coupled channel method for describing A + BC chemical reactions that have coupled electronic states. We have applied this to the Cl + HCl reaction, including for coupling between the $^2\Sigma$ and $^2\Pi$ potential surfaces that correlate to $Cl(^2P)$. The results indicate significant spin-orbit and orbital alignment effects. The relation of these results to the $ClHCl^-$ photodetachment spectrum will be discussed.

ULTRAFAST STUDIES OF ELECTRON PHOTODETACHMENT AND SOLVATION IN AQUEOUS IODIDE ANION SOLUTIONS

A.P. Baronavski and Steven McCauley*
Naval Research Laboratory
Chemistry Division
Washington, DC 20375-5000

We will describe experiments which to provide insight into the formation and subsequent evolution of electrons in aqueous solutions. Electrons are produced by photo-detachment from the hydrated iodide anions at 308 nm, and are probed by transient absorption spectroscopy using a femtosecond continuum. The photodetached electrons first go through a very short-lived (~100fs) "trapped state." They then undergo radiationless relaxation to the presolvated state, which relaxes to the fully hydrated electron in ~ 400fs. We will discuss the mechanisms involved in these processes and the spectroscopy of the three states observed. Our results will be compared with those of Eisenthal[1] and Antonetti.[2]

[1]F.H. Long, H. Lu, K.B. Eisenthal, Chem. Phys. Lett. 160, 464 (1989).

[2]A. Migus, Y. Gaudel, J.L. Martin, and A. Antonetti, Phys. Rev. Lett. 58 1559 (1987).

* On sabbatical from California State Polytechnic University, Pomona, CA.

THE DYNAMICS OF THE ELECTRONIC QUENCHING AND CHEMICAL REACTIONS OF THE IMIDOGEN RADICAL

Paul J. Dagdigian
Department of Chemistry, The Johns Hopkins University, Baltimore, MD 21218

The dynamics of several collisional processes involving $NH(X^3\Sigma^-, a^1\Delta)$ has been investigated through measurement of product nascent internal state distributions by laser fluorescence detection. The state distribution of $NH(X^3\Sigma^-)$ formed in the electronic quenching of $NH(a^1\Delta)$ by Xe and CO has been determined in a crossed beam experiment, in which the electronically excited radical was prepared by 193 nm photolysis of HN_3. Product $NH(X^3\Sigma^-)$ vibrational levels up to v=4 have been observed through laser fluorescence excitation in the $A - X$ $\Delta v=0, -1, -2$ sequences. Very little rotational excitation is found in the quenched molecules. Population in all three $X^3\Sigma^-$ fine structure levels is observed. These results are interpreted in terms of the general theory for collision-induced spin-orbit coupling [Dagdigian, Alexander, and Werner (in preparation)] and are compared with the state distribution in the $NH(X^3\Sigma^-)$ fragment from the spin-forbidden decomposition of vibrationally excited HN_3 previously investigated by the NIST group.

The dynamics of the $NH(X^3\Sigma^-) + NO \rightarrow OH + N_2$ and $O(^3P) + NH(X^3\Sigma^-) \rightarrow H + NO$ reactions have also been investigated through measurement of the OH and NO product internal state distributions, respectively. For the former, very little OH internal excitation is observed, despite a substantial exothermicity for this pathway. The dynamics of the NH + NO reaction are compared with that of $H + N_2O$, for which the OH internal state distribution has been measured in other laboratories. The NO internal state distribution from the H + NO reaction is interpreted in terms of what is known about HNO potential energy surfaces.

REACTION DYNAMICS OF RADICAL SPECIES FROM CROSSED BEAM STUDIES

N.Balucani, P.Casavecchia, and G.G.Volpi
Dipartimento di Chimica, Universitá di Perugia, 06100 Perugia, Italy

We have recently undertaken the study of the reaction dynamics of ground, ^3P, and electronically excited, ^1D, oxygen atoms with simple molecules by using the crossed beam scattering method with mass spectrometric detection [1,2]. We exploit the capability of generating intense and continuous supersonic beams containing both $O(^3P)$ and $O(^1D)$, and of resolving their distinct contributions in high-resolution angular and velocity distribution measurements.

The first reactions we have looked at are those with hydrogen halides forming the halogen oxide, which are strongly endoergic for $O(^3P)$ while exoergic for $O(^1D)$. These reactions are of importance in atmospheric chemistry. The dynamics of the XO (X=Cl, Br, I) forming channel has been characterized at different collision energies and its importance with respect to the competing OH channel assessed. It is concluded that the H-displacement pathway plays an important role in the overall reaction of $O(^1D)$ with HX. In particular, the dynamics of IO formation is found to be significantly different with respect to that of ClO and BrO.

Reactions which are exoergic for both $O(^3P)$ and $O(^1D)$, as those with H_2S, have also been investigated. The reaction channels leading to HSO + H and SO + H_2 products have been examined by carrying out experiments at different collision energies ranging from the threshold for the ground state reaction up to about 12 kcal/mol. The reactions are the prototype for the atmospheric oxidation reactions of sulfur compounds and are important in the processes associated with the combustion of sulfur contaminated fossil fuels. While the H-displacement reaction of $O(^1D)$ with H_2S is found to proceed through the formation of a long-lived complex, that of $O(^3P)$ has a drastically different dynamics, being direct (rebound mechanism) with the barrier located in the exit channel. The heat of formation of the HSO radical is established very accurately and a direct insight into the geometry of the transition state is also provided [3]. The effect of electronic excitation on the reaction dynamics of atomic oxygen is examined in detail. The SO + H_2 channel, although strongly exoergic, is neither seen to occur with $O(^1D)$ nor with $O(^3P)$.

Experiments aimed at elucidating the reaction dynamics of $O(^3P)$ and $O(^1D)$ with other interesting molecules (H_2, CH_4, C_2H_6, N_2O, CS_2, CH_3SH, halogens, and chloro-fluoro-carbons) are currently under way. Some results will be presented and discussed at the meeting. The investigation of the reaction dynamics of other important radical species (Cl, OH) by the same technique is currently also being pursued.

References

[1] N.Balucani, L.Beneventi. P.Casavecchia. and G.G.Volpi, Chem.Phys.Lett. 180, 34 (1991).
[2] N.Balucani, L.Beneventi, P.Casavecchia, D.Stranges, and G.G.Volpi, J.Chem.Phys. 94, 8611 (1991).
[3] N.Balucani, L.Beneventi, P.Casavecchia, D.Stranges, and G.G.Volpi, J.Chem.Soc. Faraday Discuss. 91, 47 (1991).

Influence of vibrational and translational motion on the reaction dynamics of $O(^1D) + H_2(v) \rightarrow OH(v,J) + H$

Karl Heinz Gericke and Klaus Mikulecky

Institut für Physikalische und Theoretische Chemie, Johann Wolfgang Goethe – Universität, Niederurseler Hang, 6000 Frankfurt am Main 50, FRG

The OH product state distribution from the reaction $O(^1D) + H_2(v) \rightarrow OH(v,J,\Omega,\Lambda) + H$ was determined by laser–induced fluorescence (LIF) in the $\Delta v=-3$ band for $v''=3$ and 4 with resolution of the J, Ω–and Λ–sublevels. The rotational state population distribution is inverted strongly in v=3, weaker in v=4. There is a strong propensity for the production of OH in the $\Pi(A')$ state, i.e. an antiinversion of the Λ–doublets. Therefore, the reaction of $O(^1D)$ with H_2 occurs via an insertion mechanism.

Vibrational excitation of H_2 was achieved by Stimulated Raman Pumping (SRP). We observed an approximately 70% higher population in OH(v=4) when $H_2(v=1)$ was used in the reaction. The H_2 vibrational excitation does not show a strong effect on the OH product rotational state distribution. Low rotational and high vibrational excitation of the OH product is expected for an abstraction path but not for an insertion reaction. Thus, there seems to be a change in the reaction dynamics when vibrationally excited H_2 is used as reactant. Perhaps "head on" collisions become more favorite and contribute additionally to the OH product rotations.

Higher OH product states are populated than it would be expected from the mean available energy of the reaction. The collision energy is significantly transferred into product rotation, and thus the product rotation becomes more and more dynamically controlled.

A PRELIMINARY INVESTIGATION OF THE $O(^1D)+H_2,D_2,HD$ REACTIONS: CHEMICAL LASER DETERMINATION OF THE NASCENT PRODUCT VIBRATIONAL DISTRIBUTIONS AND THE $O(^1D)+HD$ MACROSCOPIC BRANCHING RATIO

Junlong Shao, Li Yuan, Hongyi Yang, Yukun Gu,
Kaiba Li, Ke Wang, Yusheng Tao

(Dalian Institute of Chemical Physics, Chinese Academy of Sciences, Dalian, China)

Abstract

Concentric Xe flashlamp pumped chemical lasers of different lengths were built to study the $O(^1D)+H_2,D_2$ reaction. $O(^1D)$ was produced by photolyzing high purity ozone to ensure the successful operation of the OD^1 vibrotational chemical laser. The times to threshold of lasing were found to be decreasing with increasing of the reactants pressure or of the discharge voltage of the flashlamp. Thirty three vibrotational laser emissions were identified under free-running chemical laser operations. In addition, fifteen new OH^1 laser emissions were identified.

The nascent product vibrational distributions of the reactions

$$O(^1D)+H_2(^1\Sigma_g^+,v=0,J)\rightarrow OH(^2\pi_i,v',J')+H(^2S_{1/2}),\Delta H_{300}=-181.6KJ/mol \quad (1)$$
$$O(^1D)+D_2(^1\Sigma_g^+,v=0,J)\rightarrow OD(^2\pi_i,v',J')+H(^2S_{1/2}),\Delta H_{300}=-180.8KJ/mol \quad (2)$$
$$O(^1D)+HD(^1\Sigma_g^+,v=0,J)\rightarrow OH(^2\pi_i,v',J')+D(^2S_{1/2}),\Delta H_{300}=-181.6KJ/mol \quad (3)$$
$$O(^1D)+DH(^1\Sigma_g^+,v=0,J)\rightarrow OD(^2\pi_i,v',J')+H(^2S_{1/2}),\Delta H_{300}=-184.9KJ/mol \quad (4)$$

were studied with a four meter Xe flashlamp pumped grating selection chemical laser. The preliminary results obtained were as follows:

reaction	reactants ratio	total pressure torr	vibrational distributions			
(1)	$O_3:H_2:He=1:3:50$	54	N_1/N_0	N_2/N_1	N_3/N_2	N_4/N_3
			0.72±0.01 (1.02)*	0.90±0.12 (0.99)*	.082±0.02 (0.96)*	0.52±0.06 (0.40)*
(2)	$O_3:D_2:He=1:6:10$	34	<0.69	0.95±0.07	0.71±0.03	0.87±0.01**
(3)	$O_3:HD:He=1:3:50$	54	0.76±0.10***	0.83±0.09	0.90±0.15	
(4)	$O_3:DH:He=1:6$	28		0.94±0.08		

* figures in the parenthesis are the results of modelling calculation based upon experimental time to threshold and relaxation rate constants of OH(v') by various species involved in the reaction.
** $N_3/N_4 > 1.0$
*** $O_3:HD:He=1:3:30$, total pressure=34 torr

The effect of the thermalization of $O(^1D)$ before reaction and the rotational equilibrium of OH^1 product on the vibrational distribution were taken into consideration and believed to be of minor influence on our results. Our results are compared with the experimental results of infrared chemiluminescence and laser induced fluorescence and also the results of theoretical calculation based upon different potential energy surfaces.

The macroscopic branching ratio of $O(^1D)+HD$ reaction was studied by varying the concentration of hydrogen in the $O(^1D)+H_2$ reaction, so that the times to threshold were identical for the same laser transition of both reactions. The macroscopic branching ratio thus obtained was 1.8 ± 0.2, which is different from the result obtained by the H(D) atomic detection with laser induced fluorescence by Bersohn. Our results authenticated that the theoretical calculation based upon SL (Schinke-Lester)-type surface is better than those based upon either Murrel-Carter or diatomics in molecules surfaces.

The chemical laser technique is a valuable method for the determination of the nascent product vibrational distributions, especially when it is complemented by modelling calculations if all the necessary relaxation rate constants are available. The potentiality for the improvement of the chemical laser grating selection technique to obtain more accurate results is finally elucidated.

Mechanisms for the Vibrational Deactivation of Large Molecules

John R. Barker

Department of Atmospheric, Oceanic, and Space Sciences
The University of Michigan
Ann Arbor, Michigan 48109-2143
[313-763-6239; usergblg@um.cc.umich.edu]

In recent experiments on V-V energy transfer, on isotope effects in energy transfer, and on the deactivation of various benzene derivatives, some aspects of the mechanisms involved in the vibrational deactivation of large molecules have become clearer. To a large extent, these results support earlier notions of large molecule energy transfer, which are based on the behavior of small species, but there are a few features peculiar to larger species. Larger species have many vibrational modes and thus intramolecular vibrational relaxation and vibrational state quantum statistics may be important. It is also possible that "super-collisions" occur, in which surprisingly large amounts of energy are transferred. In this paper, the results of several experimental investigations will be used to illustrate the principles involved.

COLLISIONAL DEACTIVATION OF HIGHLY EXCITED AZULENE: TRANSITION PROBABILITIES OF ENERGY TRANSFER DETERMINED BY KINETICALLY CONTROLLED SELECTIVE IONIZATION MEASUREMENTS.

U. Hold, T. Lenzer, K. Luther, and A. Symonds
Institut für Physikalische Chemie der Universität Göttingen,
Tammannstrasse 6, D-3400 Göttingen, Germany

An increasing interest in collisional energy transfer probabilities of highly excited molecules has been stimulated by recent observations of some cases with small fractions of very efficient collisions in vibrational deactivation and by the experimental possibility to measure actual evolutions of energy distributions even in the quasi-continuous density of states regime. Predictions of important consequences of small numbers of "strong" collisions in cases like unimolecular fall-off behaviour ask for complementary experimental data, to determine when and to which degree energy transfer probability distributions occur with low amplitude extensions toward very large E values. We report the results of an in-depth study on the collisional relaxation of highly vibrationally excited azulene. The "kinetically controlled selective ionization" (KCSI) technique is used for energy selective detection of molecular populations during their collisional deactivation. The time-resolved observations at various "energy windows" include relaxations at two different initial energies (19800 and 30700 cm^{-1}) and in a variety of collider gases. Detailed master equation analysis is used to derive the time dependent full energy distributions, first and higher moments of energy transfer, as well as transition probability functions of collisional energy transfer.

Diode Laser Studies of Energy Transfer from Highly Vibrationally Excited Aromatic Molecules

A. J. Sedlacek, G. E. Hall, and R. E. Weston, Jr.
Chemistry Department, Brookhaven National Laboratory
Upton, New York 11973
and
G. W. Flynn
Department of Chemistry, Columbia University
New York, New York 10027

We are using time-resolved infrared diode laser absorption spectroscopy to study energy transfer to CO_2 from highly excited aromatic molecules (C_6H_6, C_6D_6, C_6F_6). An excimer laser (KrF, 248 nm) excites the aromatic molecule to the S_1 state, which is converted by rapid internal conversion to the vibrationally excited electronic ground state. Collisional energy transfer to carbon dioxide is followed by probing specific vibrational-rotational states of the CO_2 molecule with the diode laser. Using a tunable etalon, it is also possible to measure absorption line profiles, from which translational temperatures can be determined. Thus, it is possible to measure vibrational, rotational, and translational energy contents of the collisionally excited carbon dioxide.

In previous experiments[1], the kinetics of the excitation of the antisymmetric stretching mode (ν_3) were examined. It was found that the average amount of energy transferred to this mode is only a few wavenumbers per collision; moreover, the rotational temperature of the molecules in the 00^01 state is not significantly increased over the ambient temperature. Yet, experiments by Barker and coworkers[2] show that the average energy loss from aromatic molecules to CO_2 is a few hundred cm^{-1} per collision, and the question arises as to the partitioning of this energy among the CO_2 degrees of freedom. Our present experiments are designed to probe the ground vibrational state (00^00), which is difficult because of background absorption. However, it has been possible to measure line shapes of molecules in high rotational states (J up to 70), and these are compatible with a translational excitation of ~550 cm^{-1} per collision with hexafluorobenzene. At lower J values near the maximum at the ambient temperature, the line shape appears to be a difference of two Gaussians, an absorption increase due to molecules being scattered into the specific rotational state at a high translational temperature combined with a decrease due to molecules being removed at the ambient temperature. A simple two-temperature model fits the observed rotational population distribution reasonably well, and leads to an estimate of ~450 cm^{-1} of rotational energy transferred per collision. The contrast between the rotational and translational energy contents of the ground vibrational state with those of the 00^01 excited state is striking. The basis for this difference will be discussed in terms of the usual Born approximation model of vibrational energy transfer.

We believe that these initial experiments demonstrate that the diode laser technique provides an unequalled method for studying the details of energy transfer processes.

This research was carried out at Brookhaven National Laboratory under Contract No. DE-AC02-76CH00016 with the U. S. Department of Energy and supported by the Division of Chemical Sciences, Office of Basic Energy Science. Support to GWF was provided under Department of Energy Grant No. DE-FG02-88ER13937.

---

[1] A. J. Sedlacek, R. E. Weston, and G. W. Flynn, *J. Chem. Phys.* 94, 6483 (1991).

[2] M. L. Yerram, J. D. Brenner, K. D. King, and J. R. Barker, *J. Chem. Phys.* 94, 6341 (1991).

"Supercollision" Effects on Thermal Unimolecular Reactions

J. Troe
Institut für Physikalische Chemie
Universität Göttingen
Tammannstraße 6, D-3400 Göttingen, Germany

There is photophysical and photochemical evidence that vibrationally highly excited molecules are collisionally deactivated by a majority of weak collisions in the presence of a minority of strong collisions, recently termed "supercollisions". Trajectory calculations seem to confirm the presence of a few strong collisions besides a majority of weak collisions. In the present work, this situation is represented by a biexponential collision model. Analytical solutions of the master equation for low pressure thermal unimolecular reactions are derived for biexponential collision models. It is shown that small fractions of supercollisions tend to fill up efficiently the non-equilibrium depletion of states below the threshold energy. Collision efficiencies β_c for biexponential and exponential models differ because of different $\langle\Delta E^2\rangle$ at a given $\langle\Delta E\rangle$. An approximate expression of the type $\beta_c/(1-\sqrt{\beta_c}) \approx \xi\, u^{\sqrt{\xi}}$ with $\xi = -\langle\Delta E\rangle/F_E kT$, $u = 2\xi(\xi+1)/\xi^2$, and $\xi^2 = \langle\Delta E^2\rangle/(F_E kT)^2$ is proposed and compared with analytical solutions of the master equation for exponential (u=1), biexponential (u < 1) and stepladder (u > 1) models.

Infrared–Ultraviolet Double Resonance Expriments on Collisional Energy Transfer in NO, HCN and C_2H_2

M J Frost*, M Islam, I W M Smith and J F Warr**
School of Chemistry, The University of Birmingham, Edgbaston, Birmingham B15 2TT, UK

*(*present address: Joint Institute for Laboratory Astrophysics, University of Colorado, Boulder, Co 80309–0440, USA)*

*(**present address: Unilever Research Port Sunlight Laboratories, Bebbington, Wirral L63 3JW, SUK*

We shall report the results of double resonance experiments on collisional energy transfer processes involving NO, HCN and C_2H_2. The measurements are performed by using tunable pulses of infrared radiation from an optical parametric oscillator (OPO) to promote molecules into a single level associated with an excited vibrational state, which is accessible by an allowed transition from the vibrational ground state. The evolution of the excited population as collisions occur is then followed in 'real–time' by carrying out laser–induced fluorescence (LIF) measurements. Two kinds of measurement are performed. Either the frequency of the LIF probe laser is fixed on a single rovibronic transition of the molecule being studied and the *time delay* between the two laser pulses is scanned, or the time delay is fixed and the *frequency* of the probe laser is scanned. Combining the results of these measurements provides information about processes of collisional energy redistribution at the state–to–state level. Information gathered at delays corresponding to the order of the average time between collisions yields rate constants for *rotational* energy transfer; that at longer time delays and higher gas pressures gives data for *vibrational* energy transfer.

We shall present results for relaxation processes involving three molecules: (i) NO initially excited to v = 2, j,Ω (and hopefully v = 3,j,Ω) observed via LIF in its $A^2\Sigma^+$–$X^2\Pi_i$ band system; (ii) C_2H_2 initially excited to single levels within one or other of the vibrational states arising from Fermi resonance between the zeroth–order states $3_1(\nu_3)$ and $2_1 4_1 5_1(\nu_2 + \nu_4 + \nu_5)$ and monitored via LIF in its $\tilde{A}^1A_u - \tilde{X}^1\Sigma_g^+$ system; (iii) HCN initiallyexcited to levels with its $3_1(\nu_3)$ fundamental C–H stretching level and observed via LIF in its $\tilde{A}^1A - \tilde{X}\ ^1\Sigma^+$ system.

Collisions of NH($A^3\Pi$,J,N,e/f,v=0) with NH_3, Ar, He

A. Kaes and F. Stuhl

Physikalische Chemie I, Ruhr-Universität, D-4630 Bochum, Germany

Abstract

The (0;0) band of the triplet NH($A^3\Pi \rightarrow X^3\Sigma^-$) transition shows a nicely structured spectrum with well separated Q-, R-, and P-branches and sufficiently resolved rotational and spin components. We have utilized these spectral features to study detailed collisional processes of single excited NH($A^3\Pi$,J,N,e/f,v=0) states. The excited NH(A) were generated by excitation of ground state NH(X) radicals with tunable dye laser light. The ground state radicals were formed in the sequential two photon ArF laser photolysis of NH_3 and by unknown secondary processes. In the absence of inert gas, the system has a temperature of about 430 K, in the presence of a rare gas (Ar, He) the system is close to room temperature.

Eleven states (N,J,e/f) were selected for kinetic investigations. We have measured their fluorescence lifetimes (by extrapolating to zero pressure), rate constants for their quenching and Λ-doublet mixing, and rotational relaxation. All kinetic processes are observed to be very fast (near collision frequency), except quenching by rare gases. The collisional processes involving NH_3 are generally faster than those caused by the rare gases. All processes slow down with increasing rotational quanta with the exception of the fluorescence lifetime which stays constant for N=3-8.

The collisional processes with He are of particular interest, because they can be compared with calculations. Good agreement is obtained for the Λ-doublet mixing with a recent calculation of inelastic cross sections[1] based on an *ab initio* potential surface[2]. The Λ-doublet mixing in collisions with the polar NH_3 can be correlated with the corresponding rotational line strengths hence suggesting dipolar interaction. The rotational relaxation by NH_3 proceeds via two different processes: The relaxation in NH(A) proceeds to the neighboring rotational levels, if spin is conserved. In case of a simultaneous spin change, however, the resulting NH(A) product states are completely thermalized. This second process is consistent with complex formation.

Financial support of the Deutsche Forschungsgemeinschaft is gratefully acknowledged.

References:

1. M. H. Alexander, P. J. Dagdigian, and D. Lemoine, J. Chem. Phys. 95, 5036 (1991).

2. R. Jonas and V. Staemmler, Z. Phys. D 14, 143 (1989).

Chemically Driven Pulsed and Continuous Visible Chemical Laser Amplifiers and Oscillators

J. L. Gole, K. K. Shen, C. B. Winstead, and D. Grantier
School of Physics, Georgia Institute of Technology,
Atlanta, Georgia 30332 Tel. (404) 894-4029

Efficient near resonant intermolecular energy transfer from selectively formed metastable states of SiO and GeO ($a^3\Sigma^+, b^3\pi$) which has been used to form pulsed thallium and gallium atom laser amplifiers at λ = 535 and 417nm has now been employed to form continuous Na atom laser amplifiers at λ = 569 and 616 nm. We have pumped $X^2P_{1/2}$ Tl or Ga atoms to their lowest lying $^2S_{1/2}$ states, and $X^2S_{1/2}$ Na atoms to their lowest excited $4d^2D$ and $5s^2S$ states respectively. Adopting a pumping sequence in which a premixed Group IV A metalloid-receptor atom combination is oxidized, we have observed a system temporal behavior which suggests the creation of a population inversion producing a gain condition in the Tl, Ga, Na, and K systems and forming the basis for full cavity oscillation on the Tl $7^2S_{1/2}$ - $6^2P_{3/2}$ and Na $4d^2D$-$3p^2P$ transitions at 535 and 569 nm respectively. When the thallium and gallium based systems are operative the reaction-energy transfer sequence produces an intense short-lived photon pulse whose intensity for the Tl-Ge-O_3 system exceeds by an order of magnitude that associated with Tl $^2S_{1/2}$ - $^2P_{3/2}$ fluorescence for a 1 cm path length. A system parameterization suggests that the observed amplification in the Tl system corresponds to a superfluorescent event whose duration does not exceed 5ns FWHM. In contrast, the corresponding behavior in the Na-Si-N_2O system produces a <u>continuous</u> amplified output which correlates with a gain coefficient $\alpha \approx 0.1$ at 569 nm and $\alpha \sim 0.03$ at 616 nm. The energy transfer pump of Tl atoms requires the oxidation of a premixed metalloid-metal mixture in order to display the manifestation of what appears to be superfluorescence; the results suggest that this sequence allows for the rapid interaction of a high concentration of the pumping metalloid oxide and receptor metal atom on a time scale comparable to the upper state radiative lifetime. The current observations are in excellent agreement with those results obtained previously in the study of "superradiance" from Tl discharges. The observation of a gain condition is further substantiated when the single pass superfluorescent Ge-Tl-O_3 system is converted to a multipass oscillator configuration (3% output coupling) with a corresponding increase in excess of 10 times the output power of the single pass configuration accompanied by well over an order of magnitude increase in the ratio of stimulated emission to fluorescence. Full cavity studies on the sodium system demonstrate celar continuous operation. Here, with 0.2% output coupling, the light output at 569 nm for the full cavity exceeds that observed with a blocked high reflector by a factor exceeding 1000/1.

Translation-to-Vibration Excitation of $H_2O(001)$ by 2.2 eV H atoms: Rotational Alignment of an Asymmetric Top

Christopher M. Lovejoy and Stephen R. Leone

Joint Institute for Laboratory Astrophysics
University of Colorado and National Institute of Standards and Technology
and Department of Chemistry and Biochemistry, Univ. of Colorado
Boulder, Colorado 80309-0440

Time-resolved Fourier-Transform Infrared (FTIR) Spectroscopy is used to study the process

$$H + H_2O \rightarrow H_2O(v, J_{KaKc}) + H$$

at 2.2 eV center-of-mass collision energy following pulsed excimer laser photolysis of H_2S in $H_2S + H_2O$ mixtures. Nearly nascent rotational distributions ($\leq$ 1.5 rotational state-changing collisions) are obtained. The reaction excites several vibrational states of $H_2O(v)$, including the (020) bend overtone, the (100) symmetric and (001) asymmetric stretches, and the (011) bend plus asymmetric stretch.

Excitation of the water (001) asymmetric stretch is accompanied by preferential in-plane rotation (J vector along the c-axis) for $7 \leq J \leq 17$, but not for low-J levels, which constitutes a unique form of rotational alignment observed without polarization-sensitive probes. We discuss mechanisms which might lead to such excitation, including nearly in-plane impulsive collisions and a "failed-reactive" process which samples the transition state leading to H_2 + OH.

COLLISIONAL VIBRATIONAL ENERGY TRANSFER OF OH ($A^2\Sigma^+$, v'=1)

Leah R. Williams and David R. Crosley
Molecular Physics Laboratory
SRI International
Menlo Park, California 94025

Collisional vibrational energy transfer (VET) and quenching rates in OH are used to calculate atmospheric OH concentrations from laser-induced-fluorescence measurements. Knowledge of the partitioning of energy after collisions, as well as the actual transfer rates, are needed. We use a laser-induced-fluorescence technique in a room temperature flow cell to measure the rotational distribution in v' = 0 after VET from v' = 1, and the VET and quenching rates for v' =1 of the ($A^2\Sigma^+$) state. OH is generated in the ground state in a microwave discharge and excited to the ($A^2\Sigma^+$, v' = 1, N' = 2) level by a frequency-doubled, excimer-pumped dye laser. Added He carrier gas ensures that the rotational distribution in the v' = 1 state remains thermal at 300 K. Time- and frequency-resolved fluorescence in the (1,1) and (0,0) bands is detected through a monochromator and recorded by both a transient recorder and a boxcar integrator.

The rotational distribution in v' = 0 after VET was examined by recording rotationally resolved spectra of the (0,0) band emission. After VET by N_2, the rotational distribution is approximately thermal at 750 K, warmer than the initial temperature in v' = 1 of 300 K. For O_2, the distribution is much hotter, approximately 2000-2500 K. Several other colliders investigated fall into three groups. The distributions for H_2, D_2 and CH_4 colliders are cooler than that of N_2; CF_4, N_2O and CO_2 colliders behave similarly to N_2. Ar appears to have a hot rotational distribution similar to that of O_2.

The VET and quenching rates with N_2 and O_2 colliders were measured and generally agree with previous results. For N_2, the VET rate is 7.5 ± 0.6 μs^{-1} $Torr^{-1}$ and the total removal rate from v' = 1 is 7.6 ± 0.6. Quenching of v' = 1 by N_2 is thus smaller than our estimated experimental error. O_2 is less efficient at VET and more efficient at quenching with rates of 0.5 ± 0.1 for VET and 6.6 ± 0.5 for total removal, yielding a v' = 1 quenching rate of 6.0 ± 0.5 μs^{-1} $Torr^{-1}$.

It is interesting to note that these two colliders, N_2 and O_2, similar in size and shape, lead to very different partitioning of energy after VET into rotational and other channels, and have very different rates for VET and quenching.

This research was supported by the NASA High Speed Research Program.

THE INFLUENCE OF VOLATILE ORGANIC COMPOUNDS OF NATURAL ORIGIN ON THE PHOTOCHEMICAL PRODUCTION OF OZONE

P.D. Goldan[1], S.A. Montzka[2], W.C. Kuster[1], M. Trainer[1,3], and F.C. Fehsenfeld[1,3]
[1]Aeronomy Laboratory, National Oceanic and Atmospheric Administration, 325 Broadway, Boulder, Colorado 80303.
[2]Climate Monitoring and Diagnostics Laboratory, National Oceanic and Atmospheric Administration, 325 Broadway, Boulder, Colorado 80303.
[3]Cooperative Institute for Research in Environmental Sciences, University of Colorado, Boulder 80309.

Volatile organic compounds (VOC's) emitted from forests are chemically active compounds. Because they are emitted in large quantities, they are thought to play a significant role in shaping regional air quality, global tropospheric chemistry, and balancing the global carbon cycle. Currently, there is considerable interest in the role that these compounds play in determining the regional distribution of ozone in the United States. The current understanding of the impact that these natural biogenic compounds have on the production of ozone and the associated regional air quality issues will be briefly outlined.

One of the principal emissions of vegetation is isoprene. The compound is found in significant quantities in most continental areas, including many urban areas. In addition, the by-products of isoprene oxidation, vinyl ketone (CH_2=$CHCOCH_3$) and methacrolein (CH_2=$C(CH_3)COH$), were measured at a rural site in the Southeastern United States during the summer of 1990. Considering all the data over the whole measurement period, the concentrations of these two carbonyls were approximately equal at this isolated rural site. The average mixing ratios for methyl vinyl ketone and methacrolein were 0.98 ppbv and 0.66 ppbv, respectively, while the medians were 0.87 ppbv and 0.57 ppbv.

The concentration of these carbonyls are sufficiently great that their oxidation can also influence the production of ozone. These carbonyls constituted a significant fraction of the volatile organic compounds that were observed. Their mixing ratios were less than that of the dominant compound, isoprene, but were considerably greater than the mixing ratios of anthropogenic compounds (e.g., benzene). In addition, their concentration relative to isoprene provides an important test of our understanding of isoprene oxidation. The mixing ratios of methyl vinyl ketone and methacrolein were found to be highly correlated and exhibited a systematic variation with respect to each other. On average, during the day methyl vinyl ketone was larger than methacrolein while methacrolein tended to be slightly larger during the night. The systematic behavior of these compounds with respect to each other and other compounds measured at the site were simulated using a one-dimensional photochemical model. These observations were consistent with the production and loss by the photochemical oxidation of isoprene, methyl vinyl ketone, and methacrolein. These results will be described.

In addition to isoprene, other reduced carbon compounds are also emitted and have been detected in the atmosphere in substantial quantities. These compounds, and the current understanding of their oxidation mechanisms and products will be briefly discussed.

THE ROLE OF HYDROCARBONS IN THE PRODUCTION OF OZONE EPISODES IN THE SOUTHERN UNITED STATES

M.O. Rodgers and W.L. Chameides

School of Earth and Atmospheric Sciences
Georgia Institute of Technology
Atlanta, GA 30332

Hydrocarbons, along with nitrogen oxides, represent the primary chemical precursors to ozone formation in the lower atmosphere. Hydrocarbons have long been thought to be the major limiting reactant in urban ozone formation with nitrogen oxides limiting in rural and remote environments. Recent research has suggested that highly reactive natural hydrocarbons, especially isoprene, emitted from vegetation may add sufficient hydrocarbon reactivity to many urban environments to make nitrogen oxides the limiting reactant. These emissions have been postulated to be especially important in the southern United States were high temperatures and extensive vegetative cover result in unusually large natural hydrocarbon emissions.

In this presentation we will present results of atmospheric measurements in urban (Baton Rouge, LA and Atlanta, GA), suburban, and rural sites in the southeastern United States and discuss the relative contributions of different hydrocarbon sources to the oxidant chemistry of each location. In each location natural hydrocarbons have been shown to play a major role in total hydrocarbon reactivity.

The Secondary Reactions in the Tropospheric Degradation of Aromatics: Rate Constants for O_2 + Benzene-OH, Toluene-OH, p-Xylene-OH and Phenol-OH

Rainald Koch, Manfred Elend, Jens Nowack, Manfred Siese and Cornelius Zetzsch

Fraunhofer-Institut für Toxikologie und Aerosolforschung
Nikolai-Fuchs-Str. 1, D-3000 Hannover 61

The reversible addition of OH to aromatics and the consecutive reactions of the adducts with NO, NO_2 and O_2 are investigated by employing the pulsed vuv photolysis/resonance fluorescence technique to the systems with benzene, toluene and phenol in Ar. The competition of the removal of the adducts by O_2 with their unimolecular decay (in N_2 containing O_2 at the ppm level) is observed in smog chamber experiments with benzene, toluene and p-xylene.

A simultaneous analysis of several decays of OH in the presence of various concentrations of the aromatics and of O_2 at constant temperature and total pressure is performed by nonlinear least squares fitting of the analytical solution of the full model. At 130 mbar the following rate constants (in units of $10^{-16}cm^3s^{-1}$ at the temperatures given) are obtained for the reactions of the adducts with O_2:

·benzene-OH	·toluene-OH	·phenol-OH
1.6±0.4(299K)	5.6±1.5(299K)	300±40 (323K)
2.1±0.2(314K)	5.6±0.2(321K)	260±30 (333K)
3.0±0.1(333K)	5.6±0.2(339K)	250±20 (337K)
3.7±0.3(354K)	5.3±0.4(347K)	290±20 (343K)
	5.9±0.6(351K)	270±20 (353K)
		320±20 (363K)

Detailed data on the pressure and temperature dependence are presented for phenol.

Upper limits $<10^{-13}cm^3s^{-1}$ are obtained by the same method for the reactions of these adducts against NO, whereas triexponential decays of OH are observed in the presence of NO_2, which are leading to rate constants of $\sim 3 \cdot 10^{-11}cm^3s^{-1}$ (fairly independent of temperature) for the removal of these adducts.

The smog chamber experiments in N_2 at atmospheric pressure and 292 K with variable O_2 at the ppm level yield half-values (of the influence of O_2 compared to atmospheric composition) of ~ 700 (benzene), ~ 450 (toluene), and ~ 250 ppm O_2 (p-xylene) in good agreement with the data for benzene and toluene from the resonance fluorescence method above.

This reactivity of the adducts against O_2 is high enough to compete successfully with NO_2 at NO_x-levels below ~3 ppm for benzene and toluene and ~300 ppm for phenol, i.e. under conditions relevant for the troposphere, and NO_x is involved not earlier than in the subsequent steps, leading to a regeneration of OH via HO_2.

PHOTOOXIDATION STUDIES BY FTIR SPECTROSCOPY OF CF_3COCl and CF_3CFH_2 (HCFC-134a)

Dimitri Boglu, Richard Meller and Geert K. Moortgat

Max-Planck-Institut für Chemie, Air Chemistry,
Saarstrasse 23, D 6500 MAINZ, Germany

Abstract

The use of alternative hydrochlorofluorocarbons, as substitution for fully halogenated species, has recently received wide attention. Those hydrogen-containing compounds are expected to be removed in the troposphere by reaction with OH radicals. This paper deals with the determination of the (photo)oxidation mechanism of CF_3COCl and CF_3CFH_2 (CFC-134a) in air by means of long-path FTIR spectroscopy. CF_3COCl was identified as product of the degradation of CF_3CHCl_2 (HCFC-123).

CF_3COCl (5-10 ppm) was photolysed in air (1 atm) at 254 nm, and the products CO, CO_2, COF_2 were identified. An unidentified IR absorption was tentatively assigned to CF_3OOCF_3 or CF_3OOOCF_3, based on GC/MS analysis.

The Cl-initiated oxidation of CF_3CFH_2 (HCF-134a) was studied by photolysing mixtures of Cl_2 (60 ppm), CF_3CFH_2 (10-20 ppm) in in O_2/N_2 (1 atm). The products, identified by FTIR, were CF_3COF, COF_2, HCOF and $CF_3O_xCF_3$ (see above). A series of experiments were performed with variation of the O_2 partial pressure from 50 mtorr to 760 torr.

Based on the product analysis, the mechanism of the (photo)oxidation of CF_3COCl and CF_3CFH_2 in air will be presented, and the role of the CF_3CFHO_2, CF_3CFHO, CF_3, CF_3O_2 and CF_3O radicals discussed.

To be presented at the XXth Informal Conference on Photochemistry, in Atlanta, Georgia , April 26 - May 1992

The Influence of the Biosphere on Important Atmospheric Gases

Steven C. Wofsy

Division of Applied Science and Department of
Earth and Planetary Science
Harvard University, Cambridge, MA 02138

The vegetation and land surface represent a principal source of many trace gases, including CO_2, CH_4, non-methane hydrocarbons, and sulfur- and nitrogen gases, and a major sink for reactive species such as O_3 and nitrogen oxides. The ABLE series of field experiments was designed to help understand the exchange of important trace gases between the earth's biosphere and the atmosphere. Direct measurement of exchange fluxes represents a difficult challenge due to the large spatial scales and long time scales relevant to the scientific issues. The basic experimental design to obtain direct quantitative measurements will be illustrated, and emerging understanding will be summarized, in discussions of two examples, net annual exchange of CO_2 (storage of carbon by terrestrial ecosystems) and deposition of O_3 and reactive nitrogen oxides.

In-Situ Measurements of Tropospheric OH and HO_2 by Laser Induced Fluorescence at Low Pressures

P.S.Stevens, J.H. Mather, and W.H. Brune
Department of Meteorology, The Pennsylvania State University
University Park, PA 16802

The hydroxyl radical (OH) is the primary oxidant in the atmosphere, and is responsible for photochemical reactions involving many species that affect global climate change. The chemical lifetimes of these species, such as alternative chlorofluorocarbons (HCFC's) and methane, are dependent on the abundance of OH in the troposphere. Another odd-hydrogen species, the hydroperoxyl radical (HO_2), is closely linked to OH by a number of rapid, chemical reactions. Thus a simultaneous in-situ measurement of both OH and HO_2 is important in order to test the photochemical mechanisms responsible for oxidation in the atmosphere.

Due to its high reactivity, OH mixing ratios in the troposphere are extremely small (less than 0.1 pptv) and thus difficult to measure accurately. One promising technique for sensitive detection of the OH radical is laser induced fluorescence (LIF) at low pressures. Ambient air is expanded through a nozzle into a cell at 3-torr and irradiated with a pulsed tunable dye laser at a frequency corresponding to the $A^2\Sigma^+(v' = 0) \rightarrow X^2\Pi(v'' = 0)$ OH transition at 308 nm. A loop injector upstream of the detection axis allows for the addition of reagent NO to convert ambient HO_2 to OH using the fast reaction $HO_2 + NO \rightarrow OH + NO_2$. The OH fluorescence is detected using a fast switching μ-channel plate detector. The detector is turned on 20 nsec after the laser pulse, reducing background interference from Rayleigh scatter, and remains on for 300 ns to collect light from OH fluorescence. This technique results in a minimal detectable OH concentration below 1×10^5 cm^{-3} (S/N = 2) in two minutes. Measurements of ambient OH and HO_2 from the roof of the Meteorology building on the Penn State campus will be presented.

Ion-Assisted Tropospheric OH Measurements

F. L. Eisele and D. J. Tanner
Physical Sciences Laboratory, Georgia Tech Research Institute
Georgia Institute of Technology, Atlanta, GA 30332

The OH radical plays a central role in tropospheric and stratospheric photochemistry. Its primary source is the photolysis of O_3 to give $O(^1D)$ which subsequently reacts with H_2O to give two OH radicals. The OH radical is highly reactive with an atmospheric lifetime of a few seconds or less which results in low, and thus difficult to measure, OH concentrations. During its brief lifetime, however, OH is responsible for the destruction of a number of otherwise relatively stable species such as: methane, CO, nonmethane hydrocarbons, NH_3, and hydrogen-containing halocarbons.

The measurement of OH concentration is accomplished by titrating all of the OH contained in a sample air flow into $H_2{}^{34}SO_4$ in an effectively wall-less laminar flow tube. The gas phase $H_2{}^{34}SO_4$ product is subsequently reacted with NO_3^- ions and the resulting $H^{34}SO_4^-/NO_3^-$ ion concentration ratio is measured by mass spectrometry and used to calculate the $H_2{}^{34}SO_4$ and OH concentration. This technique offers real time (minutes) measurement capability with a detection limit below 1×10^5 cm^{-3}. The ion-assisted technique was first used to measure OH at Mauna Loa Observatory in Hawaii in 1989. An improved version of the initial apparatus recently participated in the first successful OH intercomparison conducted at Fritz Peak Research Station in Colorado from mid July to late August 1991, where OH concentrations were compared to those obtained by NOAA's long path laser absorption technique. Agreement between the two techniques was good in both clean and polluted air masses. This intercomparative OH measurement campaign in conjunction with several supporting measurements provided the first real test of photo-chemical models of OH.

This work was supported by the Office of Exploratory Research of the United States Environmental Protection Agency and by the National Science Foundation.

THE PHOTODISSOCIATION OF CARBONYL HALIDES

F. Wu and R. W. Carr
Dept. of Chemical Engineering and Materials Science
University of Minnesota
Minneapolis, MN 55455

The carbonyl halides $COCl_2$, COFCl and COF_2 are formed in the atmosphere from photooxidation of CCl_4, $CFCl_3$ and CF_2Cl_2, respectively. Photodissociation of these species by sunlight releases F and Cl atoms, and it is necessary to know the quantum yields in order to assess the relevant timescales for photochemical removal. We have investigated the flash photolysis of $COCl_2$, COFCl and COF_2 in the presence of NOCl, which rapidly scavenges both F and Cl atoms.

$$F + NOCl = NO + ClF$$

$$Cl + NOCl = NO + Cl_2$$

Mass spectrometry has been employed to determine yields of Cl_2 and ClF, from which the photodissociation yields of F and Cl atoms from these three carbonyl halides have been inferred.

CHLORYL NITRATE: A NOVEL PRODUCT OF THE $OClO + NO_3 + M$ RECOMBINATION

Randall R. Friedl and Stanley P. Sander
Jet Propulsion Laboratory, California Institute of Technology,
Pasadena, California 91109

and

Yuk. L. Yung
Division of Geological and Planetary Sciences
California Institute of Technology, Pasadena, CA 91125

An understanding of the partitioning of atmospheric chlorine between reactive and inactive forms is essential for quantitative modeling of polar ozone depletion. Presently, the temporal and spatial behaviors of the atmospheric abundances of the major chlorine reservoir species, HCl and $ClONO_2$, are poorly characterized by field measurements. Consequently, the existence of other important chlorine reservoir species can not, at this time, be excluded by the present observational data base.

We have observed new infrared and ultraviolet spectral features arising from the reaction

$$OClO + NO_3 \rightarrow \text{Products}$$

below temperatures of 250 K. We assign these features to chloryl nitrate (O_2ClONO_2), a novel compound of potential atmospheric significance. In addition we have observed a second reaction channel that produces ClO and NO_2. Chloryl nitrate formation predominates at temperatures below 230 K. The reaction rate constant is estimated to be on the order of 10^{-14} cm^3 $molecule^{-1}$ s^{-1} in 1 - 5 torr of helium. We will present a characterization of the reaction phenomenology and discuss the possible significance of chloryl nitrate in the Earth's atmosphere.

Production of vibrationally excited oxygen from the 248 nm photodissociation of ozone.

(abstract)

Laser induced fluorescence was used to measure the nascent rotational distribution of vibrationally excited O_2 $X^3\Sigma_g^-$ (v'' = 9, 12, and 15) produced from the 248 nm photolysis of O_3 in a bulb. Although the fragments were probed in a nearly collision-free environment, it was necessary to distinguish the O_2 (v'') produced directly from the O_3 photodissociation from a small amount produced via the reaction of $O(^1D_2)$ with O_3. The resulting rotational distributions were sharply peaked at relatively low rotational energies. Comparison to statistical and simple impulsive models of dissociation indicate the rotational energy release is largely impulsive. This is consistent with previous studies of other products of the photodissociation of O_3.

Michael Daniels
Cornell University

Product State Distributions in the Photodissociation of Expansion-Cooled NO_2 near the $NO(X^2\Pi)$ v=1 Threshold

D.C. Robie, M. Hunter, J.L. Bates* and H. Reisler
Department of Chemistry, University of Southern California
Los Angeles, CA 90089-0482

ABSTRACT

The photodissociation of NO_2 near the NO v=1 threshold was studied using a supersonic molecular beam of NO_2 and multipohoton ionization detection of $NO(X^2\Pi_{1/2,3/2})$. The vibrational populations near the v=1 threshold are nonstatistical as compared with the predictions of Phase Space Theory (PST). The rotational distributions in both NO v=0 and 1 show pronounced structures and fluctuations; however, their average is described fairly well by PST, suggesting that the decomposition of NO_2 at $\lambda \geq 370$ nm can be viewed as vibrational predissociation on the mixed $\tilde{X}^2A_1/1^2B_2$ state. Similar structured rotational distributions have been observed in recent studies of the photodissociation of CO_2 at 157 nm [Miller et al., J. Chem. Phys. 96 (1992) 32]. The structures in the rotational distributions are interpreted as fluctuations inherent in the decomposition of an excited complex with many overlapping resonances (Ericson fluctuations).

* Present address: Department of Chemistry, Santa Monica College, Santa Monica, CA 90404

Photodissociation of Silane in a Supersonic Expansion

Th. Glenewinkel-Meyer[1], J.A. Bartz, and F.F. Crim
Dept. Chemistry, University of Wisconsin, Madison, WI 53706

We report on mass spectrometric investigations of the photodissociation of silane (SiH_4) in a pulsed supersonic molecular beam. Laser assisted decomposition of SiH_4 plays a major role in chemical vapor deposition of thin silicon films for semiconductors. However, information about the exact fragmentation processes leading to formation of silicon atoms, e.g. through subsequent hydrogen ligand loss, is still scarce. Very few experiments have actually been done utilizing the collision-free region of a supersonic molecular jet, where a single molecule may decay undisturbed by any possible collision partners.

In our experiments, the molecular beam is crossed perpendicularly by two counterpropagating pulsed laser beams. The first laser pulse photodissociates the target with photons in the ultraviolet range between 210 and 300 nm. They are produced by doubling the 500 to 600 nm output from a Nd:YAG pumped dye laser or further frequency mixing of those photons with the Nd:YAG fundamental. Because of the high UV fluence, the dissociative excitation observed may be due to more than one photon. After a delay time of up to 1 μs the second laser pulse ionizes the photodissociation fragments using vacuum-ultraviolet photons of 125 nm wavelength. They are produced by resonant four-wave mixing in Hg-vapor of the doubled output from another Nd:YAG/dye laser combination. The fragment ions are then accelerated into a time-of-flight mass spectrometer and detected with an ion multiplier.

The fragmentation pattern of the parent SiH_4 molecule as a function of UV excitation wavelength and delay time between the excitation and ionization step provides insight into the distribution of the electronically excited silane states, from which the decay process starts. It also indicates the possible couplings between those states and the observed product asymptotes. These results will lead to the next planned sequence of experiments, namely photodissociation of germane, GeH_4, and precursor molecules of III-V compounds, e.g. GaAs, that are important in semiconductor manufacturing.

[1]Feodor-Lynen-Fellow of the Alexander-von-Humboldt Foundation

PHOTODISSOCIATION DYNAMICS OF METHANETHIOL EXCITED IN THE FIRST ABSORPTION BAND. James S. Keller, Elke Jensen, Phillip W. Kash, and Laurie J. Butler, The James Franck Institute and Department of Chemistry, The University of Chicago, Chicago IL 60637.

We investigate the photochemistry of methanethiol excited to its lowest electronically excited state. The two photolysis wavelengths used in these experiments, 248 and 222 nm, lie within the molecule's first absorption band. We measured the velocity and angular distributions of photofragments and collected the dispersed Raman emission from photoexcited parent molecules. The results of this work are contrasted with our earlier studies involving photoexcitation to the second electronically excited state and also with the photochemistry of the analogous methanol system. In both methanol and methyl mercaptan, the preferred product channels correspond to fission of a stronger bond (O–H or S–H) over a weaker bond (C–O or C–S). The influence of low-lying Rydberg states is explored for these systems. *Ab initio* calculations of the lowest excited potential energy surface of methanethiol are also presented.

Nonadiabaticity and the Competition between Alpha, Beta, and Gamma Bond Fission upon $^1(n,\pi^*(C=O))$ Excitation in Acetyl, Bromoacetyl, and Bromopropionyl Chloride

P. W. Kash, M. D. Person, G. C. G. Waschewsky, and L. J. Butler
The James Franck Institute and Department of Chemistry
The University of Chicago, Chicago, Illinois 60637

Abstract

One of the central challenges in chemistry is to develop predictive ability for the branching between energetically allowed chemical reaction pathways. This work investigates how molecular dissociation induced by local $^1(n(O),\pi^*(C=O))$ electronic excitation at a carbonyl functional group can result in preferential fission of an alpha bond over a weaker bond beta or gamma to the functional group and how nonadiabaticity in the dynamics drives the selectivity. The experiment measures the photofragment velocity and angular distributions from the photodissociation of acetyl chloride, bromoacetyl chloride and bromopropionyl chloride at 248 nm, identifying the branching between bond fission channels and the mechanism for the selectivity. The anisotropic angular distributions measured show dissociation occurs on a time scale of less than a rotational period, resulting in primary C-X (X = Cl, Br) bond fission but no significant C-C bond fission. While the selective fission of the C-Cl over the C-C alpha bond can be predicted from the adiabatic correlation diagram for this new class of Norrish Type I cleavage, the preferential fission of the C-Cl alpha bond over the C-Br bond beta to the carbonyl group would not be predicted on the adiabatic potential energy surface. In bromoacetyl chloride, fission of the C-Cl and C-Br bonds occurs with a branching of 1.0:1.1 (1.0:0.4 from $^1n\pi^*$ transition), compared with a predicted statistical branching ratio of 1:30. In bromopropionyl chloride, the measured ratio is 1:0.4 (with almost no C-Br fission resulting from the $^1n\pi^*$ transition). This preferential α-bond fission is attributed to a dissociation mechanism on the coupled $(n,\pi^*(C=O))$ and $(n(X),\sigma^*(C-X))$ electronic states, a model consistent with the lack of C-C fission and the measured kinetic energy and angular distributions. The selectivity results from the relative strengths of the electronic coupling between the initially excited $(n,\pi^*(C=O))$ bound configuration and the two $(n(X),\sigma^*(C-X))$ states, the weaker coupling inhibiting the adiabatic crossing over the barrier to C-Br bond fission. Our current investigation of this intramolecular electronic coupling involves calculation of the electron correlation between the relevant excited electronic states, with the goal of evaluating the relative contribution of coupling matrix elements which depend on transition dipole-transition dipole coupling and those which depend on non-zero orbital overlap. The results demonstrate the need to go beyond the Born-Oppenheimer approximation to gain predictive ability in any reactive system where the electronic configuration changes along the reaction coordinate, particularly at barriers due to configuration crossings.

Gas and Condensed Phase Photochemistry of OClO

Anne Jefferson, Erik C. Richard and Veronica Vaida

Department of Chemistry and Biochemistry
University of Colorado
Boulder, CO 80309

Abstract

The photochemistry of the $\tilde{A}\,^2A_2 \leftarrow \tilde{X}\,^2B_1$ electronic transition of OClO in the gas and condensed phases is reported. Direct absorption of OClO with an FT spectrometer and photochemistry of OClO with REMPI - MS reveal two photodissociation paths. In the UV photolysis of OClO resonant wavelength spectra of ClO and Cl photofragments were measured. ClO is formed vibrationally hot ($v = 3$-5). The formation of Cl atoms suggests OClO isomerization to ClOO with ClOO dissociating to Cl and O_2. Picosecond pump - probe experiments of OClO in water solution confirm the formation of ClO, Cl and ClOO. In mass spectroscopic experiments OClO was found to cluster readily with itself and H_2O.

Cl Atom Production from Near UV Photolysis of OClO

Elizabeth Bishenden and D.J. Donaldson
Department of Chemistry, University of Toronto,
80 St. George St., Toronto, Ontario, M5S 1A1

Near UV photolysis of OClO using a frequency-doubled Nd:YAG-pumped (532 nm) dye laser results in two reactions:

$$OClO \rightarrow OCl + O$$

$$OClO \rightarrow Cl + O_2$$

The first of these reactions occurs throughout the near UV wavelength region. Using (2+1) REMPI at 235.4 nm and 237.8 nm, respectively, we have detected both $Cl(^2P_{3/2})$ and $Cl(^2P_{1/2})$ after photolysis of OClO at wavelengths shorter than 379 nm. These short wavelengths correspond to highly vibrationally excited states of the electronically excited parent molecule. At 362 nm, the quantum yield of ground state chlorine atoms peaks at 0.15±0.1; at all wavelengths the yield of spin-orbit excited chlorine atoms is five times less than the ground state chlorine atoms.

The different wavelength ranges for the two photolysis reactions indicate that the reactions follow different pathways. Competing predissociative pathways for the photolysis of OClO are discussed.

Photodissociation Dynamics of $RN_3 + h\nu \rightarrow R + N_3$, R = H,D,CN

Stephan Baumgärtel, Karl–Heinz Gericke, Tobias Haas, Michael Lock, and Christof Maul

Institut für Physikalische und Theoretische Chemie, Johann Wolfgang Goethe – Universität, Niederurseler Hang, 6000 Frankfurt am Main 50, FRG

The uv–photodissociation dynamics of $HN_3 + h\nu \rightarrow H + N_3$ at 193nm, 243nm, 248nm and of $NCN_3 + h\nu \rightarrow CN(v,J) + N_3$ at 193nm have been analyzed by observation of the H resp. of the CN product using Doppler–resolved laser induced fluorescence and time–of–flight techniques. The quantum yield ϕ for the formation of $H+N_3$ is about ϕ = 0.2 with a minor dependence on the excitation energy. The internal energy of the N_3 product molecule, determined by the recoil velocity of the hydrogen atom, strongly increases with increasing photolysis energy. The $<\mu \cdot v>$ correlation is negative and independent of the HN_3 excitation wavelength, indicating a spatial distribution where the recoil direction of the fragments is aligned perpendicular to the transition dipole moment μ of the parent HN_3.

In the photodissociation of NCN_3 at 193nm most of the available energy is transferred into product translation. However, the CN(v,J) fragment is significantly rotationally ($f_{rot}(CN)$=9.1%) and slightly less vibrationally ($f_{vib}(CN)$=5.8%) excited. The rotational distribution is non–statistical. With increasing vibrational excitation the CN product rotation decreases. The highest populated vibrational level is v=2. The spin of the elctron is a spectator in the dissociation process. The internal energy of the N_3 partner fragment is analyzed by observation of CN Doppler profiles. The N_3 product shows a broad internal distribution, which is probably caused by strong bending motions comparable to the dissociation of HN_3. The rotational excitation of the CN fragment is essentially induced by "in–plane" and "out–of–plane" motions of the NCN ν_5(a') and ν_9(a") bending modes.

PHOTODISSOCIATION OF JET-COOLED NITROSYL CHLORIDE NEAR 380NM

M.Hippler and J.Pfab

Dept of Chemistry, Heriot-Watt University
Edinburgh EH14 4AS, Scotland

Nitrosyl chloride as a triatomic molecule may serve as a benchmark for testing ideas and theories about photodissociation, because the internal excitation of the NO fragment can be probed with great precision. In addition, good quantum mechanical calculations on the potential energy surfaces of NOCl are available.

In the experiment, a 380nm tunable dye laser is focused into the core of a freely expanding jet of nitrosyl chloride seeded in argon or helium, photodissociating the NOCl and simultaneously probing the nascent NO *via* (2+1) REMPI.

The NO fragments are highly rotationally excited. The rotational population distribution can be fitted with a Gaussian curve peaking around the quantum number j= 40. This corresponds to an average rotational energy of 2750 cm^{-1} or 21% of the dissociation energy available. The NO fragment is mainly in the vibrational ground level v= 0, however, and only slightly vibrationally excited.

It is inferred from our spectra that the π^* orbital lobe of the odd electron of NO is out of plane of rotation of the NO fragment. It is therefore concluded that the orbital lobe of NO is out of plane of the NOCl molecule in the excited state of nitrosyl chloride prior to dissociation, too.

The experimental results compare quite favorably with recent calculations by H.Reisler *et al.* [1] confirming that photodissociation near 380nm occurs *via* a very repulsive excited potential surface.

[1] Y.Y.Bai, A.Ogai, C.X.W.Qian, L.Iwata, G.A.Segal and H.Reisler, J.Chem.Phys. 90, 3903 (1989)

ABSORPTION SPECTROSCOPY OF POLARIZED TL PHOTOFRAGMENTS

D.V.Kupriyanov[1] and O.S.Vasyutinskii[2]
[1]Technical University, SU-195251, St.-Petersburg, Russia
[2]A.F.Ioffe Physico-Technical Institute, SU-194021,
St.-Petersburg, Russia

The field of photodissociation of diatomic molecules has been investigated extensively over past several decades but only recently several methods have been proposed for obtaining detailed information on the dynamics of the occurring processes.

In this work we used the absorption spectroscopy of polarized atomic photofragments (ASPAP) /1/ to study the dynamics of TlBr photodissociation at 266nm. We present both experimental and theoretical studies of polarized $6^2P_{1/2}$ ground state and metastable $6^2P_{3/2}$ thallium atoms produced in photodissociation of TlBr molecules by polarized impulse laser radiation. The atomic polarization (i.e. Zeeman population differences) led to the dichroism of the atomic vapors and the ASPAP method is based on the detection of this dichroism /2/. We studied the temporary changes of the thallium orientation (M selection) and alignment (|M| selection) in various experimental conditions.

Theoretical interpretation of the experimental results enabled to distinguish the channels of the photodissociation reaction under study and to determine the probabilities of a few early unknown radial nonadiabatic transition in the decaying molecules.

1.O.S.Vasyutinskii *Sov.Phys.JETP Lett.* 31,428,(1980)
2.D.V.Kupriyanov, B.N.Sevastianov, and O.S.Vasyutinskii *Z.Phys.D - Atoms, Molecules and Clasters* 15,105,(1990)

TIME-EVOLUTION OF THE PHOTOFRAGMENT ANGULAR DISTRIBUTION: $\beta(t)$

Janet R. Waldeck and Moshe Shapiro

Department of Chemical Physics

Weizmann Institute, Rehovot 76100 Israel

We treat the photodissociation of a linear molecule with a coherent laser pulse. Expressions are derived for the *time-dependent* the anisotropy parameter, $\beta(t)$, both during and after the excitation process. We then present a study of the photo-predissociation of NaI and show how $\beta(t)$ may be obtained from the energy resolved photodissociation amplitudes. For the range of frequencies spanned by some of the femto-second transition state experiments,[1] the spectrum reveals a sequence of narrow Fano-type resonances whose shape is due to interferences induced by curve crossing processes. We find that the more commonly known frequency resolved anisotropy, $\beta(\omega)$, can vary across these resonances from the expected value for a purely parallel electronic transition (β=2) to almost its value for a perpendicular transition (β=-1). A general *time-dependent* radial matrix element can be obtained by "folding" the laser pulse with the energy-resolved dissociation amplitudes:

$$R_J = \int dE c_E(t) e^{-iEt/\hbar} \epsilon(\omega_{Ei}) \langle EJ^- | \vec{\mu}(r) | E_i J_i \rangle$$

Here, $\langle EJ^- | \vec{\mu}(r) | E_i J_i \rangle$ denotes a frequency- resolved transition amplitude between the initial $|E_i J_i\rangle$ and final $|EJ^-\rangle$ states, $\epsilon(\omega_{Ei})$ gives the electric field amplitude distritution and $c_E(t)$ accounts for the *time-dependence* of the expansion coefficients of the excited state wavefunction. Integration is over the continuum energy. The time-dependent anisotropy, $\beta(t)$, generated from the above radial matrix elements, depends sensitively on the location and width of the pulse. Proposals are made as to ways of measuring $\beta(t)$.

[1] T.S. Rose *et al.* J.Chem.Phys. 88, 6672 (1988).

Abstract for the XXth Informal

Conference on Photochemistry, Atlanta 1992.

Time Resolved FTIR studies of the photolysis of CH_2CFCl

G Hancock and D G Weston
Physical Chemistry Laboratory
South Parks Road
Oxford
OX1 3QZ
England

Time resolved infrared chemiluminescence has been observed following the infrared multiple photon dissociation of 1–Chloro 1–Fluoro Ethylene at 10.64μm. Products from two major channels have been observed:

$$CH_2{=}CFCl \longrightarrow HF + CH{\equiv}CCl$$
$$CH_2{=}CFCl \longrightarrow HCl + CH{\equiv}CF$$

The ratio of channels (1) to (2) has been estimated at 17:1, higher than has been observed in previous studies of the irmpd of this molecule; the discrepancy has been attributed to the difference in fluence and pressure used in the studies. The rovibrational distribution of HF has been analysed under nascent and near–nascent conditions, from which we estimate a vibrational temperature of 6500K, which is higher than expected on a purely statistical basis, and a rotational 'temperature' of 1500K, considerably lower than expected statistically. The fraction of energy in HF vibration, at 0.10, is less than has been observed after photolysis at 193nm but the two sets of results can be considered consistent if a HF frequency in the 'transition state' is assumed to be less than for that of free HF. From a series of cold gas filter experiments, we estimate the vibrational temperature of HCl to be approximately 6000K.

A Time-Resolved FTIR Study of the Photodissociation of Pyruvic Acid

G. E. Hall, J. T. Muckerman, J. M. Preses, and R. E. Weston, Jr.
Chemistry Department, Brookhaven National Laboratory
Upton, New York 11973
and
George W. Flynn
Chemistry Department, Columbia University
New York, NY 10027

We have recently developed an experimental arrangement for carrying out time-resolved Fourier transform infrared (FTIR) spectroscopy to probe the emission spectra of unstable species produced by photodissociation or in chemical reactions initiated by the radiation from a pulsed excimer laser. The method is similar to those previously described by Sloan and by Leone. It differs from the earlier methods, because at each of the positions of the moving interferometer mirror, the time dependence of the infrared signal is measured for ~200 μs, or 100 channels of a transient digitizer. In this respect it is essentially the same as the method now being used by Sloan, although the specific instrumentation is different.

In an initial application of this device we have reinvestigated the gas-phase photodissociation at 193 nm of pyruvic acid (2-oxo-propanoic acid):

$$CH_3COCOOH + h\nu(193\ nm) \rightarrow CO_2 + CH_3CHO\ .$$

Previous investigations have used either low-resolution IR emission from the ν_3 vibrational manifold of the product CO_2 (at ~4.3 μm)[1], or diode laser absorption spectroscopy in the same spectral region[2]. The experiments of Rosenfeld and Weiner[1] indicated that CO_2 was produced in vibrational states higher than the 00^01 state. This was confirmed by the more quantitative measurements of the Flynn group[2], who determined populations of several levels in the 00^0p and $0n^l0$ manifolds, from which they derived vibrational temperatures of 3700±1000 K and 1800±150 K, respectively.

The emission spectrum we observe at ~10 μs after the photolysis pulse is strongly red-shifted from the room-temperature absorption spectrum of CO_2, with a maximum at ~2200 cm^{-1}. The peak gradually shifts to the blue at longer times, and by 150 μs the spectrum has clearly identifiable vibrational-rotational lines from the CO_2 00^01 state. Initial attempts to fit the nascent population distribution with thermal distributions at very high temperatures were unsuccessful. However, a statistical model using a linear surprisal gives good agreement with our observations and with the vibrational temperatures found by the Flynn group. This agreement is obtained only if the available energy is set equal to the 150 kcal/mol released if acetaldehyde is formed directly. Production of the hydroxycarbene (CH_3COH) as an intermediate releases only 98 kcal/mol, and with this energy the linear surprisal model cannot be made to agree with the experimental observations.

This research was carried out at Brookhaven National Laboratory under contract DE-AC02-76CH00016 with the U. S. Department of Energy and supported by its Division of Chemical Sciences, Office of Basic Energy Science. Support to GWF was provided under Department of Energy Grant No. DE-FG02-88ER13937.

[1] R. N. Rosenfeld and B. Weiner, *J. Am. Chem. Soc.* **105**, 3485 (1983).
[2] C. F. Wood, J. A. O'Neill, and G. W. Flynn, *Chem. Phys. Letts.* **109**, 317 (1984); J. A. O'Neill, T. G. Kreutz, and G. W. Flynn, J. Chem. Phys. **87**, 4598 (1987).

PHOTODISSOCIATION OF METHYLACETYLENE AND ACETYLENE AT 193NM

Kanekazu Seki and Hideo Okabe
Department of Chemistry, Howard University
Washington, DC 20059

The photolysis of methylacetylene(MA) at 193 nm was studied using Fourier Transform Infrared Spectroscopy for product analysis. Main primary processes are CH_3C_2H + hv-->CH_3C_2 + H and CH_3C_2H + hv--> CH_2 + C_2H_2 with a quantum yield of 0.7 $\pm$ 0.1 and 0.11 $\pm$ 0.01 respectively. Cl_2 was used as H atom scavenger. The CD_3C_2H photolysis was used to confirm that acetylene-d_1 formed is a primary product and is independent of reactant pressures. The H atom addition to the center carbon atom of CD_3C_2H produces CD_3 + C_2H_2 with a yield of 0.10 $\pm$ 0.01; C_2H_2 is reduced to almost zero above 5 Torr of MA. The remaining H atom addition to the end carbon would produce allene and propylene. The photolysis of CD_3C_2H and Cl_2 mixtures produces only HCl and DCl is not found, indicating that H atoms are dissociated immediately from the triple bonded carbon, although the C-D bond in CD_3C_2H is much weaker. The photolysis of acetylene at 193 nm is performed and the primary quantum yield of about 0.2 is obtained from C_4H_2 yield.

PHOTOLYSIS OF $NFCl_2$

Deborah B. Exton and Julanna V. Gilbert
Department of Chemistry
University of Denver
Denver, Colorado 80208

Photolysis studies of gas phase $NFCl_2$ in argon were performed with a KrF excimer laser (249 nm). Photolysis of the $NFCl_2$ samples resulted in both UV and visible emission. The UV emission consists of two short-lived (<20 ns) bands, a strong band at 258 nm and a weak band at 284 nm. These bands are consistent with the (D'-->A') transitions of Cl_2 and ClF, respectively, and are assigned as such. The approximate Cl_2(D'):ClF(D') ratio is 10:1, as calculated from the intensities of the 258 and 284 nm features. The fact that Cl_2 is the product favored by the photodissociation implies that N-Cl bond scission is preferred over N-F bond scission in this system.

The visible spectrum consists of an unresolved continuum extending from about 390 to 500 nm, with a maximum at 437 nm and several defined bands on the short wavelengths side of the continuum. At this time, the source of the visible emission remains a mystery.

The time profiles of the Cl_2 and ClF emission indicate that the Cl_2 and ClF are direct photoproducts rather than products of secondary reactions, and the fluence dependence data show that the Cl_2 and ClF are produced in a single photon process. The photolysis is assumed, therefore, to involve a concerted process in which two N-X bonds are broken, producing the halogen molecule and the corresponding nitrene, i.e.,

$$NFCl_2 + h\nu \begin{cases} \longrightarrow Cl_2^* + NF \\ \longrightarrow ClF^* + NCl \end{cases}$$

No data on the NF or NCl fragments is available from this study, however, if spin orbit coupling is weak in $NFCl_2$, ground state NF and NCl fragments are predicted from the photolysis.

Data obtained in this study suggest that $NFCl_2$ is an endothermic compound. This is consistent with estimated values of the ΔH_f for NCl_3 which have been reported.[1,2]

1. T.C. Clark, M.A.A Clyne, Trans. Fraraday Soc., 65, 2994, (1969).; T.C. Clark, M.A.A. Clyne, Trans. Faraday Soc., 66, 372, (1970).

2. W.A. Noyes, W.F. Tuley, J.Amer. Chem. Soc., 47, 1336, (1925).

Photofragmentation of CF_3I^+ Produced by Resonant Multiphoton Ionization

Leslie D. Waits, Ronald J. Horwitz, Robert G. Daniel, and Joyce A. Guest
Department of Chemistry
University of Cincinnati
Cincinnati, OH 45221-0172

Resonant (2+1) multiphoton ionization of CF_3I in the 300-306 nm range provides sufficient energy for subsequent decomposition to $CF_3^+ + I$. Absorption of a fourth photon is required to access the $CF_3 + I^+$ channel. We have used time-of-flight mass spectrometry to examine I^+ and CF_3^+ fragments following resonant excitation of CF_3I. The I^+ fragments observed are shown to be the photoproducts of single-photon dissociation of CF_3I^+. The CF_3^+ fragments observed appear to be produced by a combination of statistical dissociation of the parent CF_3I^+ and the same ion photodissociation process that leads to I^+. Photoelectron spectra taken in collaboration with J. R. Appling (University of Kentucky) show that the CF_3I^+ photoion is formed predominately in its ground $\tilde{X}^2E_{3/2}$ state. Modeled translational distributions will be used to interpret the ion decomposition dynamics.

PHOTOINITIATED REACTIONS IN MASS-SELECTED MAGNESIUM ION-MOLECULE COMPLEXES

C.S. Yeh, K.F. Willey, D.L. Robbins, J.E. Salcido and M.A. Duncan

Department of Chemistry
University of Georgia
Athens, Georgia 30602

Magnesium ion-molecule cluster complexes(e.g., Mg^+-CO_2, Mg^+-H_2O, Mg^+-CH_3OH) are produced in a modified pulsed-nozzle laser vaporization cluster source. These complexes are studied by mass-selected photochemistry in a specially designed reflectron time of flight mass spectrometer. Photoexcitation of these complexes near the Mg^+(^2S-^2P) atomic transition induces a variety of photochemistry. These photoinduced reactions are first observed in the single molecule complexes. The known thermochemistry for the reactions of non-clustered species combined with photoexcitation energy makes it possible to obtain the binding energy of the ion complex. Vibrationally resolved spectra are obtained for some of these complexes (e.g., Mg^+-CO_2).

SPECTROSCOPY AND PHOTOCHEMISTRY OF METAL DIMER RARE GAS COMPLEXES

D. L. Robbins, K. F. Willey, C. S. Yeh,
J. S. Pilgrim, B. J. Salcido, M. A. Duncan*

Department of Chemistry
University of Georgia
Athens, Georgia 30602

Resonant two photon ionization spectroscopy, has been used to obtain vibrationally resolved electronic spectra for the B states of Ag_2Ar, Ag_2Kr, and Ag_2Xe. Predissociation in these complexes is slow enough to allow sharp vibrational bands to be observed up to several hundred wavenumbers of vibrational energy in the excited state. Three vibrational modes are active in each of the silver dimer-rare gas complexes, allowing the determination of vibrational constants, anharmonicities, and cross-mode couplings. The excited state binding energies are ($D_0' = 755, 1205, 2761$ cm^{-1} for Ar, Kr, Xe, respectively). Ground state energies are ($D_0'' = 275, 394, 1234$). The anomalously high ground state binding energy of Ag_2Xe may indicate a change in geometry relative to the Ar and Kr complexes. Some hot bands are observed for the Ag_2Xe complex in the Ag_2Xe^+ channel, but also via photodissociation in the Ag_2^+ channel.

PHOTOCHEMISTRY AND CHARGE-TRANSFER IN MASS-SELECTED ORGANOMETALLIC CLUSTERS

K. F. Willey, C. S. Yeh, D. L. Robbins,
J. S. Pilgrim, M. A. Duncan*

Department of Chemistry
University of Georgia
Athens, Georgia 30602

Ion-molecule complexes are produced in a pulsed nozzle cluster source by expanding organic seed/rare gas mixtures over a metal rod during laser vaporization. The supersonically cooled ions are extracted from the molecular beam in the first stage of a reflectron time-of-flight mass spectrometer. The ion-molecule complex of interest (e.g. Ag^+-benzene, Mg^+-acetone) is then mass-selected from the normal cluster distribution by its flight time through the first stage before entering the reflectron region. Tunable visible and UV laser radiation are used to probe ions at the turning point in the reflectron. Dissociation yields charge-transfer (e.g. Ag^+-benzene $\xrightarrow{h\nu}$ Ag + benzene$^+$) in a majority of the systems studied to date. From these observed photoinduced reactions it is possible to derive energetics and mechanisms for this new photochemical process seen in the gas phase. Binding energies derived for the ground state of these complexes are compared to recent results from *ab initio* calculations.

The ArNO Van der Waals' Complex: Observation and Analysis of the A-X Electronic Transition

Michael J. McQuaid and Rosario C. Sausa
U.S. Army Ballistic Research Laboratory
SLCBR-IB-B
Aberdeen Proving Ground, MD 21005-5066

Abstract: Spectra associated with bound-bound transitions of ArNO have been observed using 1+1 REMPI/TOFMS near 226 nm. They are associated with the $A^2\Sigma$ - $X^2\Pi$ transition of the NO monomer. The features appear in the same wavelength range reported by Miller[1] for this transition of the complex, but there are significant differences between the results. The source of these differences remains to be determined. The Hamiltonian and wavelength basis set developed by Chakravarty et al.[2] is being used to analyze the data. In the current analysis a radially averaged angular potential related to the Legendre polynomials is being assumed. Estimates of the barrier to internal rotation and the geometry of the complex based on this analysis will be discussed.

---

[1] J.C. Miller, J. Chem. Phys., 90, 4031 (1989)

[2] C. Chakravarty, D.C. Clary, A. Degli Eposti, and H.-J. Werner, J. Chem. Phys. (1991)

Electronic Spectroscopy and Predissociation of Ne-CN.

Suli Fei and Michael C. Heaven
Department of Chemistry, Emory University, Atlanta, GA 30322

In previous work we have recorded and analyzed three bands of Ne-CN which were associated with the CN *B-X* 0-0 transition. These features were assigned to the electronic origin and two internal rotor levels [Y. Lin and M. C. Heaven, J. Chem. Phys. 94, 5765 (1991)]. More recently we have re-examined the Ne-CN *B-X* spectrum in the vicinity of the CN 0-0 transition, and recorded spectra for the bands associated with the CN 1-0 transition. Ten previously unobserved bands have been characterized. Features corresponding to multiple excitations of the internal rotor mode, and excitation of the -Ne stretch, are present. We are in the process of fitting a two-dimensional potential energy surface to this data.

A search for Ne-CN bands associated with the CN *A-X* 3-0 transition was made. A single feature, with a homogeneously broadened rotational envelope, was observed next to the CN $A^2\Pi_{1/2}$-*X* , 3-0, R(1) line. Complex features associated with the $A^2\Pi_{3/2}$-X transition could not be found. A possible explanation for these results is that Ne-CN(*A*, v=3) is subject to rapid predissociations caused by spin-orbit relaxation and internal conversion. The fact that fluorescence cannot be seen following excitation of the lower energy spin-orbit component suggests that internal conversion (Ne-CN ($A^2\Pi_{3/2}$, v=3) → Ne + CN(*X*)) is much faster than *A* state radiative decay. Observation of fluorescence following excitation of the higher energy spin-orbit component would then imply that spin-orbit relaxation (Ne-CN ($A^2\Pi_{1/2}$, v=3)-Ne → Ne + CN ($A^2\Pi_{3/2}$, v=3) is much faster than internal conversion. These speculations are being explored in a series of optical-optical double resonance experiments.

Development of a Three-Dimensional Potential Energy Surface for the *A* State of OH/D-Ar.

Udo Schnupf, Joel M. Bowman, and Michael C. Heaven.
Department of Chemistry, Emory University, Atlanta, GA 30322

We have calculated vibrational energy intervals for ArOH/D (*A*, v=0 and 1) using exact methods for zero rotational angular momentum (N=0), and a centrifugal sudden approximation for N=1. A modification of our previous two-dimensional potential surface for ArOH/D (*A*, v=0) [J. M. Bowman, B. Gazdy, P. Schafer, and M. C. Heaven, J. Chem. Phys. 94, 2226 (1990); 94, 8858E, (1990)] was made to include explicit OH/D vibrational dependence. By a trial-and-error procedure the potential parameters were optimized to give good agreement with the observed vibrational intervals. Rotational constants, calculated from the optimized potential surface, were also found to be in agreement with the experimental values. A novel inverse isotope effect, noted for the van der Waals stretching vibration, was predicted and rationalized by these calculations.

XXth Informal Photochemistry Meeting
April 26- May 1, 1992
Atlanta, GA

ABSTRACT

Resonances and Predissociation dynamics of Ar-OH*(v=0,1), Bela Gazdy and Joel M. Bowman, Department of Chemistry, Emory University, Atlanta, GA 30322

We report results of coupled channel calculations of low scattering of Ar+OH*(v=0) and high energy scattering of Ar+OH*(v=1). Broad resonances are seen in the former and much narrower ones for the latter. The positions of the high energy resonances are in excellent agreement with L^2 calculations of the quasibound states of Ar-OH*(v=1) which were calculated previously [U. Schnupf, J.M. Bowman, and M.C. Heaven (1992)] using a potential which gave good agreement with experiment. Rotational state distributions from the predissociation dynamics of these quasibound complexes are calculated "exactly" , and compared with experiments of Heaven and coworkers. We also compare the "exact" rotational distributions with approximate multichannel "Golden-rule" calculations.

Supported in part by the National Science Foundation

XXth Informal Photochemistry Meeting
April 26- May 1, 1992
Atlanta, GA

ABSTRACT

Wavepacket relaxation and complete absorption spectrum of HO_2, Douglas Chapman, Joseph Bentley, Bela Gazdy, and Joel M. Bowman, Department of Chemistry, Emory University, Atlanta, GA 30322

We report truncation/recoupling calculations of all bound and numerous quasibound states of non-rotating HO_2, using the DMBE potential of Varandas and Brandão. This basis of molecular eigenstates is used to study the relaxation dynamics of OH-overtone wavepackets. A simple, three dimensional dipole moment function is constructed and used in calculations of the complete absorption spectrum, which contains interesting features indicative of the two equivalent HO_2 isomers. Comparison with limited experimental data points out the need for an improved potential surface.

Supported in part by the Department of Energy.

LASER-INDUCED FLUORESCENCE OF JET-COOLED CH_3O: VIBRONIC ANALYSIS OF THE $\tilde{X}$ STATE

Yin-Yu Lee, Yuan-Pern Lee, and I-Chia Chen

Department of Chemistry, National Tsing Hua University

101, Sec. 2, Kuang-Fu Rd. Hsinchu

TAIWAN 30043, R. O. C.

The methoxy (CH_3O) radical has been produced in a pulsed suppersonic jet expansion by laser photolysis of methyl nitrite (CH_3ONO) at 248 nm. The wavelength-resolved fluorescence spectra from various vibrational levels of the $\tilde{A}\ ^2A_1$ state of CH_3O (and $^{13}CH_3O$) have been recorded. A frequency-doubled tunable dye laser pumped by the 532 nm output from a pulsed Nd-YAG laser was used for excitation. The main progression is the C–O stretching (ν_3) mode at 1046 cm^{-1}. Other modes in combination with the ν_3 progression have also been identified. We found that previous assignments of $\nu_2 = 1362\ cm^{-1}$ and $\nu_5 = 1487\ cm^{-1}$ by Foster et al. (J. Phys. Chem. 92, 5914 (1988)) was probably erroneous. Preliminary results showed that $\nu_1 = 2875\ cm^{-1}$, $\nu_2 = 1419\ cm^{-1}$, $\nu_5 = 1495\ cm^{-1}$, and $\nu_6 = 654\ cm^{-1}$. The laser-induced emission spectra of CH_3O in solid Ne also support the new assignments.

Abstract

LASER EXCITATION SPECTROSCOPY OF JET-COOLED HYDROXYL AND METHOXY RADICALS IN THE OVERLAPPING 308 - 317 NM SPECTRAL REGION

Abdullahi H. Nur, Xinming Zhu, and Prabhakar Misra
Department of Physics and Astronomy
Howard University, Washington, D.C. 20059

The hydroxyl (OH) radical is an ubiquitous presence in combustion flows and flames and is a significant reactant in the earth's atmosphere. The methoxy (CH_3O) radical plays a leading role as an oxidation intermediate in the combustion of hydrocarbons and in air pollution. In the present investigation, laser-induced fluorescence spectroscopy in conjunction with a supersonic jet expansion has been used to obtain rotationally-resolved excitation spectra of the vibronic bands of both free radicals in the near ultraviolet. Weak features due to the A $^2A_1$ - X ^2E electronic system of CH_3O in the 308 - 317 nm region have been extracted from a spectral domain dominated by strong OH transitions due to the A $^2\Sigma^+$ - X $^2\Pi_i$ (0,0) band. Implications for the population variation of rotational energy levels and insights into the electronic structure and spectroscopy of the OH and CH_3O radicals will be discussed.

Financial support from Wright-Patterson Air Force Base (Grant# F33615-90-C-2038) and the D.C. Space Grant Consortium is gratefully acknowledged.

Detection of CH_2 ($\tilde{X}\ ^3B_1$) Radicals by 3 + 1 REMPI

Karl K. Irikura and Jeffrey W. Hudgens

Chemical Kinetics and Thermodynamics Division
National Institute of Standards and Technology
Gaithersburg, MD 20899

Abstract. Spectra of triplet methylene radicals, $\tilde{X}\ ^3B_1$ CH_2 and CD_2, were produced between 380 and 440 nm using mass resolved resonance enhanced multiphoton ionization (REMPI). These spectra arose from three-photon resonances with the $\tilde{B}\ ^3A_2$ (3d), $\tilde{C}$ (3d), $\tilde{D}$ (3d), and 4d $^3A_2$ Rydberg states between 78950 and 68200 cm^{-1} above the ground state. A fourth laser photon ionized the radicals, i.e., CH_2^+ (m/z 14) and CD_2^+ (m/z 16) ion signals were generated through a 3 + 1 REMPI mechanism. Methylene radicals were produced by the reaction of fluorine atoms and methyl radicals.

The Effect of Molecular Orientation in CO/Ag(111) Scattering Probed by REMPI

Thomas F. Hanisco, Chun Yan, Andrew C. Kummel
Dept. Chem., University of California, San Diego

We have studied the cross correlations between the rotational state distributions, angular momentum alignment, angular momentum orientation, and velocity distributions of monoenergetic, rotationally cold CO and N_2 scattered at 0.75 eV off Ag(111). Measurements were made for both normal incidence versus glancing incidence beams and for specular versus off-specular detection. The comparison between N_2 and CO is most dramatic: (1) For N_2 the rotational state selected velocity distributions are very narrow while for CO the rotational state selected velocity distributions are wide. (2) For glancing incidence beams, N_2 exhibits a high degree of parallel momentum conservation than CO. (3) The velocity resolved rotational rainbows for N_2 are more prominent for glancing incidence while the velocity resolved rotational rainbows for CO are more prominent for normal incidence. (4) There is 100% cartwheeling type alignment for N_2 for medium and high exit rotational states while for CO the alignment is weak except at the very highest rotational states where it is still less than 100% cartwheeling. (5) The angular momentum orientation for CO shows backwards tumbling for molecules scattered into low J states while for N_2 no orientation in seen in low J states.

Our data can be interpreted as showing that the N_2 molecules at these relatively high energies collide with a modestly corrugated surface and have nearly linear trajectories. Conversely, the CO molecules have a permanent dipole moment and a deeper physisorption well on Ag(111) thus attain a higher velocity in the attractive well. This results in the CO molecules probing deeper into the corrugated repulsive portion of the potential and having more inelastic collisions which result in greater rotational and phonon excitation but lower exit translational energy; the CO scattering data is consistent with scattering from a fairly corrugated surface. The lower alignment for CO scattering into high *J* states is consistent with the CO molecules having curved exit trajectories and/or multiple collisions with the surface. Finally, the dramatic differences in the angular momentum orientation for CO and N_2 scattering probably results from the difference in CO gas-surface collisions in which the carbon versus the oxygen end of the molecule is orientated towards the surface.

KrF Laser-induced Photochemistry of Nitrosobenzene Adsorbed on a Cold Al_2O_3 $(11\bar{2}0)$ Surface: Desorption Dynamics of the NO Photofragment*

by

Seong-Poong Lee and M. C. Lin
Emory University
Atlanta, GA 30322

Abstract

The laser-induced photodesorption/photoframentation of adsorbed nitosobenzene on a cold Al_2O_3 $(11\bar{2}0)$ surface at 248 nm has been studied by analyzing the time-of-flight (TOF) of species emerging from the surface. Both photodesorbed and photofragmented species were detected either by electron-impact ionization (EI/TOF) or resonantly enhanced multiphoton ionization (REMPI/TOF) with mass selection using a quadrupole mass spectrometer.

The NO fragment was found to carry two uniquely different translation energy distributions. The REMPI spectra of each component taken near the peak of the deconvoluted TOF distributions reveal distinctively different rotational temperatures. The surface coverage dependence of the rotational spectra for NO (0-0), (0-1) and (0-2) vibrational bands will be presented. Additionally, the reaction and desorption of the phenyl radical on the sapphire single crystal surface will be discussed.

---

* Work supported by the Department of Energy (DE-FG05-91ER14191).

Photodesorption of Benzene Adsorbed on Single Crystals of SiO_2 and LiF at 308, 248 and 193 nm.*

Y. Bu, S.-P. Lee and M. C. Lin
Department of Chemistry
Emory University
Atlanta, GA 30322

Abstract

The dynamics of photodesorption of C_6H_6 and C_6D_6 absorbed on a z-cut quartz and a LiF(001) single crystal surface has been investigated at 308, 248 and 193 nm. The photon energies of these wavelengths correspond to the electronic energies of the T_1, S_1, and S_2 states of benzene, respectively. For C_6H_6 adsorbed on the quartz surface, no desorption could be detected following 308 and 248 nm photolysis probably because of the low extinction coefficients for excitation to the T_1 and S_1 states. The desorption of C_6H_6 at 193 nm, however, could be readily detected.

For benzene on LiF(001), on the other hand, excitations at all three wavelengths resulted in detectable desorption with comparable intensities and only slightly different translational energies. For example, the translational temperatures of C_6D_6 desorbed at 308, 248 and 193 nm were measured to be 285 K, 305 K and 400 K, respectively, for fluence = 12.7 mJ/cm^2, dosage = 0.1 L (Langmuir). At 193 nm, the photofragmentation of benzene was noted with fluence greater than 14 mJ/cm^2.

The observed photodesorption at 308 and 248 nm in the experiment with the LiF substrate could be attributed entirely to F-center excitation. The results obtained from our studies on these two different substrates will be presented and discussed in detail.

---

* Work supported by ONR (N00014-89-J-1235)

XXth Informal Photochemistry Meeting
April 26- May 1, 1992
Atlanta, GA

ABSTRACT

Vibrational overtone-induced desorption of HF from LiF(001), Keh-Dong Shiang, and Joel M. Bowman, Department of Chemistry, Emory University, Atlanta, GA 30322.

We describe a many-body potential for HF physisorbed to LiF(001). This potential is then used in a classical trajectory study of the desorption dynamics of HF(v=1-5). The final state vibrational, rotational, and kinetic energy distributions of the desorbed HF are calculated, and the desorption mechanism is elucidated. These calculations were stimulated by experiments in progress by Lin and coworkers on this system, and by experiments on HBr-LiF by Polanyi and co-workers.

Supported in part by the National Science Foundation

Photochemistry of Group V Hydrides on GaAs: Dynamics and Mechanism*

X.-Y. Zhu and J. M. White
Center for Materials Chemistry, Department of Chemistry and Biochemistry
University of Texas, Austin, TX 78712

Ammonia , phosphine, and arsine are commonly used group V precursor molecules in the growth and fabrication of III-V compound semiconductor devices. Presently, most applied processes employ thermal activatio . but the continued trend toward microminiaturization places strict spatial and chemical requirements on interfaces and necessitates the use of nonthermal activation, e.g., photochemical activation. This motivated us to study the photochemistry of monolayer group V hydrides adsorbed on GaAs(100) under low-power excimer laser (193, 248, and 351 nm) irradiation. One common feature found for the surface photochemisty of all three hydrides is that photoreaction occurs at photon energies much lower than the UV absorption thresholds in the gas phase, indicating substrate mediated excitation. Despite of the common excitation mechanims, the photochemical pathways vary dramatically depending on individual hydrides.

For molecular arsine, adsorbed on GaAs(100) at 100 K, UV laser irradiation results in photodissociation, which is characterized by the sequential formation of AsH_2, AsH, and GaH on the surface. The final steps, photochemical removal of hydrogen from Ga-H and As-H, lead to *As deposition at 100 K*. Isotope effects have been observed in all photodissociation steps and are related to the mass-dependent substrate quenching of the excited states, as implied in the classic Menzel-Gomer-Redhead (MGR) model.

For monolayer molecular ammonia adsorbed on GaAs(100) at 100 K, UV laser irradiation leads mainly to photodesorption and a small amount of photodissociation The minor photodissociation channel enables the *nitridation of GaAs at 100 K*, with surface NH group as an important intermediate. The photodesorbing ammonia is characterized by a mean translational temperature of $\langle E_{trans}/2k \rangle \approx 300$ K, independent of photon energy or isotope substitution. A surprisingly large isotope effect is observed for the photodesorption channel: $\sigma_{NH_3}/\sigma_{ND_3} = 4.1 \pm 0.5$. This cannot be accounted for by the mass difference in the two molecules, using existing photodesorption models, e.g., the MGR model. We take this as the first evidence for *vibration-mediated UV photodesorption from surfaces*. Calculation using model potential energy surfaces supports our interpretation.

*Supported in part by the Science and Technology Center Program of NSF, Grant CHE 8920120

LOW ENERGY ELECTRON ENHANCED ETCHING OF SEMICONDUCTOR SURFACES

H.P. Gillis, J.L. Clemons, and J.P. Chamberlain
School of Chemistry and Microelectronics Research Center
Georgia Institute of Technology
Atlanta, GA 30332-0400

Anisotropic etching without ion bombardment damage is essential for fabrication of nanometer-scale quantum devices, which require lateral resolution of 1000 Å and vertical resolution of 100 Å.

As an alternative to Reactive Ion Etching (RIE), we have investigated etching of Si(100)-(2x1) by beams of H or Cl atoms, with simultaneous bombardment by a low energy (10-1000 eV) electron beam. A steady flux of atoms is provided by a microwave discharge flowing through a differentially pumped collimating aperture. Adsorption of reactants is studied by LEED, UPS, ESD, and TSD. Products of steady-state etching are detected by a differentially pumped quadrupole mass spectrometer.

Results will be presented for non-patterned samples, showing kinetics of removal of several Si_xH_y and Si_xCl_y species in steady-state electron enhanced etching, as well as effects of etching on LEED patterns. Results on patterned samples will illustrate anisotropy from electron-enhanced etching.

Investigation of Distortion and Damage of Mo-Si Multilayer Reflective Coatings with High Intensity UV Radiation

Howard A. Bender and William T. Silfvast
Center for Research in Electro-Optics and Lasers
University of Central Florida, Department of Physics
12424 Research Parkway, Orlando, Florida 32826

Kenneth M. Beck
University of Central Florida
Departments of Chemistry and Physics, Orlando, Florida 32816

Summary

We report on studies of optical distortion and damage thresholds of Mo-Si multilayer soft x-ray reflective coatings using 308 nm pulsed radiation from a XeCl excimer laser to simulate soft x-ray irradiation. Preliminary experimental results yielded values of 260 mJ/cm^2 and 500 mJ/cm^2 for distortion and damage thresholds.

Studies have been performed on the thermal stability of soft x-ray Mo-Si multilayer mirrors under steady state irradiation[1]. Under pulsed irradiation, rapid lattice expansion and increased reflectivity changes have been observed[2]. Also, real time reflectivity decreases and wavelength shifts have been measured under high intensity pulsed x-ray flux[3]. It would be desirable to understand and quantify the specific distortion and damage effects caused by such high flux intensities.

As a preliminary step, optical microscopy was used to analyze gross visual material changes. Low intensity laser flux caused visible discoloration or distortion changes at values above the quoted distortion threshold. When these regions were subsequently illuminated with higher intensities the damage threshold was observed to increase by 50%, suggesting that significant permanent changes in the layers had occurred with the annealing pulse. These changes will be investigated in more detail with electron microscopy.

Time dependent optical reflectivity measurements of the irradiated regions were also investigated and compared to samples of pure silicon at flux levels which caused melting of the silicon.

The sample multilayer used was a 40 bi-layer Mo-Si coating on a single crystal silicon (100) substrate. Each layer had approximate thicknesses of 40 Å.

Calculated values of melting a thin layer of the surface (as a gauge for induced damage) indicated much higher thresholds near 1 J/cm^2. However, these models did not account for the extremely thin layers in relation to heat diffusion depths.

These results will be compared and correlated with values obtained using soft x-ray flux from a laser plasma source.[2,3]

REFERENCES

1. A.V. Vinogradov, unpublished communication, 1991.
2. A. Zigler, J.H. Underwood, J. Zhu and R.W. Falcone, "Rapid Lattice Expansion and Increased X-ray Reflectivity of a Multilayer Structure Due to Pulsed Heating", Appl. Phys. Lett. 51(23), 1873-1875, 1987.
3. B. McGowan, private communication, LLNL, 1992.
4. M. Sparks, "Theory of Laser Heating of Solids: Metals", Journal of Applied Physics, Vol. 47, No. 3, 837-849, 1976.
5. H.S. Carslaw and J.C. Jaeger, Conduction of Heat in Solids, 2nd ed., Oxford University Press, Oxford, 1959.
6. D.H. Auston, et. al., "Time Resolved Reflectivity of Ion-Implanted Silicon During Laser Annealing", Appl. Phys. Lett. 33(5), 437-439, 1978.

ENERGY AND ELECTRON TRANSFER PROCESSES IN THE QUENCHING OF TRIPLET STATES OF ORGANIC COMPOUNDS BY 1,3-DIKETONATE METAL CHELATES. LASER FLASH PHOTOLYSIS STUDIES

Bronislaw Marciniak and Gordon L. Hug
Radiation Laboratory, University of Notre Dame, Notre Dame, Indiana 46556

The wide range of redox potentials of 1,3-diketonate transition metal chelates (ML_n) and their numerous low-lying excited states make them suitable for the study of both energy and electron transfer quenching. Moreover, 1,3-diketonates of Cu(II) and Ni(II) are known to undergo photoreduction sensitized by triplet states of aromatic ketones in H-donating solvents. The mechanism of interaction of excited triplets with these chelates is still unclear and requires further examination.

In this work we have studied, with nanosecond laser flash photolysis, the quenching of triplet states of various organic compounds by acetylacetonates and hexafluoroacetylacetonates of transition metals Cu(II) and Ni(II), lanthanides Tb(III) and Gd(III), and Mg(II) in acetonitrile solution. No sensitized luminescence was observed (except for Tb(III)), and no nanosecond transients were observed that could be ascribed to sensitized excited states or to electron transfer intermediates. However, rate constants for the quenching of a series of triplet states of organic compounds by simple ML_n complexes were measured. Indirect evidence concerning the nature of the quenching mechanisms was obtained from correlations of these quenching rate constants with the standard free energy changes for energy transfer and electron transfer. These correlations (extended in the case of Cu(II) and Ni(II) 1,3-diketonates to the quenching involving a combination of energy and electron transfer) allow us to estimate the values of transmission coefficients and intrinsic barriers for both mechanisms of quenching. It was found that the quenching of triplet states of most organic donors by acetylacetonates of Cu(II), Ni(II), Tb(III), Gd(III), and Mg(II) was adequately described by the energy transfer. The exceptions were the quenching of benzophenone triplets by these complexes and quenching of aromatic hydrocarbons with low-lying triplet states by $Cu(acac)_2$, where electron transfer processes play a significant role. The quenching by hexafluoroacetylacetonates of Cu(II) was found to be mainly due to electron transfer.

ATMOSPHERIC OXIDATION OF SELECTED TERPENES AND RELATED CARBONYLS: GAS PHASE CARBONYL PRODUCTS

Daniel Grosjean* (a), Edwin L. Williams II (a) and John H. Seinfeld (b)

(a) DGA, Inc., 4526 Telephone Road, Suite 205, Ventura, CA 93003

(b) Department of Chemical Engineering, California Institute of Technology, Pasadena, CA 91125

Biogenic hydrocarbons including terpenes have recently received renewed attention for their contribution to ozone and aerosol formation in urban and rural areas. However, very little is known regarding the atmospheric oxidation of terpenes and the nature and fate of their reaction products. In this study, the carbonyl products of three major terpenes, alpha pinene, beta pinene and d-limonene, have been identified and their concentrations measured in experiments involving sunlight irradiations of mixtures of terpene (1-2 ppm) and NO (0.25 ppm) in air. In turn, sunlight irradiations of carbonyl-NO_x mixtures have been carried out for the major high molecular weight carbonyl products of beta pinene (nopinone) and d-limonene (4-acetyl-1-methylcyclohexene), and the corresponding carbonyl products have been identified. The nature and yields of these carbonyl products are discussed in terms of oxidation mechanisms involving the OH-terpene and ozone-terpene reactions.

PEROXYACYL NITRATES: ATMOSPHERIC FORMATION AND REMOVAL PROCESSES

Daniel Grosjean

DGA, Inc.
4526 Telephone Road, Suite 205
Ventura, CA 93003

Ambient levels of peroxyacyl nitrates ($RC(O)OONO_2$) including PAN ($R = CH_3$) and PPN ($R = C_2H_5$) have been measured during three consecutive smog seasons (1989-91) at two southern California mountain forest locations impacted by urban photochemical smog. The highest levels recorded were 22 ppb for PAN and 4.3 ppb for PPN; 24-hr averages were 2-10 ppb for PAN and 0.25-1.7 ppb for PPN. Diurnal variations of PAN and PPN coincided with those of ozone in all cases. PPN and PAN were highly correlated, with PPN/PAN ratios of 0.28 (summer 1989), 0.18 (1990) and 0.14 and 0.19 (1991). The PPN/PAN ratio reached a maximum at the time of ozone maximum and increased with increasing PAN concentrations. PAN/ozone and PPN/ozone concentration ratios increased substantially at night and decreased with increasing temperature.

Diurnal and seasonal variations in PPN/PAN ratios are discussed in terms of formation and removal processes for PAN and PPN including in-situ photochemical production, thermal stability and loss by chemical reactions. An inventory of hydrocarbons that are precursors to PAN and PPN has been constructed and is discussed in terms of the relative contribution of olefins, aromatics, carbonyls and paraffins to the observed PPN/PAN ratio as a function of air mass transport time. Other peroxyacyl nitrates observed included PnBN ($R = n\text{-}C_3H_7$) and possibly its isomer PiBN ($R = i\text{-}C_3H_7$). The isoprene oxidation product MPAN ($R = CH_2 = C(CH_3)$-) was synthesized using two methods and was further characterized in the laboratory but was not observed in ambient air at the two mountain forest locations studied.

Time resolved UV spectroscopy of CF_3CFHO_2

M. Matti Maricq
Research Staff
Ford Motor Company
P.O. Box 2053, Drop 3083
Dearborn, Michigan 48121

Abstract

HFC-134a (CF_3CFH_2) is a likely replacement for CFC-12, currently used in automobile air conditioning systems. This compound has a much shorter atmospheric lifetime than CFC-12 owing to the presence of hydrogen atoms which make it reactive toward OH radicals. Following hydrogen abstraction from HFC-134a by OH, the resulting CF_3CFH radical reacts rapidly with O_2 to form the corresponding peroxy radical (CF_3CFHO_2). The subsequent atmospheric fate of this peroxy radical, however, is not currently well understood.

This paper reports the results of an experimental investigation into the kinetics of the formation and self reaction of the CF_3CFHO_2 radical. Time resolved UV absorption spectroscopy is used to follow the addition of O_2 to CF_3CFH to form CF_3CFHO_2, the self reaction of the peroxy radical to form CF_3O_2, and the disappearance of CF_3O_2 by self reaction. Quantitative determinations of the concentrations of these species as a function of time are made by comparison of the UV spectrum of the reaction mixture to reference spectra of CF_3CFH, CF_3CFHO_2, and CF_3O_2, also measured as a part of this study.

The measured concentration profiles are compared to predictions from a model reaction mechanism. The data are in good agreement with a simplified model in which 2 CF_3CFHO_2 → 2 CF_3O_2, CF_3CFHO_2+CF_3O_2 → CF_3O_2+Prod, and 2 CF_3O_2 → Prod. The rate constants for these processes are reported and a more complete model for CF_3CFHO_2 self reaction is discussed.

THE ACTION SPECTRUM OF THE O_2 10-0 SCHUMANN-RUNGE BAND IN THE ATMOSPHERE

T. G. Slanger
Molecular Physics Laboratory
SRI International
Menlo Park, CA 94025

ABSTRACT

In determining the rate of O_2 photodissociation in the 40-110 km region, the assumption is generally made that solar radiation is quasi-continuous, and varies smoothly with wavelength over the 174-205 nm range of the dominant absorption features, the Schumann-Runge (SR) bands. However, it is well-known that there are emission and Fraunhofer absorption lines in this region of the solar spectrum, and to the extent that there are resonances of these features with SR lines, this standard assumption is not valid. The 181.6-181.8 nm pair of Si^+ lines occur at the head of the SR 10-0 band, overlapping three SR rotational lines. As the Si^+ lines have 20-30 times the intensity of the adjacent continuum, the contribution of the 10-0 band to O_2 photodissociation has been greatly underestimated. For zero optical depth, the 10-0 band is twice as effective as any other band in dissociating O_2, which may impact modeled determinations of O_3 density profiles.

QUANTUM YIELDS FOR OXYGEN ATOMS FROM THE PHOTOLYSIS OF NO_3

J. J. Orlando, G. S. Tyndall, G. K. Moortgat[‡] and J. G. Calvert

Atmospheric Chemistry Division, National Center for Atmospheric Research, PO Box 3000, Boulder, CO 80307, USA

[‡] Abteilung Luftchemie, Max-Planck-Institut für Chemie, Postfach 3060, D-6500 Mainz, Federal Republic of Germany.

Photolysis by visible radiation is normally considered to be the major loss process for NO_3 in the atmosphere.

$$NO_3 + h\nu \rightarrow NO_2 + O \qquad \lambda \leq 640 \text{ nm}$$

$$\rightarrow NO + O_2 \qquad 585 \leq \lambda \leq 640 \text{ nm}$$

There has been only one previous study of the photolysis of the NO_3 radical (Magnotta and Johnston, *Geophys. Res. Lett., 7,* (1980) 769). In this work, the NO_3 concentration was calculated from measured N_2O_5 and NO_2 in an equilibrium mixture. The quantum yields reported were greater than unity at many wavelengths. Clearly, a further study of this process is necessary to understand the photochemistry and thermodynamics of NO_3.

Quantum yields for the production of oxygen atoms in the photolysis of NO_3 radicals are being measured as a function of wavelength using pulsed laser photolysis. The NO_3 radicals are produced in a discharge flow system by the reaction of F atoms with HNO_3, and the O atoms produced from the photolysis are detected by resonance fluorescence. Actinometry is performed relative to ozone photolysis. If possible, a qualitative estimate of the channel to give $NO + O_2$ will be made using time resolved chemiluminescence from the reaction $O_3 + NO$.

KINETIC STUDY OF THE REACTION OF CH_3S WITH NO_2

Niann S. Wang*
Department of Applied Chemistry, National Chiao Tung University
1001, Da-Hsieh Rd. Hsinchu,
TAIWAN 30050, R. O. C.

J. M. Jen and Yuan-Pern Lee
Department of Chemistry, National Tsing Hua University
101, Sec. 2, Kuang-Fu Rd. Hsinchu,
TAIWAN 30043, R. O. C.

Methyl thiyl radical (CH_3S) is an important intermediate in the atmospheric oxidation processes of reduced sulfur compounds. Further oxidation of CH_3S eventually leads to the production of H_2SO_4 in the atmosphere.

A laser photolysis system with laser induced fluorescence detection of CH_3S has been set up to study the reaction kinetics of CH_3S. The CH_3S radicals were produced by photolyzing CH_3SSCH_3 (DMDS) with an excimer laser output at 248 nm. The concentration of CH_3S was monitored by exciting the CH_3S at 371 nm ($\tilde{A}\ ^2A_1 - \tilde{X}\ ^2E_{3/2}$ transition) with a XeCl excimer (308 nm) pumped dye laser and collecting the fluorescence at 450±5 nm with a lens-bandpass filter-PMT arrangement. The signal from the PMT was averaged by a boxcar integrator and processed by a microcomputer.

The temperature dependence of the rate coefficient for the reaction CH_3S+NO_2 has been studied. Preliminary results show near-zero activation energy for this reaction and $k = 4.8\times10^{-11}$ cm^3 molecule^{-1} s^{-1} at 298 K with no pressure effect between 20 and 200 torr. Our results are compared with other previous reports. The significance of this reaction in the atmosphere will be discussed.

CHEMICAL KINETICS OF THE REACTIONS OF THE OH RADICAL WITH SEVERAL HYDROCHLOROFLUOROPROPANES

David D. Nelson, Jr., Mark S. Zahniser and Charles E. Kolb
Aerodyne Research, Inc.
45 Manning Road
Billerica, MA 01821

ABSTRACT

We report discharge flow kinetic studies of the reactions of OH with several alternative hydrohalocarbons. Detailed results including temperature dependences are reported for HCFC-225ca, HCFC-225cb, and HCFC-243cc. Preliminary results are reported for several other compounds. The reaction of these species with OH radicals in the troposphere is expected to determine their tropospheric lifetimes. Their tropospheric lifetimes, in turn, largely determine the extent of their role in stratospheric ozone depletion. The rate constants for HCFC-225ca, -225cb, and -243cc were measured in the temperature range 295 K - 370 K and the resulting Arrhenius plots (ln(k) vs. 1/T) showed no curvature within the experimental uncertainties over this temperature range. Expressing the rate constant as $k(T) = A \exp[-E/(RT)]$, we find $A=(6.5 \pm 1.3)\times10^{-13}$ cm^3 $molecule^{-1}$ s^{-1}, $E/R = 970 \pm 115$ K for HCFC-225ca, $A=(3.9 \pm 0.7)\times10^{-13}$ cm^3 $molecule^{-1}$ s^{-1}, $E/R = 1120 \pm 125$ K for HCFC-225 cb, and $A=(7.1 \pm 2.8)\times10^{-13}$ cm^3 $molecule^{-1}$ s^{-1}, $E/R = 1690 \pm 230$ K for HCFC-243cc. The uncertainties in the rate constants calculated from the above expression are estimated to be ~10% for HCFC-225ca and HCFC-225cb and ~15% for HCFC-243cc over the measured temperature range. Using thermochemical transition state theory, we show that these Arrhenius parameters are consistent with those of analogous ethane based HCFCs. Surface reactions in the flow tube reactor prevented the direct measurement of rate constants for these reactions at temperatures below room temperature. However, using the reported Arrhenius parameters, we calculate the rate coefficients at 277 K, the weighted mean temperature of the troposphere, and derive tropospheric lifetimes for HCFC-225ca, -225cb, and -243cc of 4, 8, and 44 years respectively.

Kinetics and Mechanism for the Reaction of OH with Ethyl *t*-Butyl Ether in the Presence of NO_x.
T.E. Kleindienst, D.F. Smith, E.E. Hudgens, and C.D. McIver. ManTech Environmental Technology, Inc. - Environmental Sciences. Research Triangle Park, NC 27709. J.J. Bufalini, Atmospheric Research and Exposure Assessment Laboratory, US EPA, RTP, NC 27711.

The Clean Air Act Amendments passed in Congress in 1990 stipulate reductions in the emissions of toxic air pollutants, particularly aromatic compounds. This legislation and the considerable difficulty in meeting the National Ambient Air Quality Standard for ozone and CO in many metropolitan areas have resulted in initiatives to produce reformulated fuels. Maintaining octane number while removing aromatic compounds has resulted in the introduction of aliphatic ethers into gasoline blends. While methyl *tertiary*-butyl ether has been most widely used, ethyl *tertiary*-butyl ether (ETBE; $(CH_3)_3C\text{-}O\text{-}C_2H_5$) has also been proposed for use, since ethanol can be used as a precursor for its production. The impact of these ethers on oxidant formation must be evaluated by modeling and experimental studies. However, relatively few determinations have been made of the atmospheric lifetime constant of ETBE and little is known regarding the degradation mechanism. The present study was conducted to measure rate constant of OH with ETBE (and its major reaction products) and to determine the likely atmospheric degradation products and their yields in the presence of NO_x.

Experiments to measure the OH rate constants and measure product yields were performed in 150-L Teflon reaction chambers. OH was generated through the photolysis of methyl nitrite or nitrous acid. For the rate constant measurements, a relative rate technique was used. The disappearance of the reactant and reference compounds were measured using GC/FID. Reference compounds used were *n*-butane, propane, and *n*-hexane and were appropriately selected to avoid chromatographic interferences. For the mechanistic studies, reactant and product concentrations were measured by GC/FID, HPLC, or GC/MS. The mass spectrometer was initially operated in the total ion mode for product identification, then in the selected ion monitoring mode for selected quantitative measurements. For GC analysis of the gas samples, the precision and accuracy of the measurements were largely dependent on the integrity of the sampling and injection systems and considerable effort was devoted to ensure the worthiness of these systems. Gas samples for GC and GC/MS analysis were collected using a cryogenic sampling system. GC separations were performed with an HP-5 capillary column with helium as the carrier gas. Oven temperatures were programmed from 35 to 210 °C. While most of the product yields were measured using GC/FID, carbonyl compounds produced by gas-phase reactions were determined by impinger sampling in a derivatizing solution of 2,4-dinitrophenylhydrazine (DNPH). Hydrazones formed by derivatization were separated and quantitatively measured by HPLC using a three-component gradient solvent program. All measurements were performed at 25 °C.

The observed products produced by the reaction of OH + ETBE were *t*-butyl formate (TBF), formaldehyde, acetaldehyde, *t*-butyl acetate (TBA), ethyl acetate, and acetone. OH rate constants were measured for ETBE, TBF, and TBA and gave values of 9.7, 0.74, and 0.44×10^{-12} cm^3 $molecule^{-1}$ s^{-1}, respectively. The value for ETBE gives an atmospheric lifetime of 1.2 days, for an average diurnal OH concentration of 1×10^6 molecules/cm^3. OH reacts with ETBE by H-atom abstraction from either side of the molecule. Attack of the ethyl group results in the formation of TBF (molar yield of 0.64), TBA (0.13), and acetaldehyde. Attack of OH on the *t*-butyl side leads to the formation of ethyl acetate (0.043), acetone (0.019), and acetaldehyde. The yield measured for acetaldehyde was 0.16. Formaldehyde is formed from methyl and methoxy radicals generated in the system and gave a molar yield of 0.53. From the detection of *t*-butyl nitrite, it was determined that *t*-butoxy radicals are also formed during the photooxidation. Generation of these products occurs through standard tropospheric oxidation mechanisms following OH reaction with organics in the presence of NO_x. Actual product yields measured result from the disposition of the alkoxy radicals formed following abstraction. Consideration of the mechanisms will focus on the probability of the alkoxy radicals undergoing decomposition versus reaction with molecular oxygen.

KINETICS AND THERMOCHEMISTRY OF C_2Cl_5 FORMATION FROM The $Cl(^2P_J)$ + C_2Cl_4 ASSOCIATION REACTION

J. M. Nicovich, S Wang[a], and P. H. Wine

Physical Sciences Laboratory, Georgia Tech Research Institute,
Georgia Institute of Technology, Atlanta, GA 30332

The reaction of atomic chlorine with tetrachloroethylene (C_2Cl_4) has been the subject of several recent laboratory studies. Both the kinetics [1] and mechanism [2-4] of C_2Cl_4 photooxidation under atmospheric conditions have been investigated. Tetrachloroethylene appears to react with chlorine atoms much more rapidly than with hydroxyl radicals; hence, C_2Cl_4 oxidation in the troposphere appears to be initiated primarily by $Cl(^2P_J)$, despite the very low tropospheric concentration of this radical species. There is evidence reported in the literature that the $Cl(^2P_J)$-initiated oxidation of C_2Cl_4 can result in production of CCl_4, a compound with a very high ozone depletion potential [2].

Although it is known that reaction (1) proceeds via an addition mechanism, the temperature and pressure dependencies of k_1 have not been systematically investigated.

$$Cl(^2P_J) + C_2Cl_4 + N_2 \rightarrow C_2Cl_5 + N_2 \qquad (1)$$

We have coupled laser flash photolysis of $Cl_2CO/C_2Cl_4/N_2$ mixtures with time resolved detection of $Cl(^2P_J)$ by atomic resonance fluorescence spectroscopy to investigate the kinetics of reaction (1) over the temperature range 233-298K and the pressure range 3-700 Torr; over this range of experimental conditions the reaction is found to be in the falloff regime between third- and second-order, although the high pressure second-order limit is approached at low temperature and high pressure. At higher temperatures, i.e. 332-390K, $Cl(^2P_J)$ regeneration is observed on the time scale of the experiment (tens of milliseconds), thus indicating the occurrence of the reverse dissociation reaction, i.e.

$$C_2Cl_5 + N_2 \rightarrow Cl(^2P_J) + C_2Cl_4 + N_2. \qquad (-1)$$

Analysis of equilibration kinetics as a function of temperature provides information about the thermochemistry of reaction (1) and, therefore, about the heat of formation of C_2Cl_5.

This work was supported by the National Aeronautics and Space Administration.

(a) Present address: Dalian Inst. of Chemical Physics, Chinese Academy of Sciences, P.O. Box 110, Dalian, Peoples Republic of China

(1) R. Atkinson and S. M. Aschmann, Intl. J. Chem. Kin. 19, (1987) 1097.
(2) H. B. Singh, D. Lillian, A. Appleby and L. Lobban, Environ. Letters 10, (1975) 253.
(3) E. C. Tuazon, R. Atkinson, S. M. Aschmann, M. A. Goodman, and A. M. Winer, Int. J. Chem. Kin. 20, (1988) 241.
(4) E. Mathias, E. Sanhueza, I. C. Hisatume, and J. Heicklen, Can. J. Chem. 52, (1974) 3852.

LASER FLASH PHOTOLYSIS STUDIES OF RADICAL-RADICAL REACTION KINETICS: THE $O(^3P)$ + BrO REACTION

R. P. Thorn[a], J. M. Cronkhite[b], J. M. Nicovich, and P. H. Wine

Physical Sciences Laboratory, Georgia Tech Research Institute,
Georgia Institute of Technology, Atlanta, GA 30332

The $O(^3P)$ + BrO reaction is the rate-limiting step in a potentially important mid-stratospheric ozone destruction cycle.

$$O(^3P) + BrO \rightarrow Br + O_2 \quad (1)$$

$$Br + O_3 \rightarrow BrO + O_2 \quad (2)$$

Net: $O(^3P) + O_3 \rightarrow 2\,O_2$

We are employing a dual laser flash photolysis technique with time-resolved, simultaneous detection of $O(^3P)$ (using atomic resonance fluorescence spectroscopy) and BrO (using long path UV absorption spectroscopy) to study the kinetics of reaction (1) as a function of temperature and pressure. Following 248 nm laser flash photolysis of $O_3/Br_2/N_2$ mixtures, Br_2 is rapidly titrated to BrO via reactions (2) and (3).

$$O(^3P) + Br_2 \rightarrow BrO + Br \quad (3)$$

Subsequently, due to the occurrence of reactions (1) - (5), a near-steady state situation is established with a small, slowly decaying $O(^3P)$ level, a small, slowly rising Br_2 level, and a large, slowly decaying BrO level.

$$BrO + BrO \rightarrow Br_2 + O_2 \quad (4a)$$
$$\rightarrow 2\,Br + O_2 \quad (4b)$$

$$O_2(^1\Delta) + O_3 \rightarrow O(^3P) + 2O_2 \quad (5)$$

After an appropriate time delay following the first laser flash, a small fraction of the residual O_3 is photolyzed at 532 to produce additional $O(^3P)$. Decay of $O(^3P)$ back to its near-steady state level is dominated by reaction (1) and provides the desired kinetic information.

The temperature and pressure dependence of k_1 will be discussed as will the role of reaction (1) in stratospheric BrO_x chemistry.

This work was supported by the National Aeronautics and Space Administration.

(a) Also affiliated with the Georgia Tech School of Earth & Atmospheric Sciences.
(b) Also affiliated with the Georgia Tech School of Physics.

Determination of Rates Constant for the ClO Self Reaction

Scott L. Nickolaisen, Randall R. Friedl, and Stanley P. Sander
Jet Propulsion Laboratory, 183-901, 4800 Oak Grove Drive, Pasadena, CA 91109

Abstract

Rate constants for the reactions

$$ClO + ClO + M \longrightarrow Cl_2O_2 + M \quad (2)$$
$$ClO + ClO \longrightarrow Cl_2 + O_2 \quad (3)$$
$$ClO + ClO \longrightarrow Cl + ClOO \quad (4)$$
$$ClO + ClO \longrightarrow Cl + OClO \quad (5)$$
$$Cl_2O_2 + M \longrightarrow ClO + ClO + M \quad (7)$$

were determined using a flash photolysis/UV absorption technique with M = He, Ar, O_2, N_2, CF_4, and SF_6. ClO was formed by the reaction $Cl + Cl_2O \longrightarrow ClO + Cl_2$ in which atomic chlorine was generated by the photolysis of Cl_2. The transient absorption of ClO was detected at 277.5 nm, and OClO was detected at 350 nm. Rate constants were extracted from the ClO decay and OClO formation curves by fitting the transient signals to an analytical expression for second-order kinetics or by an iterative least-squares routine. In a mixture with excess Cl_2O, the bimolecular rate constants of reactions 4 and 5 were measured. The rates for dimer formation and dissociation (reactions 2 and 7) were also measured under these conditions. In experiments with excess chlorine atoms, the rate constant for reaction 2 was determined, as well as the rate constant for the sum of reactions 3 and 4. By combining the results measured under the various stoichiometric conditions, reaction rates for each channel of the ClO self reaction were determined. Rate constants were also measured as a function of temperature with either helium or nitrogen as a bath gas. The preliminary results indicate a positive activation energy for the sum of the bimolecular processes, and a small negative activation energy for the termolecular process.

A Study of the Reactions of $O(^1D)$ with Bromocarbons

John E. Thompson and A.R. Ravishankara

National Oceanic and Atmospheric Administration
Aeronomy Laboratory, 325 Broadway, Boulder, Colorado 80303
and
Department of Chemistry and Biochemistry,
University of Colorado, Boulder, Colorado

The release of brominated organic compounds into the atmosphere leads to the destruction of stratospheric ozone via catalytic cycles involving bromine. One of the processes that can liberate Br from the organic compounds is their reaction with $O(^1D)$ present in the stratosphere. The reaction of $O(^1D)$ with a series of bromocarbons was studied. $O(^1D)$ was produced by pulse laser photolysis (pulse width of 20ns) of ozone at 248nm. The formation of $O(^3P)$ was observed using the technique of vacuum UV atomic resonance fluorescence. This formation rate was used to deduce the overall rate coefficients for the reactions of $O(^1D)$ with these compounds. The branching for the quenching of $O(^1D)$ to $O(^3P)$ was also determined by measuring the $O(^3P)$ yields in the presence of the haloalkanes relative to the quenching of $O(^1D)$ in the presence of N_2. These results will be discussed in terms of trends in reactivity and their atmospheric relevance.

Cl_2O_3 : A KINETIC AND SPECTROSCOPIC STUDY

James B. Burkholder, R.L. Mauldin III, R. Yokelson,
and A.R. Ravishankara

Aeronomy Laboratory, NOAA
325 Broadway Boulder, CO 80303 and
The Cooperative Institute for Research in Environmental Sciences
University of Colorado, Boulder,CO 80309

ABSTRACT

The UV absorption spectrum of Cl_2O_3 was measured over the wavelength range 220 to 320 nm using time resolved transient absorption. Cl_2O_3 was produced using 193 nm pulsed laser photolysis of $N_2O/Cl_2/OClO/N_2$ or $CF_2Cl_2/OClO/N_2$ gas mixtures to initiate the reaction $ClO + OClO + M \rightleftarrows Cl_2O_3 + M$ (k_1, k_{-1}). The Cl_2O_3 UV absorption spectrum peaks at 267 nm with a cross section of 1.60×10^{-17} cm^2. The forward rate coefficient, k_1, was measured over the temperature range 200 to 260 K at number densities over the range (1.1 - 10.9) $\times 10^{18}$ molecule cm^{-3} (M = N_2) using time resolved transient absorption. The reaction showed a negative temperature dependence with $k_1 = 5.54 \times 10^{-32} (300/T)^{3.48}$. The equilibrium constant for reaction 1, $K_{eq} = k_1/k_{-1}$, was measured at five temperatures over the range 232 to 258 K. A van't Hoff plot of this data yields $\Delta S = -21.2$ cal $mole^{-1}$ K^{-1} and $\Delta H = -11.1$ kcal $mole^{-1}$. These photochemical and kinetic results are compared with previously reported values. The implications of Cl_2O_3 to polar stratospheric chemistry are discussed.

Gas Phase Reaction Kinetics of CF_3O_2 and CF_3O

Thomas J. Bevilacqua, David R. Hanson, and Carleton J. Howard

NOAA Aeronomy Laboratory and
Cooperative Institute for Research in Environmental Sciences,
Boulder, CO

The trifluoromethyl-peroxy (CF_3O_2) and trifluoromethoxy (CF_3O) radicals have been identified by several investigators as key intermediates in the atmospheric degradation of some hydrofluorocarbons (HFC's) and hydrochlorofluorocarbons (HCFC's). We have used a low-pressure flow tube reactor, coupled to a chemical-ionization mass spectrometer (CIMS), to study the kinetics of the reactions of CF_3O_2 and CF_3O with tropospherically significant species. For the reaction of CF_3O_2 with NO, we have measured a room temperature rate constant of $(1.42 \pm 0.16) \times 10^{-11}$ cm^3 $molecule^{-1}$ s^{-1}, in very good agreement with previous reports. The relatively gentle ionization conditions of the CIMS detector have enabled us to observe CF_3O as the principle product, along with NO_2, of this reaction. Experimental studies of CF_3O thermolysis and of its reactions with NO and NO_2 will also be detailed.

LONG PATH FTIR STUDY OF ATMOSPHERIC REACTIONS INVOLVING CF_3OO AND CF_3O RADICALS

J. Chen, T. Zhu and H. Niki
Center for Atmospheric Chemistry and Department of Chemistry
York University, 4700 Keele St. North York, Ontario, Canada, M3J 1P3

Long path FTIR based product studies were carried out in the visible photolysis ($\lambda > 400$ nm) of mixtures containing CF_3NO and NO/NO_2 in mTorr range in 700 Torr of O_2-N_2 diluent at 298 ± 1K, in attempts to characterize the potential atmospheric fate of CF_3 radicals formed from some of the HCFCs and HCFs. Under the conditions employed, CF_3NO was photodissociated selectively at the rate ca. 2% per minute and yielded CF_3OO via reactions (1) and (2).

$$CF_3NO + h\nu\ (\lambda > 400\ nm) \rightarrow CF_3 + NO \qquad (1)$$

$$CF_3 + O_2 + M \rightarrow CF_3OO + M \qquad (2)$$

In the CF_3NO-NO-O_2 mixtures, stoichiometic yields of CF_2O, FNO and NO_2 were observed in the early stage of the photolysis, consistent with occurrence of reaction (3) followed by reactions (4),

$$CF_3OO + NO \rightarrow CF_3O + NO_2 \qquad (3)$$

$$CF_3O + NO \rightarrow CF_2O + FNO \qquad \Delta H = -33\ kcal/mole \qquad (4)$$

or by reactions (5)-(7).

$$CF_3O + O_2 \rightarrow CF_2O + FOO \qquad \Delta H = 6.3\ kcal/mole \qquad (5)$$

$$FOO \rightarrow F + O_2 \qquad (6)$$

$$F + NO + M \rightarrow FNO + M \qquad (7)$$

Reactions (5)-(7) were ruled out based on an F-atom scavenging experiment. Namely, the addition of C_2H_6 at sufficiently high concentrations to scavenge F-atom did not alter the product distribution. Thus, reaction (4) appears to be the predominant channel for the reaction of CF_3O with NO. This reaction may occur via the formation of CF_3ONO adduct. However, no evidence has been obtained for the formation of CF_3ONO as a stable product.

In the CF_3NO-NO_2-O_2 mixtures, the IR bands attributable to CF_3OONO_2 were observed at the early stage photolysis. Upon the addition of NO following the irradiation, these bands disappeared rapidly, i.e. ca. 5 minutes, with concomitant formation of CF_3ONO_2, CF_2O, FNO and NO_2. The results are consistent with reaction (8) followed by reaction (3) and (9).

$$CF_3OO + NO_2 \rightleftharpoons CF_3OONO_2 \qquad (8)$$

$$CF_3O + NO_2 + (M) \rightarrow CF_3ONO_2 + (M) \qquad (9)$$

Further systematic studies of atmospheric reactions involving CF_3OO and CF_3O radicals are being carried out by generating these radicals from precursors other than CF_3NO.

DETAILED MECHANISTIC STUDIES OF THE OH-INITIATED OXIDATION OF DIMETHYLSULFIDE UNDER ATMOSPHERIC CONDITIONS

A. J. Pounds[a], A. J. Hynes, T. McKay[b], J. D. Bradshaw[c], and P. H. Wine

Physical Sciences Laboratory, Georgia Tech Research Institute,
Georgia Institute of Technology, Atlanta, GA 30332

It has been proposed (Charlson et al.; Nature 326 655 (1987)) that dimethylsulfide (DMS:CH_3SCH_3), via its oxidation to sulfate aerosol, is the major source of cloud-condensation nuclei over the oceans and that it plays a central role in climate regulation. In previous work (Hynes et al.; J. Phys. Chem. 90 4148 (1986)) we have shown that the effective rate of the OH + DMS reaction is consistent with a two channel process involving direct abstraction together with reversible adduct formation followed by adduct reaction with oxygen; however we were unable to directly observe reversible adduct formation. In this work we report the direct observation of reversible adduct formation using the pulsed laser photolysis-pulsed laser induced fluorescence technique. Analysis of observed double exponential OH temporal profiles allows the extraction of the rates of the abstraction channel and the forward and reverse rates of adduct formation. By measuring the forward and reverse rates of adduct formation, and hence the equilibrium constant, as a function of temperature we have obtained the heat of reaction, which gives us the binding energy of the OH-DMS adduct. Determination of the effective rate of the OH + DMS reaction as a function of oxygen and nitric oxide concentrations has enabled us to determine the rate coefficients for the reactions of the OH-DMS adduct with oxygen and nitric oxide. Dimethyl sulfoxide (DMSO:CH_3SOCH_3) is a potential product of the OH-DMS adduct reaction with oxygen; we present evidence that the channel producing DMSO + HO_2 is a significant reaction pathway.

This work was supported by the National Science Foundation.

(a) Also affiliated with the Georgia Tech School of Chemistry.
(b) Present address: Dept. of Chemistry, Dunwoody High School, Dunwoody, GA 30338.
(c) Primary affiliation: Georgia Tech School of Earth & Atmospheric Sciences.

Stratospheric Photochemistry of OCS and its Possible Contribution to the Stratospheric Background Aerosol

Mian Chir and D. D. Davis

School of Earth and Atmospheric Sciences
Georgia Institute of Technology
Atlanta, GA 30332

Carbonyl sulfide is the most abundant sulfur gas in the atmosphere. While relatively inert in the troposphere, its transport into the stratosphere followed by photodissociation and photooxidation is believed to be the dominant source of the stratospheric background aerosol, i.e., the aerosol level observed during the periods when volcanic activity is at a minimum. In this study, the loss rate of OCS in the stratosphere and the net amount of OCS being transported into the stratosphere was evaluated using a one dimensional stratospheric model. The globally averaged photodissociation rate of OCS in the stratosphere is evaluated by using a discrete ordinate method model for radiative transfer in the plane-parallel atmosphere. Other photochemical reactions of OCS, i.e., reaction with atomic oxygen and hydroxyl radicals, were also evaluated. It was found that integrated over all altitudes, approximately 58% of OCS is lost by photodissociation process, 37% is lost via reaction with O, and only 5% is lost via reaction with OH. However, at altitudes below 25 km, reaction with O was found to be the major loss process for OCS. The stratospheric photochemical lifetime of OCS was estimated to be 16 years. The relatively long photochemical lifetime of OCS suggests that only a small portion (~23%) of OCS that is transported from the troposphere into the stratosphere is destroyed, most of it returns back to the troposphere where it is removed by vegetation. The net amount of OCS which diffuses into the stratosphere was found to be 2.5×10^{10} gS yr^{-1}. A comparison with literature estimates on the amount of sulfur needed to sustain the stratospheric background aerosol suggests that OCS may contribute only 15-60% of the stratospheric background aerosol.

An Examination of the NO_x Photostationary State Based on NASA GTE CITE-3 Data From the Tropical Atlantic

G. Chen, G. Sachse, J. Collins, J. Bradshaw, S. Sandholm, G. Gregory, B. Anderson, J. Barrick, and D.D. Davis

During the NASA GTE-CITE-3 field program (August/September, 1989), simultaneous in-situ measurements of NO, NO_2, CO, O_3, H_2O, UV solar flux and temperature were made along with measurements of C_2-C_4 hydrocarbons. This data set has been used to compare experimentally measured NO_2/NO ratios with those derived from photochemical modelling calculations. Modelling results will be presented that examine NO_2/NO ratios in terms of the simple photochemical system (e.g., NO, NO_2 and O_3) as well as a more complete system involving the additional reactions of NO with HO_2, CH_3O_2, and RO_2. The results from this analysis will be presented in terms of three altitude regimes: near surface boundary layer measurements, (.2 - 8 km), trade-wind inversion measurements (.8 - 1.8 km) and free tropospheric measurements (1.8 - 5.5 km). The uncertainties in the model calculated NO_2/NO ratios have also been assessed in terms of calculated random and systematic errors.

TUNABLE DIODE LASER STUDIES OF ATMOSPHERIC REACTION MECHANISMS

R. E. Stickel, M. Chin[a], C. A. van Dijk, Z. Zhao[a], and P. H. Wine

Physical Sciences Laboratory, Georgia Tech Research Institute
Georgia Institute of Technology, Atlanta, GA 30332

Coupling laser flash photolysis production of free radical reactants with product detection by time-resolved tunable diode laser absorption spectroscopy is a potentially powerful technique for examining atmospheric chemical reaction mechanisms. Product appearance can be temporally resolved on a microsecond time scale, thus providing kinetic information which helps constrain potential product formation mechanisms. Also, gas phase processes can be investigated in complete isolation from reactor surfaces.

In this paper we describe recent studies carried out in our laboratory of (1) OCS, CO, and SO_2 production from the OH + CS_2 + O_2 reaction and (2) HCl production from the Cl + CH_3SCH_3 reaction. In the OH + CS_2 + O_2 studies, observed product temporal profiles provide information not only about the primary yields of OCS, CO, and SO_2 from the reaction of the OH-CS_2 adduct with O_2, but also tell us something about the possible production of S and/or SO and the possible regeneration of OH. In the case of the Cl + CH_3SCH_3 reaction, the results indicate that hydrogen abstraction is the dominant reaction mechanism at low pressure. However, a competing process (apparently involving stabilization of an adduct) which does not lead to HCl production becomes competitive at higher pressure.

This work was supported by the National Science Foundation and by an internal research grant from Georgia Tech Research Institute.

(a) Also affiliated with the Georgia Tech School of Earth & Atmospheric Sciences

Kinetics of Elementary Reactions at Low Temperatures

L Herbert, K Li, P Sharkey and I W M Smith
School of Chemistry, The University of Birmingham, Edgbaston, Birmingham B15 2TT, UK

A Defrance, J L Queffelec, C Rebrion, B R Rowe and I R Sims
Department de Physique Atomique and Moleculaire, Université de Rennes, 35042 Rennes Cedex, France

We shall report the results of two kinds of experiment on the kinetics of elementary reactions at low temperatures. Both are based on the production of free radicals (CN or OH) by pulsed laser photolysis (PLP) of a suitable precursor (eg, NCNO for CN and OH for HNO_3) followed by observation of the decrease in radical concentration by time-resolved, laser-induced fluorescence (LIF). In the first experiment (performed in Birmingham), reaction is initiated in a tubular reactor, with photolysis and probe laser beams counterpropagating along the axis of the flowtube. This reaction cell has two jackets, allowing it to be cooled to temperatures as low as 80 K using conventional refrigerants [1]. Although the radical precursors are above their saturated vapour pressures at the lowest temperatures, sufficient concentration remains in the cooled gas to produce detectable concentrations of radicals.

From these experiments, we expect to report the values of rate constants for a number of reactions of both the OH and CN radical. They will include examples of all three types of rapid elementary reaction: radical + saturated molecule (eg, OH + HCl, CH_4 and CN + CH_4, C_2H_6), radical + unsaturated molecule (eg, OH + CO, CN + C_2H_4, C_2H_2) and radical + radical (eg, OH + NO, CN + O_2).

In the second kind of experiment (performed in Rennes), gas mixtures are cooled by expansion through a Laval nozzle producing a well-defined, uniform supersonic flow in a large evacuated chamber. This apparatus is an adaption of the CRESU (Cinétique de Réactgions en Ecoulement Supersonique Uniforme) apparatus which has been used successfully to study a number of ion-molecule reactions at temperatures as low as 8 K [2]. In the experiments which we shall report, PLP-LIF measurements are used to determine rate constants for some reactions of the CN radical, in particular that with O_2.

[1] I R Sims and I W M Smith, Chem. Phys. Letters,
[2] B R Rowe and J B Mrquette, Int. J. Mass Spec. Ion Processes, 80, 239 (1987).

Time-Resolved Infrared Spectral Photography: Applications in Atmospheric Chemistry

J. Shi, E. W. Kaiser, and L. Rimai

Ford Motor Company, Scientific Research Laboratories
P. O. Box 2053, Drop 3083, Dearborn, Michigan 48121-2053

Time-resolved infrared spectral photography (TRISP) uses a pulsed, broad-band infrared beam to probe a reaction mixture following the initiation of the reaction by UV or visible laser photolysis. This infrared beam is generated by Stimulated Electronic Raman Scattering (SERS) in a dye laser pumped alkali metal heat pipe. After multi-passing (5 passes) through the reaction cell, the transmitted infrared light is up-converted to visible by four-wave mixing in another alkali metal vapor heat pipe, and the visible is detected and analyzed by a multi-channel array detector. The advantages of TRISP over other kinetics techniques result from the combination of the product finger printing capability of a conventional FTIR technique with submicrosecond time resolution. Therefore, this technique can simultaneously monitor the reactants, products and, possibly, intermediates of these reactions.

TRISP can potentially be useful in atmospheric photochemical kinetics studies, including the oxidative chemistry of organic compounds and the free radical reactions of halogen oxides (such as ClO and BrO). In order to test the applicability of this technique, it has been used to measure the absolute rate constants of the Cl-atom initiated reactions of C_2H_6, C_2H_5Cl, and several hydrochloroflorocarbon (HCFC) and hydroflorocarbon (HFC) molecules at 298°K in 760 torr of N_2 or O_2, by monitoring the growth of HCl by its absorption at 2798.8, 2821.5, and 2843.6 cm^{-1}. The broad-band infrared radiation (2600-3200 cm^{-1}) is generated in Rb vapor in a 1-meter heat pipe, and a shorter Rb pipe is used for the up-conversion. Absolute rate measurements will be presented, and comparison will be made with previous absolute and relative measurements. In addition, the atmospheric degradation mechanisms of several HCFC and HFC molecules will be discussed based on the TRISP and other infrared spectroscopic studies.

REAL-TIME DETECTION OF ATMOSPHERIC DMS, DMSO, AND SO_2 USING SELECTED ION CHEMICAL IONIZATION MASS SPECTROMETRY

Harald Berresheim and Fred L. Eisele
Georgia Institute of Technology, Atlanta, GA 30332

Recently, Charlson et al. (1987) hypothesized that the photochemical oxidation of oceanic DMS in the marine boundary layer may play a major role in global climate regulation. In order to verify this hypothesis in the field new analytical techniques capable of measuring DMS and its major oxidation products in real time and at low/sub-pptrv levels are urgently needed. In this paper new techniques are presented making real-time detection at low/sub-pptrv levels possible for a variety of atmospheric trace gases including sulfur gases. These techniques are based on chemical ionization mass spectrometry using a selected ion chemical ionization flow reactor at atmospheric pressure in combination with a mass spectrometer or as a gas chromatograph/mass spectrometer interface. The ion chemistry in the reactor is well controlled due to the initial production of selected reactant ion species which form known product ions with the sample molecules. Uncontrolled bulk ionization of the sample gas is avoided. Wall effects are virtually eliminated by maintaining a laminar carrier gas flow in the reactor. Laboratory and field measurements of the sulfur gases CH_3SCH_3 (DMS), $CH_3S(O)CH_3$ (DMSO), and SO_2 are presented demonstrating the extreme sensitivity achievable with this device. Corresponding detection limits (2σ) are 0.5 pptrv, 0.2 pptrv, and 0.2 pptrv, with estimated precisions of ± 20%, ± 5%, and ± 5%, respectively.

The Measurement of H_2O_2 and CH_4 in the Atmosphere Using Fixed-Frequency Infrared Gas Lasers and FM Detection Techniques

by
James J. Schwab and Markos Hankin
Atmospheric Sciences Research Center
University at Albany, State University of New York

Hydrogen peroxide and methane are important trace species in the study of atmospheric chemistry and "global change" science. H_2O_2 is a strong oxidant that is produced primarily in polluted atmospheres via photochemical reactions. CH_4 is produced in large part by biological activity at the earth's surface and is photochemically oxidized throughout the troposphere and stratosphere. While measurement methods for both of these species have been demonstrated (Kolb, 1991), the method described here aims to improve the sensitivity, measurement frequency, and/or reliability of current measurements.

A key aspect of the research has been the development of an infrared rare gas laser tunable over seven infrared transitions. The laser displays strong emission at 3.39 μm ($\approx$20 mW) and weaker emission at six discrete wavelengths between 7.6 and 8.1 μm. The laser will operate with a pure neon gas fill, but better power is obtained with a mixture of helium and neon. The present design uses a helium to neon ratio of 9:1 at a total pressure of 1 torr.

There is a well-known overlap between the 3.39 μm neon laser line and the P(7)F_1(2) CH_4 absorption line (Barger and Hall, 1969). Results will be presented showing the overlap of a neon line near 8.06 μm and a pressure broadened (30-50 torr) H_2O_2 line. Work in progress to exploit these overlaps to obtain ultra-high detection sensitivity using an external electro-optic modulator will also be described.

References

Barger, R.L., and J.L. Hall, *Pressure shift and broadening of the methane line at 3.39 μm studied by laser saturated molecular absorption*, Phys. Rev. Lett. 22, 4-8, 1969

Kolb, C.E., *Instrumentation for Chemical Species Measurements in the Troposphere and Stratosphere*, Rev. of Geophys., Supplement, pp. 25-36, April 1991

Acknowledgement - This work is supported by the National Science Foundation grant No. ATM-8900933.

CHARACTERIZATION OF THE AQUEOUS-PHASE PHOTOCHEMICAL FORMATION OF PEROXYL RADICALS AND SINGLET MOLECULAR OXYGEN IN CLOUD WATER SAMPLES FROM ACROSS THE UNITED STATES.

John M. Allen and Bruce C. Faust, School of the Environment,
Environmental Chemistry Laboratory, Duke University, Durham, NC 27706 USA

Aqueous-phase photochemical oxidation reactions in clouds are known to play an important role in the overall chemistry of the troposphere. Unfortunately, the present understanding of the sources, rates of formation, and concentrations of oxidants in clouds is limited. Several investigations, none of which involved authentic cloud waters, have suggested that aqueous-phase photochemical reactions are a significant source of hydroxyl radical in cloud drops. Analogous sources of other oxidants have not been identified. An investigation was therefore undertaken to quantify the aqueous-phase photochemical production of these oxidants in cloud water samples.

Authentic cloud water samples from North Carolina, Virginia, New York, Washington, and Oregon were found to absorb ultraviolet (UV) radiation at $\lambda > 290$ nm. This absorption was due to the presence of chemical species containing chromophoric functional groups in the cloud water. Measurements of the UV-VIS spectra for blanks in which pure deionized/distilled water was used to rinse all surfaces of collectors and storage containers did not show the characteristic absorption typical of the cloud water samples. We have conducted experiments demonstrating that the absorption of UV radiation by these samples gives rise to the sensitized aqueous-phase photoproduction of peroxyl radicals ($RO_2\cdot$ and $HO_2\cdot$), and singlet molecular oxygen $O_2(^1\Delta_g)$.

The steady-state concentrations of $O_2(^1\Delta_g)$ and peroxyl radicals were determined using a kinetic probe technique in which a small amount of a chemical probe compound was added to the cloud water. The added probe was chosen so as to react rapidly and selectively with a single chosen photooxidant. The cloud water sample with the added chemical probe was then illuminated using sunlight, simulated sunlight, or a single wavelength of light in a closed quartz vessel. The oxidation kinetics of the probes were monitored by high pressure liquid chromatography. Corrections were made for direct photolysis of the probes and for any dark (thermal) reactions. The concentration of the probe was kept low to minimize any perturbations to the overall chemistry of the cloud water. At low concentrations, the probe has little effect on the steady-state concentration of the photooxidant. The experimentally determined rate expression for the loss of the chemical probe (P) is: $d[P]/dt = -k[P]$ where $k = k_2[OX]_{ss}$, k_2 is the bimolecular rate constant for the reaction of the oxidant with the chemical probe, and $[OX]_{ss}$ is the steady-state concentration of the oxidant. The steady-state concentration of the oxidant was determined by measuring k for a chemical probe with a known value for k_2. The compound 2,4,6-trimethylphenol (TMP) was used as a probe for determining steady-state concentrations of peroxyl radicals (Fig. 1). Furfuryl alcohol (FFA) was used as a chemical probe for measuring the steady state concentration of $O_2(^1\Delta_g)$ (Fig. 2). FFA and TMP were chosen as probes because of their high reactivities toward $O_2(^1\Delta_g)$ and peroxyl radicals, respectively. Neither FFA nor TMP reacted appreciably in dark controls or when exposed to illumination in distilled water.

Atmospheric water drop models do not presently incorporate aqueous-phase photochemical sources of $O_2(^1\Delta_g)$, $RO_2\cdot$, and $HO_2\cdot$. An upper bound of 5×10^{-15} M for $O_2(^1\Delta_g)$ concentration in cloud drops is calculated from equilibrium partitioning of gas-phase $O_2(^1\Delta_g)$ (1×10^6 molecules/cm^3). We have measured $O_2(^1\Delta_g)$ concentrations ranging from 3×10^{-14} to 1.5×10^{-12} M in cloud waters. Model predictions of peroxyl radical concentrations in cloud drops range from 2×10^{-12} to 2×10^{-10} M. We have measured steady-state peroxyl radical concentrations in cloud waters ranging from 1×10^{-9} to 4×10^{-8} M. We conclude that: i) aqueous-phase photochemical formation of oxidants in clouds can be an important, and in some cases a dominant, source of these oxidants and, ii) atmospheric models that do not include aqueous-phase sources of oxidants could seriously underestimate the concentrations of these oxidants in clouds and fog.

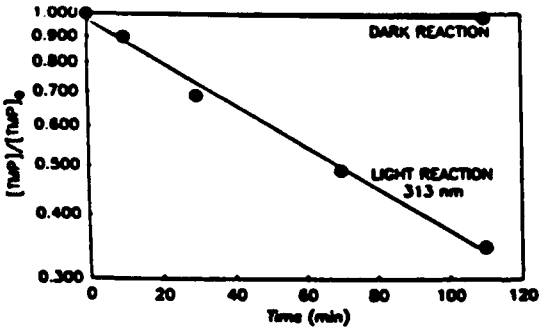

Figure 1. Photolysis of 2,4,6-trimethylphenol (TMP) in a cloud water sample from Shenandoah Park, Virginia.

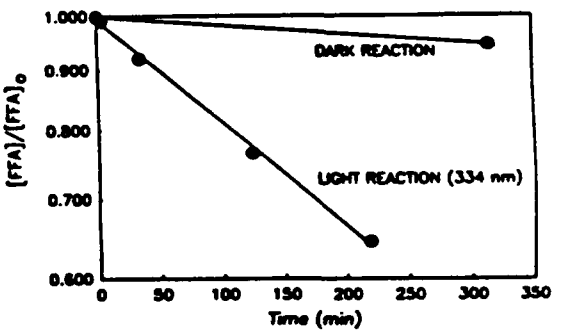

Figure 2. Photolysis of furfuryl alcohol (FFA) in a cloud water sample from Whiteface Mtn., New York.

References

Faust, B.C.; Allen, J.M., submitted to *J. Geophys. Res.*, 1991.

Faust, B.C.; Allen, J.M., in "Effects of Solar Ultraviolet Radiation on Biogeochemical Dynamics in Aquatic Environments", Woods Hole Oceanographic Institution Technical Report 90-09 (eds. N.V. Blough and R.G. Zepp), 1990.

Faust, B.C.; Anastasio, C.; Allen, J.M., in preparation.

XX[th] Informal Conference on Photochemistry
Georgia Institute of Technology, Atlanta, Georgia, April 26 - May 1, 1992

AQUEOUS-PHASE PHOTOCHEMICAL FORMATION OF PEROXIDES IN AUTHENTIC CLOUD WATERS

Cort Anastasio, John M. Allen, and Bruce C. Faust
School of the Environment, Environmental Chemistry Laboratory
Duke University, Durham, North Carolina 27706 USA

Peroxides in atmospheric waters are important for several reasons, most notably for the crucial role of H_2O_2 in the aqueous-phase oxidation of SO_2 to H_2SO_4 (1). Models of atmospheric water-drop chemistry have traditionally focused on gas-to-drop partitioning of peroxides and peroxyl radicals as the sole sources of aqueous-phase peroxides. However, recent research in our laboratory with authentic cloud water samples has shown that direct aqueous-phase photochemical formation is a significant source of peroxides to cloud waters (2).

Cloud water samples were collected by collaborators during spring through fall of 1990 and 1991, from several high elevation sites across the U.S. and by airplane from clouds over Ontario, Canada. All of the collected samples exhibited UV/VIS light absorption in a region that overlapped with the solar radiation incident on the troposphere (samples were first filtered through 0.2 or 0.5 μm Teflon filters; distilled water was used as a reference).

Samples were irradiated in teflon-stoppered quartz cuvettes at 20°C with continuous stirring. Several rinse water controls (distilled water that was sprayed into the cloud collection apparatus immediately prior to cloud collection, collected, and handled in the same manner as actual samples) were irradiated using the same procedure as a check for contamination. Four types of illumination were used: sunlight; simulated sunlight (from the filtered output of a Xenon lamp), and monochromatic light (313 or 334nm). Dark (thermal) controls of the samples were carried out under conditions identical to that of photolysis except for illumination.

Aqueous-phase photochemical peroxide production occurred in nearly all of the samples photolyzed. This is a result of light absorption by chromophores in the samples and, presumably, the formation of peroxyl radical intermediates ($HOO^{\cdot}$ and $ROO^{\cdot}$), which are considered to be the dominant precursors of peroxides in atmospheric waters. For the most recent samples, studied in the summer of 1991, 17 of 18 (94%) yielded measurable aqueous-phase photo-production rates. Dark controls showed no peroxide production for any of the samples tested. Irradiation of rinse waters yielded an average of less than 5% of the initial rate of peroxide photo-production seen with the associated samples: in half of the tested rinse waters there was no observed peroxide photo-production.

Typical initial rates of aqueous-phase photochemical production of peroxides (scaled to clear sky illumination of midday, autumnal equinox, Durham, NC sunlight at an altitude of 980 m) were approximately 1-2 μM/hour with actual or simulated sunlight. Quantum yields (for 313 and 334nm) for aqueous-phase peroxide photo-production are currently being calculated and will be reported. Additional experiments have indicated that the initial rate of aqueous-phase peroxide photo-production is linearly dependent on the actinic flux.

Based on several reports of the frequency distributions of measured concentrations in cloud waters (3-5), the formation rates reported on here are large enough to indicate that the aqueous-phase photochemical formation of peroxides is a significant, and in some cases dominant, source of peroxides to cloud waters.

References

(1) Gunz, D.W., Hoffman, M.R. 1990. *Atmos. Environ.* **24A**:1601-1633.
(2) Faust, B.C., Anastasio, C., Allen, J.M. In preparation. 1991.
(3) Kelly, T.J., Daum, P.H., Schwartz, S.E. 1985. *J. Geophys. Res.* **90D5**:7861-7871.
(4) Mohnen, V.A., Kadlecek, J.A. 1989. *Tellus* **41B**:79-91.
(5) Olszyna, K.J., Meagher, J.F., Bailey, E.M. 1988. *Atmos. Environ.* **22(8)**:1699-1706.

ONE-ELECTRON OXIDATION OF INORGANIC ANIONS BY INORGANIC RADICALS. TEMPERATURE DEPENDENCE IN AQUEOUS ACETONITRILE SOLUTIONS.

S. Padmaja P. Neta, and R. E. Huie
Chemical Kinetics and Thermodynamics Division
National Institute of Standards and Technology
Gaithersburg. MD 20899

Rate constants for several reactions of inorganic radicals with inorganic anions have been measured as a function of temperature and solvent composition in aqueous acetonitrile solutions. The reactions studied were those of the radicals $\cdot SO_4^-$, $\cdot Cl_2^-$, $\cdot Br_2^-$, and $\cdot N_3$ with several anions, CO_3^-, Cl^-, N_3^-, SCN^-, and I^-. The rate constants ranged from $10^7 - 10^9$ $M^{-1}s^{-1}$ before correction for ionic strength and the calculated activation energies from 2 to 40 kJ mol^{-1}. The rate constants decreased upon addition of acetonitrile to the aqueous solution by up to an order on magnitude. The values of E_a and log A varied with the variation in mole fraction of acetonitrile. The trend generally depends on the inorganic radical. For the oxidation of anions by $\cdot SO_4^-$, the rate constants depend more on the change in the pre-exponential factor than on the change in the activation energy. The pre-exponential factor decreased considerably with an increase in mole fraction of acetonitrile. In all other cases, both the pre-exponential factor and the activation energy changed with changing acetonitrile mole fraction. For the oxidation of I^- ions by $\cdot N_3$, an isokinetic effect is observed, with the activation energy and the pre-exponential factor increasing and then decreasing with mole fraction of acetonitrile. In the case of the other inorganic radicals, the k_{298} values varied linearly with the mole fraction of acetonitrile.

CHEMICAL KINETIC, THERMOCHEMICAL, AND SPECTROSCOPIC CHARACTERIZATION OF THE $(CH_3)_2S$-Br ADDUCT

C. J. Shackelford[a], J. M. Nicovich, K. D. Kreutter[b], E. P. Daykin[c], S. Wang[d], and P. H. Wine

Physical Sciences Laboratory, Georgia Tech Research Institute, Georgia Institute of Technology, Atlanta, GA 30332

We have studied the kinetics of the $Br(^2P_{3/2})$ + CH_3SCH_3 reaction over the temperature range 260 - 310K using time-resolved resonance fluorescence spectroscopy to follow the decay of $Br(^2P_{3/2})$ generated via 266 nm laser flash photolysis of $CF_2Br_2/CH_3SCH_3/H_2/N_2$ mixtures. Observed kinetics clearly demonstrate that the dominant reaction mechanism is $Br(^2P_{3/2})$ addition to the sulfur atom, and that the addition reaction is reversible on the time scale (~10 ms) of the experiment. Analysis of observed double exponential decays gives rate coefficients for adduct formation (k_f) and decomposition (k_d) as a function of temperature and pressure. From the temperature dependence of the equilibrium constant, i.e. $k_f(T)/k_d(T)$, a $(CH_3)_2S$-Br bond strength of 14.6 ± 1.1 kcal mole^{-1} is obtained (error is 2σ).

In a separate set of experiments, 248 nm laser flash photolysis of $CF_3Br/CH_3SCH_3/H_2/O_2/N_2$ mixtures was coupled with time-resolved long path absorption spectroscopy to investigate transient species which absorb in the near UV. The initial intent of these experiments was to see if BrO is generated via the potentially important atmospheric reaction $(CH_3)_2SBr + O_2 \rightarrow (CH_3)_2SO + BrO$. Indeed, a strong transient absorbance signal was observed at 338.3 nm, the λ_{max} of the strongest BrO absorption band. However, the transient absorbance did not show the band structure characteristic of BrO and was unaffected when N_2 was substituted for O_2 as the buffer gas. Analysis of the absorbance rise time as a function of $[CH_3SCH_3]$ clearly demonstrates that the absorbing species is $(CH_3)_2SBr$. The observed absorption spectrum is broad and unstructured over the wavelength range 320 - 440 nm, with λ_{max} ~ 370 nm; the absorption is relatively strong, i.e. σ_{max} is of the order of 10^{-17} cm^2.

This work was supported by the National Science Foundation.

(a) Also affiliated with the Georgia Tech School of Physics.
(b) Present address: Dept. of Biochemistry, Duke Univ., Durham, NC 27706.
(c) Present address: EG&G, P. O. Box 1912, MS A1-24, Las Vegas, NV 89125.
(d) Present address: Dalian Inst. of Chemical Physics, Chinese Academy of Sciences, P.O. Box 110, Dalian, Peoples Republic of China.

KINETICS OF THE REACTIONS OF $O(^3P)$ WITH CF_3NO AND $(CF_3NO)_2$

J. M. Cronkhite[a], S. Wang[b], R. P. Thorn[c], J. M. Nicovich, and P. H. Wine

Physical Sciences Laboratory, Georgia Tech Research Institute
Georgia Institute of Technology, Atlanta, GA 30332

Time-resolved atomic resonance fluorescence spectroscopy has been employed in conjunction with 266 nm laser flash photolysis of $O_3/CF_3NO/(CF_3NO)_2/N_2$ mixtures to investigate the kinetics of reactions (1) and (2) as a function of temperature and pressure.

$$O(^3P) + CF_3NO \rightarrow \text{products} \qquad (1)$$

$$O(^3P) + (CF_3NO)_2 \rightarrow \text{products} \qquad (2)$$

The rate coefficient for reaction (1) is found to be independent of pressure over the range 25-400 Torr. Reaction (1), however, is found to have a significant activation energy. Over the temperature range 243-424K, the temperature dependence of k_1 is well described by the Arrhenius expression

$$k_1(T) = (4.6 \pm 0.6) \times 10^{-12} \exp[-(560 \pm 40)/T] \text{ cm}^3\text{molecule}^{-1}\text{s}^{-1}.$$

Errors in the above expression are 2σ and represent precision only. Reaction (2) has been studied at pressures of 25 Torr and 100 Torr and at temperatures of 298K and 369K. The rate coefficient is found to be independent of temperature and pressure, with

$$k_2 = (2.1 \pm 0.3) \times 10^{-11} \text{ cm}^3\text{molecule}^{-1}\text{s}^{-1}.$$

The quoted uncertainty is 2σ and represents an estimate of absolute accuracy. The implications of the kinetic data for elucidation of reaction pathways will be discussed.

This work was supported by the National Aeronautics and Space Administration.

(a) Also affiliated with the Georgia Tech School of Physics.
(b) Present address: Dalian Inst. of Chemical Physics, Chinese Academy of Sciences, P.O. Box 110, Dalian, Peoples Republic of China.
(c) Also affiliated with the Georgia Tech School of Earth & Atmospheric Sciences.

Kinetics of the Gas Phase Reactions of Cl^- with CH_3Br and CD_3Br: Strong Evidence for Nonstatistical Behavior

A.A. Viggiano, Robert A. Morris, John S. Paschkewitz and John F. Paulson
Phillips Laboratory, Geophysics Directorate, Ionospheric Effects Division (GPID)
Hanscom AFB MA 01731-5000

Bimolecular nucleophilic displacement (S_N2) is one of the most basic types of chemical reaction. In contrast to many other types of gas phase ion-molecule reactions, nucleophilic displacement reactions are often slow.[1] There has been speculation that the inefficiency results from the reaction coordinate being a double well, i.e., two ion-molecule complexes separated by a chemical barrier.[2,3] The magnitude of the rate constant is often predicted by statistical theories such as RRKM theory.[2,4] The existence of both the entrance and exit channel complexes has been recently established. In contrast, several recent studies have called into question the ability of statistical theories to describe the reactivity. These studies all involved comparing statistical predictions to experimental results.

In order to test the validity of the statistical theories in a more direct fashion, we have studied the rate constants for the reactions of Cl^- with CH_3Br and CD_3Br,

$$Cl^- + CH_3Br \rightarrow Br^- + CH_3Cl \qquad \Delta H = -29.7 \text{ kJ/mole},$$

as a function of ion-neutral average center-of-mass kinetic energy, $\langle KE_{cm} \rangle$, at several temperatures. This allows us to determine the dependence of the rate constants on the internal temperature of CH_3Br. Statistical theories predict that the rate constant depends only on the total energy and total angular momentum.

The reactions are inefficient, proceeding at only a few percent of the collision rate constant. Both increasing temperature and increasing kinetic energy are found to decrease the rate constant as approximately $T^{-0.8}$ or $\langle KE_{cm} \rangle^{-0.8}$. At a fixed $\langle KE_{cm} \rangle$, no dependence of the rate constants on temperature was found. This indicates that the reactions do not depend on the internal temperature of the CH_3Br or CD_3Br. At the temperatures of the experiments, a significant amount of the CH_3Br or CD_3Br molecules are vibrationally excited, and therefore the rate constants are not strongly dependent on vibrational energy. A strong temperature dependence is found when comparing rate constants at a given total energy, which shows that total energy is not the only parameter governing reactivity. This strongly indicates that the reactions cannot be described by statistical theories.

1. Ikezoe, Y.; Matsuoka, S.; Takebe, M.; Viggiano, A. A. *Gas Phase Ion-Molecule Reaction Rate Constants Through 1986.*; Maruzen Company, Ltd.: Tokyo, 1987.
2. Olmstead, W. N.; Brauman, J. I. *J. Am. Chem. Soc.* **1977**, *99*, 4219.
3. Farneth, W. E.; Brauman, J. I. *J. Am. Chem. Soc.* **1976**, *98*, 5546.
4. Caldwell, G.; Magnera, T. F.; Kebarle, P. *J. Am. Chem. Soc.* **1984**, *106*, 959.

Kinetics of CN Radical Reactions with Selected Cycloalkanes: CN Reactivity Towards Secondary C-H Bonds*

D. L. Yang, T. Yu and M. C. Lin
Department of Chemistry
Emory University
Atlanta, GA 30322

Abstract

The reaction of CN radicals with hydrocarbons play an important role in many reactive processes including combustion and atmospheric photochemistry. In this series of studies, we have systematically examined the reactivity of CN radicals with saturated and unsaturated hydrocarbons and, for the former case, have determined the reactivity of CN radicals towards primary, secondary, and tertiary C-H bonds. The present paper represents a continuation of this series of studies.

The rates of CN radical reactions with c-C_3H_6, c-C_5H_{10}, c-C_6H_{12}, and c-C_8H_{16} have been measured over a broad temperature range. These hydrocarbons contain only secondary C-H bonds whose bond strengths, except for c-C_3H_6, are similar to each other. It was determined that the reactivities per secondary C-H bond in c-C_5H_{10}, c-C_6H_{12}, and c-C_8H_{16} are similar and are larger than the corresponding reactivity in c-C_3H_6. A small negative temperature dependences on the rates for c-C_5H_{10}, c-C_6H_{12}, and c-C_8H_{16} observed here are attributed to long range dipole-induced dipole attractive interactions. All experimental results as well as the comparison with primary and secondary reactivities in ethane and propane will be presented.

---

* Work supported by NASA under contract no. NAGW-1544

KINETICS OF CN REACTIONS WITH C_3H_6, $C_3H_3D_3$, C_3D_6, AND C_2H_3CN*

M. T. Butterfield, T. Yu and M. C. Lin

Department of Chemistry

Emory University

Atlanta, GA 30322 USA

Abstract

The two-laser pump-probe technique has been used to study the kinetics of the reaction of CN radicals with C_3H_6, $C_3H_3D_3$, C_3D_6, and C_2H_3CN at temperatures between 297 and 673K with varying pressures. CN was generated by 248 nm photolysis of ICN. Laser-induced fluorescence probing has been used for CN(B←X). The values for the rate constants, given in units of cm^3/molec sec, are reported as

$$k(C_3H_6) = 10^{(-9.88\pm0.24)} \exp(+244\pm96.3/T)$$

$$k(C_3H_3D_3) = 10^{-9.76\pm0.09} \exp(+143.4\pm35.1/T)$$

$$k(C_3D_6) = 10^{-9.87\pm0.12} \exp(+231.4\pm47.01/T)$$

$$k(C_2H_3CN) = 10^{(-10.52\pm0.05)} \exp(+103.6\pm20.3/T).$$

The absolute rates of CN reactions with $CH_3CH{=}CH_2$, $CD_3CH{=}CH_2$ and $CD_3CD{=}CD_2$ are essentially the same and are somewhat faster than that of the CN + CH reaction. The rate of the CN + C_2H_3CN reaction, however, was found to be a factor of six slower than that of CN + C_2H_4, indicating a substantial electron withdrawing effect of the CN group in vinyl cyanide. The CN reactions with these olefin molecules are believed to occur mainly by addition mechanism.

---

* Work supported by NASA under contract no. NAGW-1544

REMPI/MS Kinetic Spectrometer: A Test with CH_3 Radical Reactions[1]

S.-P. Lee, J. A. Tarr and M. C. Lin

Department of Chemistry

Emory University

Atlanta, GA 30322

Abstract

The technique of resonance-enhanced multiphoton ionization/mass spectrometry (REMPI/MS) has been employed in conjunction with laser photolysis and the high-pressure molecular beam sampling method developed by Saalfeld and coworkers[2,3] for kinetic studies of nonfluorescing ("dark") radicals. This new experimental arrangement can, in principle, be applied to cover a broad experimental condition: $300 \leq T \leq 1100$ K, $0 \leq P \leq 1$ atm, depending on the size of sampling hole and the pumping speed of the system. A preliminary test with CH_3 reactions has been made with satisfactory results.

References

1. Work supported by the Office of Naval Research under contract No. N00014-89-J-1949.

2. J. R. Wyatt, J. J. DeCorpo, M. V. McDowell and F. E. Saalfeld, Rev. Sci. Instrum. 45, 916 (1974).

3. J. R. Wyatt, J. J. DeCorpo, M. V. McDowell and F. E. Saalfeld, Rev. Sci. Instrum. 16, 33 (1975).

XXth Informal Conference on Photochemistry

ABSTRACT

Vacuum UV Absorption Spectra of Hydrazine Fuels

Valerie I. Lang and Alfred T. Pritt, Jr.
Space and Environment Technology Center,
The Aerospace Corporation, Los Angeles CA 90009

Many experiments involving the kinetics of hydrazine molecules require UV photochemical initiation and/or UV monitoring. There has previously been a lack of absorption cross-section data for these fuels, particularly for the methylated derivatives. We have measured the vacuum UV absorption spectra of hydrazine, monomethyl hydrazine and 1,1-dimethyl hydrazine in a 12.4 cm flow cell, using several rare gas continuum sources and a photodiode detector. Absolute absorption coefficients from 110 -190 nm have been obtained. These results will be combined with similar measurements to be made at wavelengths longer than 200 nm.

Photochemistry of Hydrazine: UV Absorption Cross Sections and Photoproduct Yields Between 200 and 285 nm

Ghanshyam L. Vaghjiani
University of Dayton Research Institute
Phillips Laboratory, PL/RFT
Edwards AFB, CA 93523
(805) 275 6179

Hydrazine and methylated hydrazines are important liquid rocket fuels. Emission of both ultraviolet and infrared radiation is observed during their combustion with N_2O_4, and the radiating radical species have been identified. However, the elementary reactions involved in the production of these excited state species that emit ultraviolet radiation are not well understood.

Our laboratory has initiated a study to elucidate the chemical mechanism(s) important in the production of ultraviolet radiation. To aid in accurately determining the fate of N_2H_4 during its reaction with radical species such as O, H, OH, NH_2, etc., the ultraviolet absorption cross sections of N_2H_4 have been measured in the wavelength range from 200 to 285 nm. Photolysis product yields of $H(^2S)$ have also been measured.

The experiments carried out and the results obtained will be presented, and compared with those from previous studies.

MULTIPHOTON DISSOCIATION OF NICKELOCENE FOR GAS-PHASE KINETIC STUDIES OF NICKEL ATOM ASSOCIATION REACTIONS

C. E. Brown, M. A. Blitz, S. A. Decker and S. A. Mitchell

Steacie Institute for Molecular Sciences, National Research Council of Canada, 100 Sussex Drive, Ottawa, Ont., K1A 0R6

Ground-state and metastable excited-state nickel atoms are produced by pulsed, visible laser induced multiphoton dissociation (MPD) of nickelocene at 650 nm in a static pressure reaction cell at room temperature. Association reactions of ground-state nickel atoms with unsaturated hydrocarbons and simple O-donor ligands have been studied by using resonance fluorescence excitation to monitor the kinetics of nickel atom removal. In some cases, effects due to collisional relaxation of metastable excited-state nickel atoms have been seen. These effects have been investigated by estimating the relative populations of metastable states following MPD at 650 nm, and by measuring rate constants for collisional relaxation of metastable states. The results of these studies will be discussed with reference to the mechanism of MPD of nickelocene at 650 nm, and implications for kinetic studies of ground-state nickel atoms.

FTIR studies of mechanisms of HF production from H atom/radical reactions

Paul W. Seakins and Stephen R. Leone

Joint Institute for Laboratory Astrophysics, N.I.S.T., and Dept. of Chemistry and Biochemistry, University of Colorado,Boulder, CO, 80309-0440.

HF elimination from atom/radical reactions (e.g. reaction (1)) can occur via

$$CF_3 + H \longrightarrow HF + CF_2 \qquad (1)$$

addition/elimination or abstraction mechanisms. In a recent paper Tsai et al (J. Phys. Chem. 1989, *93*, 2471) suggested that reaction (1) proceeds via a direct abstraction mechanism. More recent work on the HF product distribution from reaction (1) (Arunan et al J. Phys. Chem. 1991, *95*, 1539) revealed a monotonic decrease in HF vibrational population with vibrational energy which is consistent with the break up of a CF_3H complex. In the light of this controversy we have investigated a number of atom/radical reactions using both conventional FTIR emission and Time Resolved/Laser Flash Photolysis FTIR techniques.

$CF_3 + H(D) \longrightarrow H(D)F(v) + CF_2$

H(D) atoms have been generated by microwave discharge and flash photolysis and CF_3 radicals from reaction with excess H atoms or directly by photolysis. HF vibrational distributions from both experiments are broadly consistent with those of Arunan et al. Experiments were performed with translationally excited H atoms (2.2 eV). Under single collision conditions no HF emission was observed, favouring an addition/elimination mechanism for this reaction.

$CF_3CH_2 + D \longrightarrow CF_2CH_2 + DF(v)$ or $CF_2CHD + HF(v)$

Studies of this system should yield definitive evidence regarding the mechanisms of H atom/radical reactions. HF(v) can only be formed if the reaction proceeds via a complex (CF_3CH_2D). Preliminary experiments indicated that the major product from this reaction was DF. HF emission was observed showing that the complex is indeed formed, however, the raw HF emission was only 2% of that of DF. This suggests that, at least for this system, direct abstraction is the predominant pathway. Further experiments to determine that these are indeed the nascent product distributions from the above reaction are in progress. Analogous experiments with CF_2H + D are planned. The results of these experiments will be discussed in terms of direct abstraction or addition/elimination mechanisms.

Product State Distribution from the Reaction: N + OH → NO + H, and the Influence of Reagent Vibrational Excitation on the Reaction: N + NO(v) → N_2 + O

I W M Smith, R P Tuckett and C J Whitham
School of Chemistry, The University of Birmingham, Edgbaston, Birmingham B15 2TT, UK

We are carrying out measurements to determine the nascent product state distributions from the simple, protypical radical–radical reaction: N + OH → NO + H. The experiments use a combination of discharge-flow and pulsed photolysis techniques. Flowing nitrogen gas is partially dissociated (0.1–1.0%) in a microwave discharge to produce the N atoms for the reaction. HNO_3 or H_2O_2 is then added to the flow and is partially photolysed to produce OH radicals, using the pulsed output at 266 nm of a frequency-quadrupled Nd:YAG laser. Laser-induced fluorescence (LIF) measurements are then performed on the NO formed when the OH radicals and N atoms react. In this unusual system, the NO product is removed by reaction with N atoms, N + NO(v) → N_2 + O, more rapidly than it undergoes vibrational relaxation. Consequently, our measurements yield information of two kinds. LIF spectra at short delays reveal the distribution of NO over its vibrational states when it is formed from the N + OH reaction, and kinetic measurements on NO in individual vibrational levels disclose how the rate of the fast N + NO reaction is influenced by vibrational excitation in the NO.

The observation of a broad vibrational state distribution for the NO formed in the N + OH reaction and the slight effect of reagent vibration on the rate of the N + NO(v) reaction will be discussed in terms of what is known about the potential energy surfaces for there reactions. We also hope to present new dynamical results on the reaction of NO_2 with translationally 'hot' O atoms.

Dynamics of the $O(^1D)$ + ClNCO Reaction

S. Singleton and R.D. Coombe
Department of Chemistry, University of Denver
Denver, Colorado 80208

Photochemically initiated reactions of HNCO and the analogous halogen isocyanates have proven to be effective means for studying the NCO radical, an important intermediate in the combustion of nitrogenous and hydrocarbon fuels in the air. Recently, our laboratory reported[1] the results of extensive experiments directed toward understanding the reaction of HNCO with excited oxygen atoms, $O(^1D)$. This work has now been extended to investigations of the reaction of $O(^1D)$ with ClNCO.

$O(^1D)$ + HNCO has been shown to proceed primarily by electrophilic attack of the oxygen atom on the electrons of the NCO linkage, generating CO_2 and NH. The NH is produced predominantly in the excited $a(^1\Delta)$ state in accord with overall spin conservation. $O(^1D)$ + ClNCO also appears to proceed by electrophilic attack by the oxygen atoms, but in this case on the electrons associated with the chlorine atom. The primary products are ClO and NCO. To understand this reaction, it is necessary to address several important dynamical phenomena in the production of NCO from the reaction and from direct photochemical dissociation of ClNCO. These phenomena are included in an overall kinetic model for the system which agrees well with the observed behavior.

1. X. Liu, N.P. Machara, and R.D. Coombe, J. Phys. Chem., 95, 4983 (1991).

Radiative and Collisional Relaxation of NCl($a^1\Delta$)

A.J. Navratil and R.D. Coombe
Department of Chemistry, University of Denver
Denver, Colorado 80208

The $a^1\Delta$ metastable excited state of the NCl radical has been shown to be a major product of a number of spin-constrained chemical reactions.[1] In addition, it is thought to have potential utility as an energy storage agent in lasers, much like the analogous species $O_2(a^1\Delta_g)$ and $NF(a^1\Delta)$. Very little is known concerning the relaxation dynamics of $NCl(a^1\Delta)$, however. Measurements and calculations of its radiative lifetime reported in the literature vary widely,[2] and only a few measurements of collisional quenching rates have been published. Among these is a recent investigation by Bower and Yang[3] indicating very rapid energy transfer from NCl(a) to iodine atoms, generating excited $I(^2P_{1/2})$. This report has stirred considerable interest in $NCl(a^1\Delta)$ as a possible alternative to $O_2(a^1\Delta_g)$ for energy storage in near IR iodine lasers.

We have performed a number of experiments directed toward an accurate, real time determination of the NCl $a^1\Delta \rightarrow X^3\Sigma^-$ radiative rate. The experiments are based on diffuse photolysis of ClN_3 in a large cylindrical cell, a geometric configuration which allows very long lifetimes to be measured with minimal interference by diffusion or wall effects. We will report the results of these experiments as well as preliminary data on energy transfer between $NCl(a^1\Delta)$, O_2, and iodine atoms.

1. D.B. Exton, J.V. Gilbert, and R.D. Coombe, J. Phys. Chem., 95, 2692 (1991).

2. See for example D.R. Yarkony, J. Chem. Phys., 86, 1642 (1987).

3. R.D. Bower and T.T. Yang, J. Opt. Soc. Amer., B8, 1583 (1991).

On the Vibrational Substructure of the 195nm Transition of Acetone

Ruth McDiarmid, NIDDK, NIH, Bethesda, Md. 20892

The analysis of the vibrational substructure of the 195 nm (3s Rydberg <- X) transition of acetone has been of interest both because of the role this transition plays in the λ = 193 nm photodissociation of acetone and because of its role as the probably source of intensity of the acetone Π^* <- n transition. It has been previously shown[1,2] that hot and sequence bands involving the methyl-centered vibrational modes -- predominantly the CH_3 torsions and the CH_3 deformations and rocks -- dominate the 195 nm acetone transition. However, the earlier analyses left ambiguous the identifications of the a_1 CCC deformation and the b_1 CO bending modes. Here we resolve this ambiguity through a reanalysis of the optical spectra of acetone and acetone-d_6 and remeasurements and reanalyses of their 2RMPI and photoelectron spectra.

1. D. J. Donaldson, G. A. Gaines, and V. Vaida, J. Phys. Chem. 92, 2766 (1989).
2. R. McDiarmid, J. Chem. Phys. 95, 1530 (1991).

Thermal Emission Spectrum of YbCl Molecule

K.Gopal, K.N.Uttam and M.M.Joshi

Saha's Spectroscopy Laboratory

Department of Physics

Allahabad University, Allahabad-211002, INDIA

Thermal Emission Spectra of YbCl Molecule have been photographed for the first time using Saha's high temperature graphite furnace about a temperature 2400°C in the spectral region λλ 4700 — 6000 A° . The observed bands have been classified into two systems : A $^2\Pi$ — X $^2\Sigma$ & B $^2\Sigma$ — X $^2\Sigma$. The vibrational constants have been suitably modified and analyses have been confirmed with the help of isotopic effect.

Ion-Pair to Valence Transitions of Jet-Cooled IBr

Xiaonan Zheng and Michael C. Heaven
Department of Chemistry, Emory University, Atlanta, GA 30322

Joel Tellinghuisen
Department of Chemistry, Vanderbilt University, Nashville, TN 37235

Metastable states of IBr ($A'(2)$ and $A(1)$) have been populated by UV excitation in the presence of a high pressure of Ar buffer gas. Absorption of the pulses from a 193 nm ArF laser populated the IBr $E(0^+)$ ion-pair state. Collisional relaxation transferred this population to the $D'(2)$ and $\beta(1)$ states, which then radiated to the $A'(2)$ and $A(1)$ states. This sequence was initiated in the early stages of a free-jet expansion. Subsequent expansion and cooling resulted in $A'(2)$ and $A(1)$ state ro-vibrational temperatures of 10-20 K. The D'-A' and β–A transitions were then characterized, at the level of rotational resolution, by laser induced fluorescence spectroscopy. Thirty valence to ion-pair vibronic bands have been recorded. Analysis of this data is in progress. Experimental details and molecular constants will be reported.

The Low-Lying Electronic States of Uranium Monoxide

Leonid A. Kaledin and Michael C. Heaven
Department of Chemistry, Emory University, Atlanta, GA 30322

Electronic states of UO belonging to the $U^{2+}(5f^37s)O^{2-}$ and $U^{2+}(5f^27s^2)O^{2-}$ configurations have been identified in absorption and wavelength-resolved fluorescence spectra. The energy spacings among the observed levels have been used to develop a semi-empirical ligand field model of the low-lying states. To fit the model to levels of the $5f^37s$ configuration, two parameters were varied: the exchange interaction between the outer 7s and 5f core electrons , and the ligand field parameter B^2_0. The effects of higher order terms (B^4_0 and B^6_0) in the point charge expansion were significantly smaller than those of the leading quadrupolar term (B^2_0). They were included by maintaining the B^k_0/B^2_0, k=4,6 ratios at the values calculated from Hartree-Fock radial wavefunctions. The remaining nineteen model parameters were held at the values for the $U^{3+}(5f^3)$ ion [1].

Predictions of the ligand field calculations are being tested in a series of wavelength-resolved fluorescence measurements. A CW ring dye laser is used to excite fluorescence from various states of gas phase UO. The emission is resolved by a 0.64m monochromator. High concentrations of UO vapor are obtained by heating samples of the oxidized metal to temperatures around 2400K in a resistively heated tube furnace. Fluorescence spectra and details of the ligand field calculations will be presented.

1. H. M. Crosswhite, H. Crosswhite, W. T. Carnell, and A. P. Paszek, J. Chem. Phys. 72, 5103 (1980)

Numerical Truncation/Recoupling Calculations of the High Energy Vibrational Spectrum of Hydrogen Peroxide

Pamela Schafer, Dr. Joel M. Bowman

Dept. of Chemistry, Emory University, Atlanta, GA 30322

Results from large-scale six-dimensional quantum mechanical calculations of the vibrational eigenfunctions and eigenvalues of hydrogen peroxide is presented. The basis set for the truncation/recoupling method contains the effects of coupling between two specified modes; in this case, the two high-energy stretching modes are chosen. This improvement over a simple direct-product basis set allows the use of fewer basis set elements in the calculation. Generalized Gaussian-like quadrature is used to evaluate the potential elements. This adapted method of integration is shown to be particularly effecient for highly coupled systems. The overtone spectrum of the two stretching modes is emphasized.

Visible Absorption Spectroscopy of Dense, High Temperature Lithium Vapor

C. William Larson and Mario E. Fajardo
Propulsion Directorate
Phillips Laboratory
Edwards Air Force Base, CA 93523

J. D. Mills and Peter W. Langhoff
Department of Chemistry
Indiana University
Bloomington, IN 47405

Paul S. Erdman and William C. Stwalley
Department of Physics and Astronomy
University of Iowa
Iowa City, IA 52242

The absorption spectroscopy of dense, high-temperature lithium vapor was measured between 450 and 750 nm at a resolution around 0.6 nm. A three-millimeter diameter jet column of dense lithium vapor, up to one atmosphere total pressure, was produced in a hot-zone whose temperature ranged between 1600 and 1850 K. The relatively low jet velocity, ~ 50 cm s^{-1}, and high density assured that local chemical equilibrium was established through the sampling volume of the hot-zone. At the highest densities achieved, absorption was virtually 100% around the atomic lithium resonant transition, (2s-2p). Transitions from the excited state of lithium (2p-3d, 2p-4d, and 2p-4s), were measured in higher temperature spectra.

The highest density spectra showed absorption greater than 90% throughout the red and blue regions of the visible spectrum, from the well known transitions of the singlet state of dilithium (A-X, B-X). Up to 20% absorption from the first dilithium triplet ($^3\Sigma_u^+ - {}^3\Pi_g$), which was predicted at ~ 600 nm more than ten-years ago by Konowalow and Rosenkrantz, was observed in the higher temperature spectra and found to be about 10 nm red-shifted from the prediction.

Absorption by trilithium, which has been observed by Resonant Two Photon Ionization between 660 and 690 nm, is obscured in this absorption experiment by the A-X bands of dilithium. Theoretical spectra are being computed to determine the contribution to the total absorption by the A-X band, so that the trilithium contribution may be quantified.

Time-resolved Resonance Raman Study of Isonicotinamide Radicals

Yali Su, G.N.R. Tripathi and R. H. Schuler

Radiation laboratory
University of Notre Dame
Notre Dame, IN 46556

During the past decade, time resolved Raman spectroscopy has developed to the stage where it can be conveniently applied to study the structure and kinetics of transient chemical species in solution. However, this important spectroscopic technique has been rarely applied to the problems of radiation biology. Isonicotinamide(ISN) is a model system for the class of compounds which shows vitamin B_5 activity. The transients produced on one-electron reduction of several compounds of vitamin B_5 family have been studied by transient absorption using pulse radiolysis methods. However, little structural data is available thus far on these transient radicals. We are currently examining the structure of these radical by Raman spectroscopy to provide an understanding of the modes of reactions of these radicals in terms of the molecular structure. On pulse radiolytic reduction of ISN , the transients which are formed have an intense absorption in the ~400nm region. By Raman excitation in resonance with this absorption, a strongly enhanced ring stretch vibration was found at 1660cm^{-1}.The transient spectrum does not change from pH~6 to pH~13, but in acidic solutions (pH~1.0) this band shift to 1678cm^{-1}. The transient in the basic solution is identified as ISNH•, and in acidic solution as $ISNH_2^{\bullet+}$. The rate constant for the e_{aq}^- reaction with ISN was measured as $3x10^{10}$, which is in excellent agreement with the results from the transient absorption study performed previously. The detailed structure of intermediates, their acid-base equilibria and redox properties will be discussed .

TIME-RESOLVED IR SPECTROSCOPY OF TRANSIENT ORGANOMETALLICS IN LIQUID RARE GAS SOLVENTS

B. H. Weiller
The Aerospace Corporation
Space and Environment Technology Center, P.O Box 92957, Los Angeles, CA 90009

The combination of time-resolved IR spectroscopy and liquid rare-gas solutions is a powerful method to characterize transient organometallic species. Photochemical transients are captured by time-resolved IR spectroscopy while liquid rare gases allow temperature-dependent kinetic measurements of reactions with small activation energies. In addition, liquid rare gases are transparent in the infrared and minimize perturbations on coordinatively unsaturated species that are observed for common solvents. This paper will discuss recent results concerning transient species formed when metal carbonyls are photolyzed in the presence of weak ligands such as CO_2, N_2O and NO_2. These reactions are relevant to the laser-driven chemical vapor deposition of metal oxide thin films by the oxidation of metal carbonyls.

FLUORESCENCE LIFETIMES OF THE VINOXY RADICAL: EVIDENCE FOR PREDISSOCIATION

Katherine I. Barnhard, Min He, Brad R. Weiner,
Department of Chemistry, University of Puerto Rico, Río Piedras, PR 00931

The vinoxy (C_2H_3O) radical is an important intermediate in photochemical smog [1] and combustion systems [2]. It has been shown to react quickly with NO_2 [3] and more slowly with O_2 and NO [4]. We report our results on the collisional quenching of the $\tilde{B}^2A'' \rightarrow \tilde{X}^2A''$ transition of C_2H_3O. Vinoxy radicals are produced by excimer laser flash photolysis of methyl vinyl ether, and are subsequently probed by laser induced fluorescence on the $\tilde{B}$-$\tilde{X}$ transition. Quenching cross-sections and radiative lifetimes for vibrational modes of the B state are measured from fluorescence decays of the vinoxy radical in the presence of a variety of collision partners. A vibrational level dependence was found for the zero pressure radiative lifetimes. Possible mechanisms for the vibrational dependence of the lifetimes will be discussed.

[1] B.J. Finlayson-Pitts and J.N. Pitts Jr., Atmospheric chemistry: fundamentals and experimental techniques (Wiley, New York, 1986) pp. 425-431

[2] R.R. Baldwin and R.W. Walker, Symp. (Intern.) Combustion Proc. 18 (1981) 819

[3] K.I. Barnhard, A. Santiago, M. He, F. Asmar and B.R. Weiner, Chem.Phys. Lett 178 (1991) 150

[4] D. Gutman and H.H. Nelson, J.Phys.Chem. 87 (1983) 3902
K. Lorenz, D. Rhäsa, R. Zellner and B. Fritz, Ber.Bunsenges.Physik.Chem. 89 (1985) 341

Spectroscopy and Fluorescence Decay Dynamics of Matrix Isolated Iodine Monobromide.

Matthew Erickson, Michel Macler, Hong-Sun Lin, and
Michael C. Heaven.
Department of Chemistry, Emory University, Atlanta, Ga 30322

The spectroscopy and relaxation processes of IBr isolated in a solid Ar matrix have been studied using laser excitation and resolved fluorescence techniques. Excitation wavelengths in the range of 400 to 600 nm yielded fluorescence from the $B(0^+)$, $A(1)$, and $A'(2)$ states. Vibrational structure was absent from both the $B(0^+)$-$X(0^+)$ excitation and emission spectra. All levels of $B(0^+)$ were subject to rapid non-radiative decay.

Emission spectra for the $A(1)$-$X(0^+)$ and $A'(2)$-$X(0^+)$ systems yielded ground state vibrational constants which were virtually identical to the gas-phase values. Electronic term energies of $T_e(A)$=12130±30 and $T_e(A')$=11180±30 cm^{-1} were determined. Radiative lifetimes of $\tau(A)$=140±10 μs and $\tau(A')$=25±3 ms were obtained from time-resolved fluorescence measurements.

193 nm excitation of IBr/Ar matrices produced an emission feature at 419 nm, which has been tentatively assigned to the D'-A' transition.

Time-dependent study of the dynamics of the collision-induced intramultiplet mixing of Ca(4s4p(^3P_J) by helium at 750 K.

F. Castaño*, M.N. Sanchez Rayo, F. Beitia and D. Husain(+)

Depart. Química Física, Univ. Pais Vasco. Apart. 644, 48080 Bilbao, SPAIN and (+)Depart. Chemistry, University of Cambridge, Cambridge CB2 1EW, ENGLAND

We present a kinetic study of the collisionally-induced intramultiplet mixing within Ca(4s4p(^3P_j)), 1.888 eV above the $4s^2(^1S_o)$ electronic ground state, in the time domain. Ca(4s4p($^3P_1$)) was generated by the pulsed dye-laser excitation of calcium vapour at l=657.3 nm (Ca(4s4p($^3P_1$) <-- Ca($4s^2(^1S_o)$)) in the presence of excess helium buffer gas in a slow flow system, kinetically equivalent to a static system, at elevated temperature (T = 750 K). The time-dependent evolution of the concentrations of the individual spin-orbit states, Ca(4^3 $P_{0,1,2}$) where the J= 0-1 and 1-2 separations are 52.2 and 105.8 cm^{-1}, were monitored by laser-induced fluorescence (LIF) of the 4s5s($^3S_1$)-4s4p(^3P_J) transitions using a second dye-laser, delayed by means of varying optical path length. The resonance transitions at λ = 610.3, 612.2 and 616.2 nm ($^3S_1$- $^3P_{0,1,2}$ respectively) were normalised, to allow for variations in laser output, and monitored in the time regime 0-50 ns for pressures of He in the range 1-15 Torr, during which diffusion and spontaneous emission from Ca($^3P_1$) could be totally neglected, the $^3P_{0,2}$ states being, so called, "reservoir states". The rate equations for [Ca($^3P_{0,1,2}$)] were solved analytically and then convoluted numerically with the digitised forms of the ^1S - ^3P excitation laser and the LIF probe laser. Absolute rate data for all the collisionally-induced spin-orbit processes in both directions, J = 2-1, 1-0, 2-0, and the reverse, are reported for He. These results, determined from concentration profiles for Ca($^3P_{0,1,2}$) in the time-domain for fixed pressures of He, are compared with analogous results for Ca(^3P_j) determined from molecular beams using J state selection optical pumping laser methods at a fixed time with varying low pressures of He. The results are further compared with spin-orbit relaxation data for metal atoms and noble gases in general and with the results of recent quantum close-coupling calculations of an atom in a ^3P state with a structureless target.

A Comparison between Oxidation Reactions of the Alkali and Alkaline Earth Atoms[a]

Chia-Fu Nien and J.M.C. Plane[b]

Rosenstiel School of Marine and Atmosphere Science
and the Department of Chemistry,
University of Miami
4600 Rickenbacker Causeway
Miami, Fl. 33149

Results from recent work on the reaction kinetics of ground-state Group 1 and 2 metal atoms with N_2O and O_2 will be presented, showing that significant differences in kinetic behavior exist between the groups. Group 1 atoms are open-shell (^2S) species so that their recombination reactions with O_2 are radical-radical processes which have no barrier along the PES. On the other hand, the Group 2 atoms are closed-shell (^1S) species, and this causes them to exhibit quite different kinetic behavior with O_2. Small negative temperature dependences and large rate coefficients characterize the recombination reactions of Group 1 metals with O_2 to form superoxides. Whereas, the analogous reactions of Mg and Ca display complex temperature dependences, and the Mg reaction is extremely slow. This behavior has been successfully modelled with RRKM theory.

The Group 1 and 2 metal reactions with N_2O are highly exothermic, by at least 100 $kJmol^{-1}$, and so the metal oxide is often formed in excited states, sometimes giving rise to strong chemiluminescence. The group 2 metal reactions also display a much greater range of activation energies than their Group 1 counterparts. Several reactions of both groups with N_2O exhibit pronounced non-Arrhenius curvature. This non-Arrhenius behavior could arise from the effect of vibrational excitation of N_2O, which has low frequency bending modes (ν_2 = 589 cm^{-1}). The non-Arrhenius effects of the Group 2 metal reactions can also follow two paths with different activation barriers: one path on the initial singlet PES and, following a non-adiabatic spin transition, a second path on the low-lying triplet PES.

[a] Supported by the National Science Foundation under grants ATM-8616338 and ATM-8820225, and the Donors of The Petroleum Research Fund, administrated by the American Chemistry Society.
[b] School of Environmental Sciences, University of East Anglia, Norwich NR4 7TJ, U.K.

COLLISIONAL QUENCHING OF AlO($B^2\Sigma^+$)

R.E. McClean, H.H. Nelson, and N.L. Garland
Chemistry Division/Code 6110
Naval Research Laboratory
Washington, D.C. 20375

and

M. Campbell
Department of Chemistry
U.S Naval Academy
Annapolis, MD 21402

Abstract

Rate constants for the electronic quenching of AlO($B^2\Sigma^+$) by CO and NO are reported. AlO molecules were produced by the reactions, Al + O_2 --> AlO + O and Al + CO_2 --> AlO + CO. An excimer pumped dye laser operating at 464.8 nm was used to excite AlO($X^2\Sigma^+$) to AlO($B^2\Sigma^+$) (the 1,0 bandhead). Aluminum atoms were produced from the 248 nm photodissociation of trimethylaluminum.

Rate constants were determined by measuring the decay rate of the laser-induced fluorescence as a function of added quencher. The measured fluorescence lifetime of AlO($B^2\Sigma^+$), τ, is 103 ($\pm$ 10) ns, and the bimolecular quenching rate constants are 4.7 ($\pm$ 0.6) X 10^{-12} and 1.8 ($\pm$ 0.3) X 10^{-10} cm^3 $molecule^{-1}$ s^{-1} for CO (4.3 - 30.5 Torr) and NO (0.60 - 10.0 Torr) respectively. The effect of He (17.2 - 201 Torr), Xe (20.3 - 285 Torr), N_2 (16.5 - 243 Torr), H_2 (3 - 60 Torr), and CO_2 (3.9 - 32 Torr) on the fluorescence lifetime of AlO($B^2\Sigma^+$) was also investigated; no reduction in τ was observed with these gases.

Possible quenching mechanisms will be discussed.

XXth Informal Photochemistry Meeting
April 26- May 1, 1992
Atlanta, GA

ABSTRACT

Semiclassical Calculations of V-V and V-T/R Rate Constants in N_2-N_2, Rosa Anna Caporusso*, Mario Cacciatore, Centro di Studio per la Chimical dei Plasmi C.N.R., Dipartimento di Chimica, BARI-Italy, and Gert Due Billing, Chemistry Laboratory III, H. C. Orsted Institute, Copenhagen-Denmark.
*Present address: Department of Chemistry, Emory University, Atlanta, Georgia 30322.

Complete sets of state-to-state *ab initio* rate constants have been computed for vibration-to-vibration and vibration-translation/rotation energy exchanges in $N_2(v)$ - $N_2(v')$ collisions in the temperature range (500-4000K) and N_2 in different vibrational states (v = 0, ..., 15). We used an accurate 3D semiclassical "coupled state" method [1,2]. The method involves a classical treatment of the translation and rotational motion of both molecules. The quantum equations of motion for the vibrational amplitudes are solved by expanding the total wave function in the basis of the Morse wave function of the two isolated oscillators.

[1] G. D. Billing: Chem. Phys. Lett., 97 (1983), 188.
[2] G. D. Billing: Comp. Phys. Rep., 1 (1984), 237.

THE PREFERENTIAL EXCITATION OF THE CO($a\ ^3\Pi$,v′) PRODUCT OBSERVED IN THE N_2($A\ ^3\Sigma_u^+$,v′) + CO($X\ ^1\Sigma^+$,v′′=0) ENERGY TRANSFER REACTION.

Joseph M. Thomas*, Glenn Stark**, and Daniel H. Katayama
Phillip's Laboratory/GPIM, Hanscom AFB, Massachusetts 01731-5000

ABSTRACT

The vibrational level distribution of the CO $a\ ^3\Pi$ produced in the N_2($A\ ^3\Sigma_u^+$,v′) + CO($X\ ^1\Sigma^+$,v′′=0) energy transfer (ET) reaction was measured as a function of N_2(A,v′) using a rapidly pumped discharge-flow reactor at a total pressure of ~2 torr and ~297 K. The CO($a\ ^3\Pi$,v′ → $X\ ^1\Sigma^+$,v′′) Cameron band emission, observed from the product CO a formed in the title reaction, was collected with a 2.2 m vacuum-ultraviolet spectrograph-monochromator utilizing both photographic and photoelectric techniques. For N_2(A,v′≤4) + CO(X,v′′=0) we obtain a CO(a,v′) population distribution of 1.00:0.88 for v′ = 0 and 1, respectively. This branching ratio differs from previous results for N_2(A,v′≥0) which did not correct for competing removal processes of the CO a state. For N_2(A,v′=0) + CO(X,v′′=0) we obtain a CO(a,v′) population distribution of 1.00:0.00 for v′= 0 and 1, respectively. Evidence that the product CO a emission is much more intense for N_2(A, v′≥1) as compared to N_2(A,v′=0) is presented. The room temperature bimolecular rate constants, k_v^{II}'s, for the CO(a,v′=0 and 1) + CF_4 reaction were determined to be ≤5 x 10^{-14} cm^3 $molecules^{-1}$ s^{-1}

---

*Research Chemist, Orion International Technologies, Albuquerque, NM, 87108

**Summer Fellow, USAF Faculty Research Program. Permanent address: Department of Physics, Wellesley College, Wellesley, Massachusetts 02181

Isotope Effects in the Vibrational Deactivation of Large Molecules[1]

Beatriz M. Toselli* **and John R. Barker**

Department of Atmospheric, Oceanic, and Space Sciences
Department of Chemistry
Space Physics Research Laboratory
The University of Michigan
Ann Arbor, Michigan 48109-2143

Abstract

The collisional energy relaxation from highly vibrationally excited gas phase toluene-d_8 and benzene-d_6 pumped by a pulsed KrF laser operating at 248 nm, has been investigated by monitoring the time resolved infrared fluorescence from the C-D stretch modes near 4.3 μ. For toluene-d_8, energy transfer data were obtained for about 20 collider gases, including unexcited toluene-d_8; for benzene-d_6, only a few colliders were investigated. For both systems the data were analyzed by an inversion technique that converts the fluorescence decay to the bulk average energy, from where the average energy transferred per collision $\langle\langle\Delta E\rangle\rangle_{inv}$ can be calculated. Data obtained earlier for benzene-d_0 were re-analyzed by the same method used here and the revised results are reported. Results for both protonated and deuterated excited species show $\langle\langle\Delta E\rangle\rangle_{inv}$ to be nearly directly proportional to the vibrational energy of the excited molecule from 5000 to 25000 cm^{-1}. However, for pure toluene-d_8, benzene-d_6 and a few other collider gases at high energies, the energy dependence of $\langle\langle\Delta E\rangle\rangle_{inv}$ is reduced and even becomes negative at sufficiently high energies. The results are discussed in terms of possible quantum effects and mechanisms for energy transfer.

---

[1] This work was funded by the Department of Energy, Office of Basic Energy Sciences.

* Present address: INFIQC, Departamento de Físicoquímica, Universidad Nacional de Córdoba, Sucursal 16, C.C. 61. 5016, Córdoba, Argentina.

The Kinetics of Ozone Recombination at High O_2 Pressures: The Effects of a Metastable Electronic State

Jichun Shi* and John R. Barker

Department of Atmospheric, Oceanic and Space Sciences
Space Physics Research Laboratory
The University of Michigan, Ann Arbor, Michigan 48109-2143

Previous studies of the $O+O_2+M$ recombination reaction have found anomalous pressure dependence at high pressures (up to 10^5 torr) of N_2, Ar and He, and the anomaly was attributed to the formation of a weakly bound electronic state of O_3 in the recombination. In this work, the O_2 partial pressure dependence of this reaction has been measured for up to 1000 torr. The kinetics measurements were carried out by monitoring the time-resolved infrared emissions at 3.4, 4.7 and 9.6 μm from the vibrationally excited $O_3(v)$ intermediates. For $M=O_2$, the recombination is third-order at $P_{O2}<100$ torr, but at higher O_2 partial pressures, the rate constant falls off significantly. For $M=N_2$, similar P_{O2} dependence has been observed: the pseudo-first order rate constant is linear with P_{N2} (0-1000 torr) at constant O_2 partial pressures, but falls off with P_{O2} at constant N_2 partial pressures. This fall-off effect superficially resembles that of a unimolecular reaction, but it is actually caused by the participation in the recombination of $O_3(E)$, an unknown metastable electronic state. The fall-off is a result of the competition between the first-order conversion from $O_3(E)$ to $O_3(v)$ and the collisional dissociation of $O_3(E)$ to produce $O+O_2$.

The collisional deactivation of the $O_3(v)$ intermediates by N_2 and O_2 has been studied by simulating the three time-resolved infrared emissions using several empirical kinetics models. The deactivation rate constants are mostly determined by the total vibrational energy content, suggesting that the vibrational modes of O_3 lose their specificity in collisional deactivations at high energies.

This work was supported, in part, by the Department of Energy, Office of Chemical Sciences, by NSF's Atmospheric Chemistry Program, and by NASA's Upper Atmosphere Research Program.

---

* Now at: Ford Motor Company, Scientific Research Laboratories, P.O. Box 2053, Drop 3083, Dearborn, Michigan 48121-2053

Laser Induced Fluorescence of Jet-Cooled 4-aminobenzonitrile - The Onset of Intramolecular Vibrational Redistribution

E.M.Joslin, H.Yu and D.Phillips

Department of Chemistry, Imperial College of Science, Technology and Medicine, South Kensington, London SW7 2AY, UK.

Abstract

Laser-induced fluorescence spectra both in excitation and emission of 4-aminobenzonitrile (4-ABN) at high excitation energies are reported. These spectra are assigned in terms of fundamentals characteristic of substituted benzenes. The dependence of the onset of intramolecular vibrational redistribution of energy (IVR) as a function of excess energy has been investigated. The relatively low onset observed is attributed to the presence of the fluxional amino group.

XXth Informal Conference on Photochemistry
Georgia Institute of Technology
Atlanta, Georgia
April 26 — May 1, 1992

Ultrafast Vibrational Relaxation in the Fluorescent State of 4-(Dicyanomethylene)-2-methyl-6-(*p*-dimethylaminostyryl)-4*H*-pyran [*DCM*]

David C. Easter* and A.P. Baronavski
Chemistry Division, Code 6110
Naval Research Laboratory
Washington, D.C. 20375-5000

ABSTRACT

Vibrational relaxation in the fluorescent state of 4-(Dicyanomethylene)-2-methyl-6-(*p*-dimethylaminostyryl)-4*H*-pyran [*DCM*] has been interrogated by time-resolved femtosecond transient absorption spectroscopy. Following a sub-picosecond rise in population, each of the six vibrational regions probed exhibits a slower population increase or decrease. The wavelength-dependent filling (depletion) rates show a trend consistent with an energy gap law. The data may indicate a unique role for the ensemble of states responsible for the fluorescence maximum. Solvent effects are explored, as are parallel processes in the *DCM* ground state.

---

*presenter

HALOGEN AMINE CHEMISTRY AND THE EXCITATION OF IODINE ATOMS

R.W. Schwenz,* J.V. Gilbert, and R.D. Coombe
Department of Chemistry, University of Denver
Denver, Colorado 80208

$NCl(a^1\Delta)$ has recently been shown to be an effective energy carrier for the collisional excitation of I atoms.[1] As such, it may be a promising alternative to $O_2(a^1\Delta_g)$ in iodine chemical lasers. We have performed a number of experiments to test the compatibility of the NCl(a)-I energy transfer mechanism with the chemistry of NCl(a) generation by halogen amine systems developed in our laboratory.[2] A flow reactor was built in which $NCl(a^1\Delta)$ is produced via the reaction of NCl_3 with hydrogen or deuterium atoms, and is reacted with ground state I atoms to generate $I^*(^2P_{1/2})$ via the energy transfer reaction $NCl(a^1\Delta)+I(^2P_{3/2})\text{--}> NCl(X^3\Sigma^-)+I^*(^2P_{1/2})$. The experiments were run at reagent densities on the order of 10^{13} to 10^{14} cm^{-3}.

The I^* density produced by this system was found to scale linearly with the reagent densities, to the maximum quantities that we were able to generate. It was observed that deuterium atoms performed significantly better than hydrogen atoms as a reagent. Further, the addition of O_2 to the system caused an enhanced quenching of NCl(a) and enhanced production of I^*. This phenomenon was investigated by pulsed photochemical experiments directed toward real time measurements of the $NCl(a)/O_2$ energy transfer process. Data from both the flow reactor and pulsed experiments suggest rapid equilibration between the NCl(a) and O_2. Taken as a whole, the data serve to show the promise of this chemical system as an alternative means for pumping iodine lasers.

1. R.D. Bower and T.T. Yang, J. Opt. Soc. Amer., B8, 1583 (1991).

2. D.B. Exton, J.V. Gilbert, R.D. Coombe, J. Phys. Chem. 95, 2692 (1991).

*Permanent address: Department of Chemistry and Biochemistry, University of Northern Colorado, Greeley, CO 80639.

Kinetics of Chemically Pumped $NF(b^1\Sigma^+)$: Study of the $NF(a^1\Delta) + I^*(^2P_{1/2}) \leftrightarrow NF(b^1\Sigma^+) + I(^2P_{3/2})$ Equilibrium

J. Brooke Koffend, B.H. Weiller, and R.F. Heidner III
Environmental Monitoring and Technology Department
Space and Environment Technology Center
The Aerospace Corporation
P.O. Box 92957
L.A., CA 90009

The fast, near-resonant energy pooling between electronically excited $NF(a^1\Delta)$ and $I^*(^2P_{1/2})$ to form $NF(b^1\Sigma^+)$ is among the few promising chemically-pumped visible laser concepts. Since both precursors can be chemically produced in high yields, it is interesting to consider a green laser system based on the $NF(b^1\Sigma^+) \rightarrow NF(X^3\Sigma^-)$ transition near 530 nm. We will present recent results obtained from pulsed I^* laser optical pumping of premixed $NF(a^1\Delta)$ and $I(^2P_{3/2})$ obtained from 193 nm photolysis of NF_2/HI/buffer mixtures. During the saturating I^* laser pulse, analysis of the $NF(b^1\Sigma^+)$ time profiles is particularly simplified due to the clamping of the $[I^*(^2P_{1/2})]/[I(^2P_{3/2})]$ ratio. Direct information on the $NF(a^1\Delta) + I^*(^2P_{1/2})$ and $NF(b^1\Sigma^+) + I(^2P_{3/2})$ reactions obtained from $NF(b^1\Sigma^+)$ rise times and amplitudes will be presented.

Chemically Driven Continuous Visible Chemical Laser Amplifiers

D. Grantier, K. K. Shen, C. B. Winstead, S. H. Cobb and J. L. Gole

Using the highly efficient and selective formation of sodium dimer excited states from the sodium trimer-halogen atom (Na_3-X(F,Cl,Br,I) reactions, we seek to develop and scale chemically driven short wavelength visible and ultraviolet lasrs based on the successful production of visible chemical laser amplifiers. The Na_3-X(Cl,Br,I) reactions have been shown to creat4e a continuous electronic population inversion based on the chemical pumping of sodium dimer (Na_2). Optical gain through stimulated emission has been demonstrated in the regions close to 527, 492, and 460 nm. The results are in close analog to optically pumped alkali dimer lasers. The observed gain (max of 3.8% at $\lambda \approx 527$ nm corres. to $\alpha \sim 8 \times 10^{-3}$/cm for an individual rovibronic level) can be enhanced with a more versatile source configuration. Further, we are currently extending the range of systems under study to both the Na_3-F and Mg_3-F(Cl) atom reactions. The considered amplifiers are being optimized with a focus to increasing amplifier gain length and amplifying medium concentration facilitating their conversion to visible chemical laser oscillators.

Laser Induced Plasma Spectroscopy of Silicon and Germanium Based Molecules and Jet Cooled Metal Based Ion-Molecule Complexes

C. B. Winstead, K. X. He, T. Hammond, D. Grantier and J. L. Gole

Electric-Field-Enhanced Laser Induced Plasma Spectroscopy is developed and used to map electronic states and internal mode structure in small metal and metalloid based clusters and their ions. The technique has been used to generate emission spectra for silicon dimer and to obtained cooled gas phase emission spectra correlating closely with both absorption bands previously observed in rare gas matrices and attributed to silicon trimer and with recent gas phase negative ion photoelectron-photodetachment studies. An analysis of these silicon molecule emission features suggests that they involve a common upper state and multiple lower states and are associated primarily with short progressions in upper and lower state symmetric stretch frequencies of $\sim$300 and between 400 (X) and 460 cm^{-1} (A) respectively. Observed transitions in the germanium based system also display short progressions in the symmetric stretch with vibrational frequencies indicative of a softer bond consistent with observed phonon spectra for silicon and germanium surfaces. High resolution studies are underway to assess whether these band systems are associated with transitions to a ground $^1A_1$ state or a very low-lying $^3A_2$ state lying only a few kcal/mole higher in energy.

EFELIPS has also been used to map electronic states and internal mode structure in small metal ion based molecular complexes. In an exemplary study, ion-molecule complexes of aluminum have been formed. Emission spectra associated with $Al^+CO(Al^+OC)$ and Al^+H_2 complexation show 80-120 cm^{-1} vibrational level separations associated with the Al^+-molecule stretch or triatomic bending mode and can be corrlated closely with transitions among several excited states of the Al^+ ion (visible and ultraviolet). Complex emissions involve singlet (Al^+)-singlet (CO,H_2,N_2) interactions as the resulting singly charged electronically excited molecular ion complexes are likely formed in orbiting collisions of Al^+ with CO and H_2. No clear evidence is obtained for Al^+-N_2 complexation, although broadening and some structure associated with an Al^{++}-N_2 interaction is apparent suggesting possible excited state complex formation which dominates that in the Al^{++}-CO system. The results are considered in the light of the potential for coulomb explosion. Extensions of these efforts to the vacuum ultraviolet in order to study ground state based Al^+ complexes and extensions to other metal based systems are considered.

Laser induced lasing in the CS_2 Vapor

By

Huei Tarng Liou*, Howard Yang, and Peilin Dan
Institute of Atomic and Molecular Sciences.
Academia Sinica, P. O. Box 23-166, Taipei
Taiwan 10764, R. O. C.

ABSTRACT

When CS_2, in a tube at pressures ranging from 350 to 450 mTorr, was optically excited by a pulsed laser at a wavelength of 343.6 nm to the $J = 29$, $v = (0,10,0)$, R^3B_2 state (i.e., the $\Sigma = 0$ component of the a^3A_2 state), six coherent emissions were observed along the same axis from both ends of the tube. These emissions possess the characteristics of the pump laser, such as linewidth, pulse duration and polarization, but do not need a cavity to gain amplification. The emissions terminate on the highly vibrational states of the ground electronic state. A time delay between the pump laser and the emissions was observed. The emission intensity depends non-linearly on the CS_2 pressure and exhibits a third order power dependence. A cooperative stimulated emission model is proposed to explain this phenomenon.

ORTHO-ALLYL PHENOLS: THE CASE AGAINST EXCITED STATE PROTON TRANSFER.

Laren M. Tolbert and Lilia C. Harvey
School of Chemistry and Biochemistry, Georgia Institute of Technology
Atlanta, GA 30332-0400. USA

Abstract.

o-Allylphenols and other *o*-allylhydroxyarenes undergo photoinduced ring closure to form benzodihydrofuran and benzodihydropyran derivatives. It has become commonly accepted that the mechanism of such cyclizations involves excited-state proton transfer (ESPT) to the allyl double bond, followed by collapse of the intermediate zwitterion. *Intermolecular* excited-state proton transfer to alkenes, however, is an unknown process, even when electron-rich olefins and "photosuperacids"--molecules with photoacidities approaching those of mineral acids--are involved. We thus no longer believe that ESPT satisfactorily accounts for the behavior of allyl phenols and that alternative mechanisms involving radicals must be considered.

The subjects of our investigation are 1-allyl-2-naphthol (1A2NpOH) and 2-allyl-1-naphthol (2A1NpOH). These naphthalene fluorophores allow convenient determination of excited-state decay rates and have been extensively investigated by Chow as a case of ESPT (see path A of Figure).

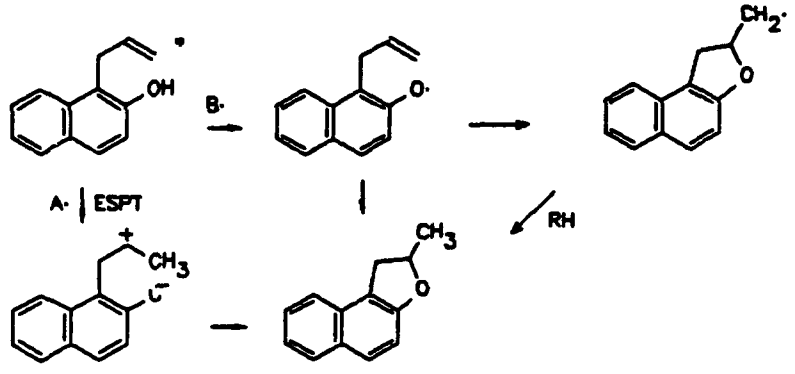

Several observations indicate that proton transfer is not involved:

1. The excited-state acidities of 1- and 2-naphthol are .5 and 2.5, insufficient for *adiabatic* protonation of a double bond.
2. Acid catalyzed cyclization of allylnaphthols 1A2NpOH and 1A2NpOH produces almost exclusively naphthofuran, but extensive six-membered (naphthopyran) formation is observed photochemically, consistent with radical but not acid-catalyzed mechanisms.
3. No evidence for anion emission from zwitterionic intermediates has been observed.
4. Both steady-state and time-resolved decay of allylnaphthols indicate little difference with the saturated derivatives 1-propyl-2-naphthol and 2-propyl-1-naphthol.

Acknowledgment. Support of this research by the U. S. National Science Foundation is gratefully acknowledged.

Cyclobutanetetracarboxylic dianhydride (CBDA) synthesis by photodimerization of maleric anhydride (MA) and the practical usage

Hideo Suzuki*, Toyohiko Abe, Noriaki Koto

Nissan Chemical Industries Ltd., Central Research Institute, Funabashi, Chiba, Japan

1. INTRODUCTION

In recent years, polyimide resins have been used as certain optical films or as electronic materials, such as insulation films and alignment films. However, because of the color, aromatic polyimides [1] have a poor percent transmission of light, and they are not very useful for such aplications and, in an extreme case, are not useful at all.

We synthesized the new polyimide, which was consisted of an aliphatic tetracarboxylic dianhydride (especially cyclobutane tetracarboxylic acid dianhydride(CBDA)) with an aromatic diamine[2].[1)2)] It had excellent transparency without coloring and good heat resistance.

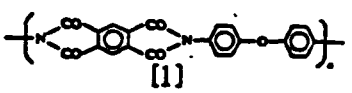

[1]

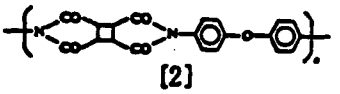

[2]

But CBDA synthetic method, which had been known, gave very low yield(8 %/KW・Hr).[3)]

2. EXPERIMENTAL and RESULTS [4)]

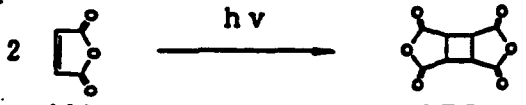

We investigated the reaction conditions of CBDA synthesis by the photodimerization of MA in liquid-phase. 100W High pressure mercury lamp(internal irradiation type) was used as light resource.

(1) SOLVENT [Temperature:6~50°C]

CBDA yield : Esters(ethyl acetate, ethylene glycol diacetate) > Ketones(acetone, acetophenone) > Ethers(tetrahydrofuran, dioxane), Nitriles(acetonitrile), Halogenated hydrocarbons (carbon tetrachloride), Nitro compounds(nitromethane), Amide compounds(N, N-dimethyl formamide > Hydrocarbons(cyclohexane), Lactones(butyrolactone)

A kind of esters is the best solvent to synthesis of CBDA, especially ethyl acetate (Y63% /KW・Hr) and ethylene glycol diacetate (Y55%/KW・Hr).

(2) TEMPERATURE

CBDA yield : 6 °C (Y75%/KW・Hr) > 20°C (Y63%/KW・Hr) > 50°C (Y43%/KW・Hr)

A lower temperature condtion is more desirable than a higher one.

(3) ADDITIVE

Addition of benzophenone(sensitizer) and benzoylperoxide(radical initiator) reduces the yield of CBDA.

3. CONCLUSION

We also investigated a kind of light resources, MA concentration, reaction time and so on. Among these reaction conditions, we found simple and better conditions.

Now we are producing CBDA for many new polyimides.

< REFERENCE >

1) H. Suzuki, T. Abe et al., Japan H 2-11615(March 15 1990)
2) H. Suzuki, T. Abe et al., U S P 5,053,480 (Oct. 1, 1991)
3) G. O. Schenck, W. Hartmann et al., Chem. Ber. 95, 1642 (1962)
4) H. Suzuki, M. Adachi et al., Japan H 2-61956 (Dec. 21, 1990)

SIMULATION OF STIMULATED EMISSION PUMPING SPECTRA IN LICN.

N. Berenguer[a], F. Borondo[a], J.M. Gomez Llorente[b] and R.M. Benito[c].

[a] Departamento de Química C-XIV. Universidad Autónoma de Madrid. 28049 Madrid. Spain.
[b] Departamento de Fisica Fundamental y Experimental. Universidad de La Laguna. 38203 Tenerife. Spain.
[c] Departamento de Física Aplicada. ETSI de Telecomunicación. Universidad Politécnica de Madrid. 28040 Madrid. Spain.

A simulation of a stimulated emission pumping spectra in the saddle point (SP) of a general two degrees of freedom model potential that closely corresponds to the real isomerization process for the LiCN molecule, shows a resonance-like spectrum (Figure a).

Resonance theory numerical techniques to project out the resonance functions show three resonance functions with increasing excitation in a mainly R mode and no excitation in the θ mode (Figure b).

Unestable periodic orbits (also shown in Figure b), whose action and stability parameters account completely for the position and width of the resonances, have been calculated in the SP region (SPPO). They are associated with the resonance behaviour.

The relaxation mechanism for the resonances involves two decay times which are the resoult of the interplay between the SPPO and a set of families of unestable periodic orbits connecting the SP region with both isomer wells.

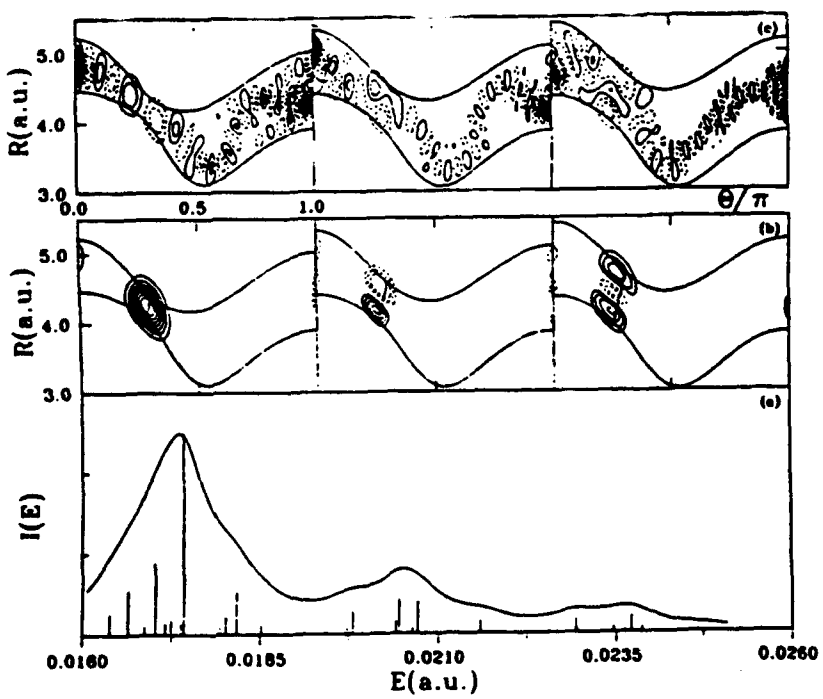

a: - Stick spectrum: features of chaotic unassignable spectrum.

- Low resolution spectrum.

b: - Results of the projection of the resonance functions. Projector:

$$P_J = \sum_{j=j_0}^{j_f} |\chi_j\rangle\langle\chi_j|$$

- Periodic orbits calculated at the first three energies that satisfy $S(E)=(n+1/2)h$.

c: - Three wavefunctions each one contributing to a different band in I(E).

A Study of Bias and Precision in the Estimation of First-Order Decay Rates from Sparse Data

Joel Tellinghuisen
Department of Chemistry, Vanderbilt University, Nashville, TN 37235

Charles W. Wilkerson, Jr., and Richard A. Keller
Chemical and Laser Sciences Division and Center for Human Genome Studies
Los Alamos National Laboratory, Los Alamos, NM 87545

It is generally well known that the mean decay time is an unbiased, maximum-likelihood estimator of the lifetime τ for an exponential decay process. Accordingly the precision of the estimate can be assessed very simply as the standard deviation of the mean, yielding the $\sqrt{N}$-dependence familiar from counting statistics. However, it is much less appreciated that this result holds only for observations extending to infinite time. When the restriction of finite time is recognized, several interesting changes occur: (1) The maximum-likelihood (ML) estimators for τ and its reciprocal Γ both exhibit bias, the extent of which varies with both the observation time window and the number of points. (2) The variance and all higher even moments formally diverge for the ML estimator of τ. (3) For a fixed number of points the standard deviation in Γ exceeds the infinite-time limiting value by an amount which increases roughly as the reciprocal of the observation time window.

In this paper, the above results are demonstrated with resort to the exact N-point distributions for random data distributed exponentially over finite time. These results are then compared with ML and least-squares results from Monte Carlo experiments in which the data are binned in various ways. In the case of least-squares, which is not an ML procedure for such data, a novel approach is presented for handling the problem of weights for empty bins; and various weighting algorithms are examined from the standpoint of the resulting bias and precision. To keep the various contingencies clear, the computations involve only background-free data. Results of these studies are directly applicable to "sparse data" situations and show that the usual methods for estimating decay rates and their precision may be inadequate in situations where there are fewer than ~100 counts and observation times shorter than ~3τ.

Cluster Ion Formation by Laser Ablation and Photofragmentation

Zhen Gao, Nan Zhang and Fanao Kong

State Key Laboratory of Molecular Reaction Dynamics
Institute of Chemistry, Academia Sinica
Beijing 100080 , China
Telephone : 2554245, Fax : 2569564

The cluster ion formation by laser ablation on some solid samples was studied using a home-made tandem time-flight mass spectrometer equipped by laser. We found that the size of cluster ion depends not only on laser fluence and the depth of the laser-generated crater on the surface of the sample, but also on the diameter of the laser spot on the surface. It has been possible now that by selecting a set of proper experimental condition, e.g. proper values of the laser fluence, the depth of the crater and the diameter of the laser spot, the cluster ions with particular n numbers can be produced. With four different sets of the experimental conditions, we have got four different results for 532 nm laser ablated carbon samples as followings:

(1). The cluster ions with n<30 and n>50 were observed at same time.

(2). The cluster ions with n<30 were formed only.

(3). The cluster ions with n>50 were formed only.

(4). In special case C_{60}^+ is much more preferred than other cluster ions.

With the aid of a mass gate in the spectrometer one kind of cluster ions with particular n can be selected and then photofragmented. The following are the examples of cluster ion photofragmentations.

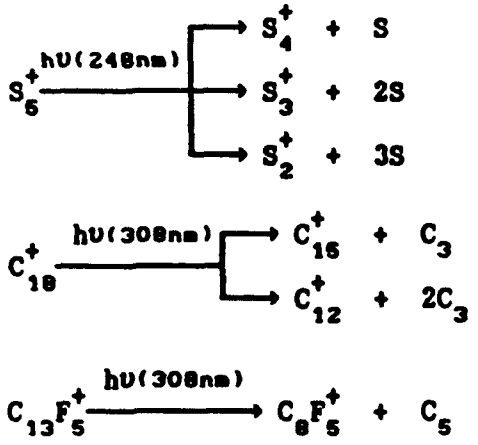

Nature of the new emission resulting from O_2 ($a^1\Delta_g$), Cl_2, and heated metal(Cu)

X.B. Xie, H.P. Yang, T.J. Cui, Q. Zhuang, and C.H. Zhang

Dalian Institute of Chemical Physics, Chinese Academy of Sciences
P.O.Box 110, Dalian 116023, P.R.China

Intense red and near-infrared emissions were observed when a heated Cu wire was placed in a chemically generated $O_2(a^1\Delta_g)$ flow, in which there was the residual chlorine. Spectra with medium resolution (0.1 cm^{-1}) were recorded by a Fourier Transform spectrometer (BOMEM, DA3.002).

The near-infrared spectrum has been assigned to an electric quadrupole transition, $^2\Delta_g(j=5/2) \longrightarrow {}^2\Pi_g(j=1/2$ and $j=3/2)$, of $CuCl_2$, based on the comparision with the absorption spectrum[1] and an *ab initio* calculation[2]. The vibrational spectral assignment has also been given. The ν_{00} of $^2\Delta_g(j=5/2)$ state is 7603 $\pm$ 2 cm^{-1}, and the separation between $^2\Pi_g(j=1/2)$ (ground) and $^2\Pi_g(j=3/2)$ states is 178 $\pm$ 2 cm^{-1}, which are excellent agreement with that of theoretically expected. The population of $^2\Delta_g(j=5/2)$ state must come from the near resonant energy transfer between the ground state of $CuCl_2$ and the $a^1\Delta_g$ state of O_2.

In the red spectrum, the interference-fringe-like fine structures with an energy spasing of approximately 21-25 cm^{-1} have appeared. This fine structure could not result from the rotational structure, and looks like the interference structure in a bound-free transition in diatomic molecules. Contrary to Tokuda et al[3] and Bouvier et al[4], we insist that the red emission is not originated from $CuCl_2$. An extended discussion on the spectroscopic recognition of the red emission has been given. More experimental studies are necessary for finally identifying the red emitter.

[1] C.W.Decock and D.M.Gruen, J.Chem.Phys., 44 (1966) 4387.
[2] C.W.Bauschlicher Jr. and B.O.Roos, J.Chem.Phys., 91 (1989) 4785.
[3] T.Tokuda et al., Chem.Phys.Letters, 174 (1990) 385.
[4] A.J.Bouvier, R.Bacis et al., Conf. Laser M28, Grenoble, July 9-11, 1991.

CHEMICAL DYNAMICS STUDIES USING TIME RESOLVED INFRARED EMISSION SPECTROSCOPY

Vernon R. Morris, Fida Mohammed, and William M. Jackson, Department of Chemistry, University of California, Davis, CA 95616

Time resolved infrared emission spectroscopy has been used to characterize the nascent vibrational populations of internally excited molecules formed as a result of direct photolysis, radical-radical and atom-molecule reactions. The 193 nm photolysis of $(CH_3)_2CO$ in He and Ar has been studied over the pressure range 13-1900 mTorr. Evidence for vibrationally excited C_2H_6 formed as a recombination product of CH_3 radicals has been observed. Prompt emission is detected at 3135 cm^{-1}, the band origin and intensity of which is not consistent with the spectroscopy of the ν_3 (antisymmetric stretch) mode of methyl radical. Arguments will be presented to explain the observed spectral features and their time behavior. In emission studies of the CN + O_2 reaction, seven vibrational states of CO have been identified. Translational to vibrational (T→V) energy transfer has been observed from hot H atoms formed from the 193 nm photolysis of H_2S to HCN. Hot HNC emission has also been identified in these studies and evidence of population inversion in both HCN and HNC as a result of this T→V transfer will be presented. The reaction of hot H atoms with ClCN has also been studied. This reaction is unique because it yields three spectroscopically well-separated emitters; HCN, HNC, and HCl. The nascent vibrational populations of these reactants have been characterized and the implications to the energetics and dynamics of this atom-molecule reaction are discussed.

The authors gratefully acknowledge the support of NSF under grant # CHE90-D0895. Vernon R. Morris also acknowledges the support of Lawrence Livermore National Laboratory under Task # 52NCFA. Fida Mohammed thanks US-AID, Washington D.C..

INDEX